TGFβ MODULATION OF IMMUNOPATHOGENESIS DURING ALPHAVIRAL ENCEPHALOMYELITIS IN IL-10 DEFICIENT MICE

by

Nina M. Martin

A dissertation submitted to Johns Hopkins University

in conformity with the requirements for the degree of Doctor of Philosophy

Baltimore, MD

November 2017

ABSTRACT

Alphaviruses are an important cause of mosquito-borne outbreaks of arthritis, rash and encephalomyelitis. Sindbis virus (SINV) causes viral encephalitis in mice, with different SINV strains leading to varying degrees of morbidity and mortality. Previous studies in mice with a virulent strain (NSV) of SINV identified a role for Th17 cells and regulation by IL-10 in the pathogenesis of fatal encephalomyelitis (Kulcsar et al, Proc Natl Acad Sci USA 111:16053-16058, 2014). The current study considers the role of another regulatory cytokine, transforming growth factor beta (TGFβ). Comparisons of IL10KO and WT mice after infection with avirulent TE, intermediate virulent TE12, and virulent NSV show that NSV-infected IL-10KO mice have greater amounts of both TGFβ1 and TGFβ3 proteins, while TE and TE12-infected IL-10KO mice have greater induction of TGFβ1, but not TGFβ3 when compared to WT control mice. These findings support the hypothesis that TGFβ3, but not TGFβ1 is responsible for promotion of the differentiation of pathogenic TH17 cells. In addition, more severe disease and impaired virus clearance in IL-10KO mice compared to wild type mice were associated with more Th1 cells; fewer Th2 cells, innate lymphoid type 2 cells, regulatory cells and B cells and delayed production of antiviral antibody in the central nervous system without an effect on Th17 cells. Therefore, IL-10 deficiency led to more severe disease, for example, in TE12-infected mice by increasing Th1 cells and by hampering development of the local B cell responses necessary for rapid production of antiviral antibody and virus clearance from the CNS. In addition, the shift from Th17 to Th1 responses with decreased virus virulence indicates that the effects of IL-10 deficiency on immunopathologic responses in the CNS during alphavirus infection are influenced by virus strain.

ACKNOWLEDGMENTS

This work was supported by a research grant from the National Institutes of Health (R01 NS87539) to D.E.G. and training grant (T32 AI007417) for N.M.M.

We would like to thank Johns Hopkins School of Public Health animal facility technicians Mary Archer and DJ Johnson for help with animal maintenance and Dr. Victoria K. Baxter and Elizabeth Troisi, for animal breeding assistance.

We would like to thank members of the thesis committee, past and present, for their continued support and time. This includes Diane Griffin, Alan Scott, Peter Calabresi, Fengyi Wan, Andrew Pekosz, Bill Moss, Jay Bream, and Gary Ketner.

I would also like to thank my mentors who have provided support and guidance throughout the doctoral process, including Gundula Bosch, Arturo Casadevall, Alan Scott, Peter Agre, Vincent Rancaniello, and Radames Cordero.

Table of Contents

ABSTRACT

Sindbis virus (SINV) causes viral encephalitis in mice, with different SINV strains leading to varying degrees of morbidity and mortality. During infection with the fatal NSV strain, previous work showed that the cytokine IL-10 is an important modulator of IL-17 and TH17, whereas TH1-associated pro-inflammatory cytokines like IFNγ and TNFα were decreased in mice lacking IL-10. These changes were associated with accelerated morbidity and mortality, as well as delayed viral clearance. The current study considers the role of another regulatory cytokine, transforming growth factor beta (TGFβ). Comparisons of IL10KO and WT mice after infection with avirulent TE, intermediate virulent TE12, and virulent NSV show that NSV-infected IL10KO mice have greater amounts of both TGFβ1 and TGFβ3 proteins, while TE and TE12-infected IL10KO mice have greater induction of TGFβ1, but not TGFβ3 when compared to WT control mice. These findings support the hypothesis that TGFβ3, but not TGFβ1 is responsible for promotion of the differentiation of pathogenic TH17 cells. TGFβ1 may play a role in the suppression of the TH2/B cell/antibody responses because this isoform was elevated and TH2 and antibody responses were suppressed after infection with all three strains in IL-10 deficient mice.

1 INTRODUCTION

1.1 Sindbis Virus

1.1.1 Alphaviruses: distribution and disease

Mosquito borne disease is an important cause of viral encephalitis worldwide (**Figure 1.9.1.A**). With increases of international travel and climate change, these diseases are spreading to new locations and vectors. Alphaviruses are an important cause of outbreaks of mosquito borne disease, with some leading to viral encephalitis (Figure 1.6.B), and others to painful, arthritic diseases. Alphaviruses cause disease in wide range of vertebrates, including humans, horses, and a number of domestic animals. Alphaviruses are maintained in the environment through a continuous transmission cycle between reservoir hosts, like birds and small mammals, and mosquito vectors; humans are typically a dead end host [1]. Based upon differences is geography and disease characteristics, alphaviruses are classified as either New World or Old World [2].

Alphaviruses that are geographically spread in Europe, Asia and parts of Africa are termed Old World viruses. These include Chikungunya (CHIKV), Sindbis (SINV), and Ross River (RRV). Old World alphaviruses typically cause painful, but not life-threatening disease with symptoms of arthritis of the small joints, rash, and other flu-like symptoms. Most cases are asymptomatic to mild. Nonetheless, Old World alphaviruses are responsible for millions of cases of painful disease that greatly impacts global health and Disability Adjusted Life Year (DALY). CHIKV has in more recent years been of concern because of its spread to the Caribbean region and potentially to the United States

(**Figure 1.9.1 C**). According to the CDC, SINV, which infects all age ranges across Asia and Europe and Africa, is the most widely distributed of the arboviruses [3, 4].

New World alphaviruses, distributed throughout North and South America, are a major public health threat by virtue of their ability to cause encephalitis, inflammation of the brain and spinal cord, and a high fatality rate ranging from 30 to 70%. Those patients that survive often have debilitating, chronic neurological defects. Three of the new world alphaviruses cause major outbreaks: Eastern (EEEV), Western (WEEV), or Venezuelan Equine Encephalitis (VEEV). EEEV was first documented in the nineteenth century from an outbreak in Massachusetts where 75 horses died from encephalitis and several decades later was isolated from horse brains. Presently, EEEV is commonly distributed in Eastern and Gulf Coast states. Florida reports several human from EEEV every year. Multiple states report a large economic loss from poultry and equine deaths every summer.

VEEV outbreaks occur in Central and South America. There have been a total of 21 outbreaks of VEEV since it was first isolated in 1938. One such outbreak spanning Venezuela and Colombia impacted an estimated 75,000 people with 300 deaths and 3000 debilitated with neurological complications [5]. The economic losses were increased by the equine losses: of the50, 000 horses infected, 8% died. In one region, out of 500 reported equine cases, there were 475 deaths.

WEEV is commonly seen in states and Canadian provinces west of the Mississippi River. WEEV has the lowest human-related fatality rate of the three new world alphaviruses at 4%. Most of these deaths occur within elderly populations, with a minority in infant and other immune compromised populations. The majority of WEE

cases are subclinical. WEEV still has a serious impact on the economy as 15-20% of horses that acquire this virus are either euthanized or die.

Despite the differences between Old and New World alphaviruses, they all share some common characteristics. The genus of alphavirus includes 26 related RNA viruses which all contain a genome of a single positive sense strand RNA, an envelope and an icosahedral capsid. Their genomes encode for four nonstructural proteins as well as two envelope proteins, E1 and E2.

One prototype alphavirus, SINV, is commonly used to study alphaviral infection, replication and clearance. SINV was first isolated in 1952 from mosquitoes captured in the village of Sindbis near Cairo, Egypt. Despite being an Old-World alphavirus that causes arthritis and flu like symptoms in humans, SINV is classified as a part of the Western equine encephalitis complex of viruses because of its closely related genomic sequence. Perhaps because of this, in mice, SINV infects both brain and spinal cord neurons, causing classical symptoms of viral encephalitis. Therefore, SINV is widely used in a mouse model to study the host immune response to viral replication in the central nervous system (CNS).

1.1.2 SINV life cycle and replication

SINV is a prototypical alphavirus with a 11.7 kb positive sense, single-stranded RNA genome. The positive-sense RNA genome contains a 5' methylguanylate cap and 3' polyadenylate tail (**Figure 1.9.2**). Entry into the target host cells occurs via receptor-mediated endocytosis, though the host receptor remains unknown. As characteristic of all alphaviruses, the genome consists of four nonstructural proteins at the 5' end, called

nsP1-4, and a capsid and two envelope proteins, E1 and E2, at the 3' end. During translation, nsp1-4 is first made as a polyprotein. Before cleavage, it is involved in replication of negative sense RNA strands, which serve as templates for additional nsP proteins, new positive sense strands, and 26S subgenomic RNAs [6].

This 26S subgenomic RNA contains all of the structural proteins. Translation of the subgenomic region results in another polyprotein that ultimately contains the capsid and envelope proteins, E1 and E2. Final processing of this polyprotein happens in several steps: first, there is autocleavage of the capsid protein, followed by translocation of the remaining polyprotein (pE2-6k-E1) to the endoplasmic reticulum for additional proteolysis, glycosylation, and posttranscriptional modifications. Subsequently, the precursor pE2 is cleaved into E2 and E3. Virus assembly and packaging is initiated by capsid proteins interacting with positive sense genomic RNA to form intracellular icosahedral nucleocapsid cores. After transport of these structures to the plasma membrane where budding occurs, E1 and E2 heterodimers trimerize to form the spikes. Theses spike proteins are in turn important for eventual attachment to new target host cells for infection [7].

1.2 Sindbis virus infection of the central nervous system

1.2.1 Virus induced encephalomyelitis in mice

This study exclusively uses an intranasal route to infect mice, but both intranasal and intracranial infections produce a similar course of encephalitis in mice. The only difference is that viral replication and spread are slightly delayed using intranasal challenge. SINV spreads quickly throughout the CNS via the cerebrospinal fluid central

canal and neuronal pathways. Neurons of the brain and spinal cord are the primary target cells and motor neurons are particularly susceptible to SINV infection [8]. During intranasal infection, virus replication begins in the olfactory neurons and then spread back to front in the brain.

Generally, virus clearance happens in three stages: clearance of infectious virus (days three to seven), clearance of viral RNA (days 8 to 60), and maintenance of low levels of viral RNA (> day 60) [9].

1.2.2 Virus and host determinants of disease

Mouse host and virus strain play a large role in the severity of SINV clinical scores, immunopathology and neuronal/host death. Factors include mouse age and genetic background (i.e. C57Bl/6 versus BALB/c) and the virulence of virus strain (i.e. virulent NSV versus avirulent TE strains) [10, 11].

In a mouse host, severity of disease is both mouse age- and strain-dependent. For example, the AR339 SINV strain causes fatal encephalitis in newborn mice, but weanling mice recover [12]. Newborn mice are more susceptible to fatality because their infected neurons die soon after they are infected while mature mice are able to produce anti-apoptotic factors, clear virus, and recover. Immature neurons have been shown, both in vivo and in vitro, to be more susceptible to SINV infections due to higher viral titers and virus-induced apoptosis [13, 14]. Mature neurons are intrinsically more resistant to SINV infection and virus-induced cell death, resulting in persistent infection of neurons in the absence of an immune response.

Susceptibility to SINV infection also depends on the genetic background of the host. Neuroadapted SINV (NSV – more on this in next section) causes uniformly fatal disease in adult C57Bl/6 mice, but adult Balb/c mice recover from infection [15]. Susceptibility in C57Bl/6 mice was associated with more neuronal apoptosis, more robust inflammatory response, and more severe neurologic disease [16]). Resistance to infection in Balb/c mice was associated with higher antibody titers as well as more Regulatory T cells producing IL-10 [16, 17].

Severity of disease is also linked to virulence of the infecting SINV strain, linked to amino acid changes in the E1 and E2 glycoproteins of SINV. These changes confer neurovirulence by altering an early step of virus replication [18, 19]. Recombinant virus studies have pinpointed that an important determinant of neurovirulence in adult mice to a single amino acid change, glutamine to histidine, at position 55 of the E2 glycoprotein [19]. The three recombinant SINV strains employed in this current study are neuroadapted SINV (NSV), TE12, and TE (**Figure 1.9.3**).

NSV causes severe encephalomyelitis associated with hind limb paralysis and death in adult mice within 7 to 8 days [10]. Fatal disease is associated with increased viral replication and the ability to cause death of infected mature neurons either directly by inducing apoptosis or indirectly by triggering immune response-mediated tissue damage [14, 20]. Originally, NSV was isolated after six intracerebral passages of avirulent wild type strain AR339, alternating between suckling and weanling mice [21]. After sequencing [10], it was found that NSV contains amino acid changes in E2 (Gly-55 to His and Leu-209 to Gly) and E1 (Val-72 to Ala and Gly-313 to Asp) which lead to increased virulence.

TE is the least virulent of the three strains and causes mild encephalomyelitis in adult mice, with nearly 100% survival and recovery rates. TE is a recombinant strain that contains the E2 gene from NSV and the E1 gene from the avirulent wildtype strain AR339. Immunocompromised weaned mice infected with TE develop an acute infection and clear infectious virus within 7 to 8 days without signs of paralysis or neurological damage [19, 22]. However, there is 100% mortality in suckling mice within a few days of infection.

1.3 Host immune responses to SINV infection

Neurons are highly specialized, nonrenewable cells. Therefore, the immune responses to viral infections of the CNS must do minimal damage to these important cells. Both SINV-specific innate and adaptive SINV-specific immune responses must be noncytolytic for survival and recovery. The immune responses are implicated in mouse survival, viral clearance, as well as immunopathology and death as summarized in **Figure 1.9.4**, the details of which will be discussed in length in the following sections.

Activation of both innate and adaptive SINV-induced immune responses occurs (1) locally in the CNS and (2) in the draining cervical lymph nodes. The spleen has little involvement in the induction of SINV-specific immunity [23]. As reviewed in [24], this is common for viral infections of the CNS, including herpes simplex virus type 1, mouse hepatitis virus, and cytomegalovirus.

1.3.1 Innate immune response to SINV infection

At 24-hours post-infection, innate immunity increases to detectable levels in the CNS. As reviewed thoroughly in [25], the first innate cell responders to viral infection are microglia which have functions in immune surveillance, antigen presentation, production of cytokines and chemokines, and debris removal [26]. It has been found recently that microglia play a critical role in survival from Dengue- and JEEV-induced encephalitis [27, 28]. Briefly, infected neurons activate microglia through cytokines and chemokines like IL-1, IL-6, IL-12, IL-23, and TNF. Activated microglial cells proliferate and up-regulate MHC Class I and Class II, which can present SINV antigens to virus-specific T cells [29]. Microglia also play an important role in recruitment of other innate cells into the CNS from the CLN via production of additional cytokines and chemokines like TNF, IL-6, and IFNβ. This triggers up-regulation of adhesion molecules on endothelial cells and increases permeability of the blood brain barrier, allowing for additional immune cells to infiltrate. Included in this infiltration are natural killer (NK) cells, dendritic cells (DC), and monocytes, with maximum activation and infiltration of innate cells at days three and four post-infection.

Early production of Type I IFN is important for initial control of virus replication and inhibition of spread [30, 31]. For example, infection of murine cells with SINV expressing a mutant nsP2 leads to higher levels of INFα and IFNβ secretion and decreased virus replication [31].

Within neurons, intracellular responses are also important for early, noncytolytic clearance of SINV. Differentiation of neurons leads to up-regulation of IRF7 and restriction of virus replication [32]. INFγ signaling and the JAK/STAT pathway are

essential for neuronal virus inhibition. First, treatment of SINV-infected differentiated neurons with IFNγ leads to neuroprotection. Subsequent inhibition of the JAK/STAT pathway within neurons completely reverses the neuroprotective and antiviral activities of INFγ in differentiated neurons [33].

1.3.2 Innate Lymphoid Cells

Before this current study, the role of innate lymphoid cells (ILC) had not been elucidated in SINV infection. ILCs derived their name from the fact that they develop from the common lymphoid progenitor, similar to B and T cells, but they do not express specific antigen receptors or undergo clonal selection and expansion when stimulated [34, 35]. Currently, there are three classes of ILCs: type 1, 2, and 3 (**Figure 1.9.5**). ILC type 1 (ILC1) have similar functions to TH1 and are important in immunity to intracellular bacteria and protozoa and chronic inflammation. They express the transcription factor Tbet and produce IL-12, IL-15, and IL-18 as well as TNF and IFNγ. Some classify NK cells as ILC1, but NK cells play a slightly different role and are important in immunity to viruses and cancer as well as chronic inflammation.

ILC type 2 (ILC2) play a similar role to TH2 in immunity to helminths, asthma and allergic diseases, as well as metabolic homeostasis. Also similar to TH2, they play an important role in activation of B cells and the antibody response via expression of the transcription factor GATA3 and production of cytokines IL-4, IL-5, IL-9, and IL-13.

The RORγt expressing ILC type 3 (ILC3) have a few subclasses and nomenclature is constantly under revision. At present, there are two major subclasses of ILC3s. Lymphoid tissue-inducer (LTi) cells are ILC3s that are similar to TH17 that

produce IL-17F, IL-22, and LTα/β. Another subclass of ILC3 is Rorγt+, Tbet+ and NKp46+ and produce IL-17A, IFNγ, IL-22 and GM-CSF. In general, ILC3s are important for lymphoid tissue development, intestinal homeostasis, immunity to extracellular bacteria, and chronic inflammation.

1.3.3 Adaptive immune response to SINV infection -- Overview

The adaptive immune response to SINV is predominately characterized by production of IFNγ by CD4+ and CD8+ T cells and antiviral antibodies by B cells [36]. At 5 days post-infection, the adaptive immune response begins to infiltrate into the CNS. Cellular immune responses include Helper T Cells type 1 and 2 (TH1 and TH2), cytotoxic lymphocytes (CTL), and B cells. Regulatory T and B cells producing IL-10 are important suppressors of the immune response and are associated with survival. An overview of helper T cell differentiation can be found in **Figure 1.9.6**. All helper T cell subsets can be found in the CNS post-infection.

1.3.4 T cell response to SINV infection

T cell production of IFNγ is known to be important for survival from SINV infection [37]. Levels of IFNγ production peak at days 5 to 7 post-infection, correlating with peak numbers of T cells. Mice lacking IFNγ have delayed viral clearance and lower amount of SINV specific IgM, IgG2a and IgG2b antibodies [37]. This suggests that IFNγ plays a role in recruiting and activating B cells to produce SINV specific antibody. Therefore, IFNγ plays a role in both immunopathogenesis via production of pro-

inflammatory factors but also neuroprotection in recruitment of B cells and production of antibody.

Helper T cells type 17 (TH17) have been implicated in the immunopathogenesis of fatal NSV infection [15, 17]. TH17 cells entering the brain of B6 adult mice infected with NSV had a pathogenic phenotype (expression of T-bet, granzyme B, IL-22, and GM-CSF) [17].

1.3.5 Antibody and B cell response to SINV infection

Antibody is known to be important for host survival and noncytolytic viral clearance. SINV-specific IgM, IgG, and IgA antibodies are produced in response to infection. Antibody secreting cells (ASC) producing IgM are detected as soon as day 5 post-infection. Starting at day 14, ASCs produce IgG and IgA [38]. In addition, these SINV-specific ASCs remain present for 12 months after recovery [39]. Non-specific SINV antibodies can also be effective in virus clearance. For example, severe combined immune deficiency (SCID) mice cleared infectious virus from the CNS within 24 hours of infection [40]. The most protective specific-SINV antibody is against E2 glycoprotein as shown by the passive transfer of various monoclonal antibodies. It is not required for the antibody to be bivalent for the antiviral effect of anti-E2 antibody to be effective [41]. The anti-E2 antibody has been shown to prevent viral budding and intracellular virus replication via crosslinking of newly formed virus glycoproteins on the host's cell surface [42]. In the *in vitro* studies, the anti-E2 monoclonal antibody is effective at restoring Na+K+ATPase function, neuronal membrane potential, and host protein synthesis [40, 43, 44].

Production of these antibodies is essential for viral clearance. Mice lacking B cells (C57Bl/6 μMT knock out mice) are unable to clear infectious virus [45].

B cells are first activated in the CLN and travel to the CNS by day 5 to 7 post-infection. Both naïve and activated B cells are detected by day 7 post-infection [9]. CD19+IgM+ B cells peak at day 10 post-infection while CD19+IgG+ B cells peak slightly later at day 14 post-infection. Because of the acute nature of the infection, there are few terminally differentiated ASCs in the CNS post-infection, as measured by CD138 and CD38 expression on B cells. CD38 is expressed on naive and activated B cells (including plasmablasts and memory B cells) and is down-regulated on mature B cells. For an ASC to differentiate into a plasma cell, CD138 is up-regulated. In addition, plasma cells do not express CD19, while earlier ASCs do express CD19. Mature plasma cells peaked by day 10 post-infection in the CNS and day 7 in CLN [9].

Factors within the CNS allow for long term, local production of antibody. For example, B cell recruitment chemokines increase early after infection [46]. In addition, infiltrating B cells express the chemokine receptors CXCR3, CXCR5, and CCR7 [46]. Last, there is a sustained increased in BAFF expression, B cell activating factor, which coincided with long-term maintenance of SINV-specific ASCs in the brain [46].

1.4 Regulation of SINV specific immune responses via IL-10

1.4.1 Overview

The CNS is the target for many acute and chronic inflammatory diseases. Suppression of resident and recruited immune cells after clearance of infection is key to preventing immune pathology and potential neural damage. In an ideal antiviral immune

response, infectious virus is eliminated and replication inhibited without host damage. It is therefore important that the immune response is tightly regulated to prevent host damage from robust or chronic inflammation. The cytokine Interleukin-10 (IL-10) is a known master regulator of immune responses and has long been recognized to play an essential role in suppression of inflammatory responses. The discovery and subsequent elucidation of molecular and cellular properties of IL-10 and its cognate receptor IL-10R is summarized in [47]. In brief, IL-10 was first described in 1989 as CSIF (cytokine secreting inhibitory factor), a factor secreted by TH2 cells to suppress inflammatory signaling [48]. The cDNA sequence was elucidated shortly later, along with a similar sequence within the Epstein Barr Virus genome. In mouse models of gastrointestinal disorders, mice lacking IL-10 develop severe and/or chronic enterocolitis [49].

It was postulated that the inhibitory effect of IL-10 was not direct, but via suppression of macrophages and other antigen presenting cells [47]. These studies were soon extended to show that IL-10 profoundly inhibited a broad spectrum of activated macrophage/monocyte functions, including monokine synthesis, NO production, and expression of class II MHC and costimulatory molecules such as IL-12 and CD80/CD86.

1.4.2 The IL-10 signaling pathway

IL-10 is part of the class II cytokine family that includes IL-19, IL-20, and IL-22 as well as types I and II interferons. IL-10 is functional as a homodimer with each subunit containing 178 amino acids [50]. The IL-10-receptor (IL-10R) is composed of two chains: a high affinity IL-10R1 chain and a lower affinity IL-10R2 chain. IL-10R1 is specific for IL-10 and is almost exclusively found on leukocytes. The IL-10R2 chain is

able to bind any of the IL-10 family cytokines (IL-22, IL-26, IL-28A, IL-28B, and IL-29) and is found on many cell types [47, 51]. Binding of IL-10 to IL-10R leads to activation of the JAK-STAT signaling pathway, ultimately leading to STAT1, STAT3, and, in some cases, STAT5 activation. Signaling via STAT3 is critical for many of IL-10's effects on immune cells [47, 52-54].

1.4.3 IL-10 is an important suppressor of immunity in SINV infection

As discussed previously, adult BALB/c mice are resistant to infection with NSV while adult C57Bl/6 mice are susceptible and experience 100% fatality. IL-10 mRNA is up-regulated upon infection with NSV in C57Bl/6 and BALB/c adult mice [15, 16]. The major producers during infection are regulatory T cells. Additionally, mice deficient in IL-10 display accelerated morbidity and mortality as well as delayed viral clearance [15]. In the BALB/c model, there was a higher frequency of regulatory T cells in the WT control group and this was associated with better clinical outcomes [16]. In the C57Bl/6 model, worse outcomes in the absence of IL-10 were associated with higher frequencies of TH17 cells, suggesting that IL-10 is an important regulator of TH17 cells during NSV infection [15, 17].

1.4.4 IL-10 plays an important role in immunity to acute viral infections

In acute viral infections, early production of IL-10 is triggered downstream of pattern recognition receptor binding of viral PAMPs, typically after a type I interferon response has already been initiated. IL-10 is produced by many innate cells, including macrophages, DCs, and NK cells in response to viral infection. Early production of IL-10

in response to viral PAMPs is thought to be important for limiting tissue damage from excessive inflammatory responses. Production can be sustained via autocrine loop in conjunction with IFNβ or antagonized by IFNγ.

In systemic, acute viral infections, CD8+ T cells are often employed to destroy infected cells. CTL's are critical in removing infected cells through recognition of viral antigens presented on MHC Class I molecules. TH1 cells, which are important in the activation and expansion of CTLs, also recognize viral antigens presented on MHC Class II molecules on APCs. IL-10 is very important for placing restraints on the effector functions of these cells once viral clearance has occurred.

IL-10 production by T cells is important in many acute viral infections, including LCMV, MCMV, and influenza [55-59].

1.4.5 IL-10 plays an important role in persistent viral infections

Persistent viral infections represent a failure of the immune response to fully clear virus. Some viruses that cause persistent infection do so intentionally by encoding for genes that actively suppress the host immune system, like viral IL-10 (vIL-10). For example, rhesus cytomegalovirus encodes for a vIL-10 that commandeers host IL-10 pathways to suppress immunity and allow for viral persistence [60]. Viral IL-10 can also be detected in patients with persistent cytomegalovirus [61]. Human herpes virus 4 (HHV-4) has also been found to have an IL-10-like protein encoded in its genome and this molecule has been found to be essential for its persistence [62].

1.4.6 IL-10 plays an important role in neurological disorders

As discussed previously, the CNS is for the most part an immune privileged compartment where timely deactivation of virus-induced immune responses is critical to neuroprotection and survival. IL-10 therefore plays an important role in control of neurological autoimmune disorders and its dysregulation has been implicated in worse clinical outcomes. In EAE, IL-10 has been found to play a crucial role in controlling inflammation in the brain and clinical outcomes are worse in its absence [63]. Moreover, treatment of EAE mice with IL-10 and antibody has improved disease outcome [64]. IL-10 also plays a protective role in neurological disorders like Alzheimer's and Huntington's by limiting glutamate toxicity via reduction in the NF-κB pathway in the CNS [65].

1.5 Regulation of SINV specific immune responses via TGFβ

1.5.1 Overview

TGFβ is an important cytokine in the regulation of acute viral infections. It has varying impacts on the immune response, depending on the context and compartment in which it is produced. It can act as either a suppressor or promoter of inflammation, as well as have an important role in modulating the antibody response. Its importance has been known for over 20 years. For example, knocking out TGFβ1 leads to embryonic lethality in most mice, with survivors demonstrating excessive inflammation, wasting disease by two weeks of age, and death at 3-4 weeks of age [66]. Histology revealed massive inflammatory lesions in multiple tissues, including T cells, macrophages, plasmablasts and plasma cells.

1.5.2 The TGFβprotein and its control by TGF-beta latency system

An overview of the TGFβ latency system can be found in **Figure 1.9.7.** The four isoforms of TGFβ(TGFβ1, 2, 3, and 4) share a highly conserved amino acid sequence which consists of N terminal signal peptide that is necessary for secretion, a pro-region called Latency Associated Peptide (LAP) and a 112-115 amino acid C terminus region that becomes the active cytokine following its release from the pro-region by proteolytic cleavage. Cleaved proteins dimerize via conserved secondary structures to form a 25kDa protein.

Once cleaved, LAP protein forms a structure that is capable of binding homodimeric TGFβ, forming a complex called Small Latent Complex (SLC). This complex remains in the cell until it is bound by another protein called Latent TGFβ-Binding Protein (LTBP), forming a larger complex called Large Latent Complex (LLC). It is this LLC that gets secreted to the extracellular matrix [67]. There are four isoforms of LTBP and specific isoforms associate with specific LAP:TGFβ isoforms. For example, LTBP-4 is reported to bind only to TGFβ1 thus, mutation in LTBP-4 can lead to TGFβ-associated complications which are specific to tissues that predominantly involves TGFβ1 [68]. Moreover, the structural differences within the LAPs provide different latent TGFβ complexes that are selective but only to specific stimuli generated by specific activators.

After its secretion, LLC remains in the extracellular matrix as an inactivated complex containing both the LTBP and the LAP which need to be further processed in order to release active TGFβ [69]. Because different cellular mechanisms require distinct

levels of TGFβ signaling, the inactive complex of this cytokine gives opportunity for a proper mediation of TGFβ signaling [69].

Only a few TGFβ activating pathways are currently known, though even these are not fully understood. This is because activation can be different depending on the cell and the tissue. Proteases, integrins, pH, and reactive oxygen species are just few of the currently known factors that can activate TGFβ. Although these mechanisms are not fully understood, it is accepted that perturbations of these activating factors can lead to unregulated TGFβ signaling levels that may cause several complications including inflammation, autoimmune disorders, fibrosis, cancer and cataracts [70, 71]. In most cases, an activated TGFβ ligand will initiate the TGFβ signaling cascade as long as TGFβ receptors I and II are available for binding. This is due to a high affinity between TGFβ and its receptors, suggesting why the TGFβ signaling recruits a latency system to mediate its signaling [69].

The consequences of this latency system are that the impacts of TGFβ are context dependent, meaning that the environment and concentration of both itself and other factors (i.e. cytokines) impacts its effect on immunity. It also consequently makes characterization of its impact more difficult as mRNA transcript levels often have little correlation with protein level; activated T cells produce high levels of TGFβ1 mRNA within 2 hours; the TGFβ protein is slowly secreted over several days [72].

1.5.2 The TGFβ signaling pathway

Figure 1.9.8.A and **1.9.8.B** illustrate the key components of the TGFβ signaling pathway. Upon activation, TGFβ binds to constitutively present kinase receptor

TGFBRII. Binding to TGFBRII triggers up-regulation of TGFBRI to the surface which forms a dimer with the TGFBRII:TGFβ complex. TGFBRII phosphorylates key residues on TGFBRI, which transduces a signal downstream.

SMAD proteins are a pivotal superfamily of signal transduction molecules that are pivotal intracellular mediators of TGFβ superfamily signaling and are reviewed in [73]. In summary, there are three types of SMADs: receptor-mediated SMADs (R-SMADs), common partner SMADs (co-SMADs), and inhibitory SMADs (I-SMAD). Isoforms of the TGFBRI class interact specifically and transiently with R-SMADs. Subsequently, the activated R-SMADs recruit Co-SMADs and heteromeric complexes accumulate in the nucleus. Nuclear SMAD complexes can bind to DNA directly or indirectly through other DNA binding proteins, and regulate the transcription of target genes.

Figure 1.9.8 shows a specific example of how this pathway important for viral clearance. Activated TGFBR1 recruits and phosphorylates a specific R-SMAD, SMAD2/3, which in turn recruits a co-Smad, SMAD4. Upon trimerization, this complex translocates to the nucleus where it up-regulates important immunity genes like STAT3. Conversely, an I-smad, such as SMAD7, can inhibit this translocation by binding to TGFBRI/II and physically blocking attachment of SMAD2/3 to the receptor. It has been shown that SMAD7 is key in determining the duration of the TGFβ response [74].

The combinations of SMAD proteins will lead to different cellular responses, a complete review of which can be found in [75]. It's thought that the concentration of TGFβ can lead to activation of different SMADs which in turn leads to, for example, different T cell differentiation fates. Higher concentrations of TGFβcan lead to induction

of regulatory T cells while lower levels leads to differentiation of TH17 cells [76]. This is thought to be accomplished via differential activation of SMAD isoforms depending on the concentration of TGFβ. As exemplified in **Figure 1.9.9**, low TGFβ levels activate SMAD2, leading to RORγt and pSTAT3 up-regulation (TH17). Higher levels of TGFβ are thought to activate SMAD3/4 and NFAT and thus lead to the development of regulatory T cells [77-79]. Furthermore, it is thought that different isoforms of TGFβ will lead to either non-pathogenic or pathogenic TH17 cells, as shown in **Figure 1.9.10**. Pathogenic TH17 cells produce IL-17 and IFNγ, as well as GM-CSF. The TGFβ3 isoform is thought to induce pathogenic TH17 cells, while TGFβ1 does not [80].

1.6 Suppression of SINV specific immune responses by regulatory T cells (Treg)

1.6.1 Regulatory T cells are important suppressors of inflammation – overview

Nearly 40 years ago, T cells were discovered to not only promote immune responses, but also suppress and regulate [81]. Regulatory T cells control the balance between different arms of the immune response, and play an important role in the immune suppression associated with certain infections and cancers. Dysregulation of migration and suppressive markers on regulatory T cells is associated with severe clinical outcomes in patients with, for example, multiple sclerosis and myasthenia gravis [82, 83]. It is hypothesized that these autoimmune disorders arise, at least in part, because of genetic abnormalities in Treg suppressive markers CTLA-4 and CD25, while others have shown a decreased expression of FoxP3 and IL-10 [83]. It has also been found that regulatory T cells control the balance between TH17 responses and regulatory responses; disruption of this balance can lead to severe immunopathogenic disease [84, 85].

1.6.2 Suppression of SINV specific immune responses by regulatory T cells

Regulatory T cells are important suppressors of inflammation and have been shown to play a critical role in host survival after SINV infection. BALB/c mice survive infection with fatal NSV while C57Bl/6 mice have a 100% fatality rate, at least partially due to the higher frequency of IL-10 producing regulatory T cells in C57Bl/6 animals [17].

Regulatory T cells play an important part in control of inflammation post-NSV infection in C57Bl/6 mice. For example, mice lacking IL-10 have fewer regulatory T cells and experience accelerated morbidity and mortality compared to wild type controls [15, 17].

1.7 Regulatory B cells are important suppressors of inflammatory diseases

1.7.1 Overview

Regulatory B cells (Breg) are known to be important suppressors of inflammation and act similarly to regulatory T cells. The role of regulatory B cells in SINV infection was unknown prior to this study.

1.7.2 Regulatory B cells are modulators of neurological autoimmune disorders

A recent review has underscored the importance of regulatory B cells in the resolution of neurological autoimmune disorders like MS, EAE, and MG [86]. For example, regulatory B cells play a large part in recovery by suppressing the infiltrating T

cells in the CNS that are implicated in leading to progressive demyelination [87]. Han et al. [86] sum up the evidence to date to support the importance of regulatory B cells. Briefly: mice were not able to survive EAE in the absence of B cells [88], addition of CD19+CD5+IL-10+ B cells (but not other B cells) were able to suppress EAE and decrease numbers of infiltrating T cells [64, 89-91]. It's also been found that regulatory B cells specifically improve EAE symptoms by inducing the formation of IL-10-producing regulatory T cells [92], which is important for limiting neuronal damage from inflammation. They also act by suppressing TH1 and TH17 cells, which have also been implicated in the immunopathogenesis of MS [93, 94].

1.7.3 Regulatory B cells play an important role in acute viral infection

In certain acute viral infections, regulatory B cells may contribute to pathogenesis. Coxsackievirus B3 is a positive strand virus and one of the major causes of viral cardiac myocarditis. BALB/c mice infected with coxsackievirus B3 display higher frequency of splenic IL-10 producing B cells than the controls [95]. The authors conclude that regulatory B cells may play a pathogenic role in the development of myocardiopathy, however, it may just be that there are higher numbers of IL-10 producing Bregs to control the higher levels of inflammation caused by the acute viral infection of the cardiac myocytes. This mirrors results seen with patients with cardiomyopathy [96]. However, these studies did not address if the regulatory B cells are actually contributing to pathogenesis or if they are present to try to control damaging inflammation post-infection as in other models.

1.7.4 Regulatory B cells play an important role in persistent viral infections

Regulatory B cells play an important role in chronic viral infections by suppressing effector T and enhancing regulatory T functions, which is important for immune tolerance. For example, patients with chronic hepatitis B virus infection were enriched in regulatory B cells whereas nephritis patients were lacking regulatory B cells [97, 98]. Additionally, when regulatory B cells from the HBV patients were co-cultured with CD4+CD25- helper T cells, the cells from these patients produced less IFNγ and IL-17 and more IL-4, plus their conversion to regulatory T cells producing IL-10 was enhanced [97]. Increased regulatory B cell function is also associated with the persistence of HCV. Patients with chronic HCV infection have increased numbers of both IL-10 producing regulatory B and T cells [99, 100].

1.7.5 Characterization of the regulatory B cell phenotype

Although the idea of B cells performing regulatory functions is not new [88], the definitive proof for their existence and characterization is recent. The delay in the elucidation of this cell type was because a unique molecular marker does not exist to distinguish Bregs from other B cells, unlike, for example, CD4 for helper T cells. Using flow cytometry approaches two groups identified which subpopulations of B cells could be generalized to produce IL-10 and be labeled as "Bregs" aka "B10 cells" [91, 101]. They discovered in mouse models of contact hypersensitivity and experimental autoimmune encephalitis that IL-10-producing regulatory B cells all have CD19, CD5, and CD1d (hi) on their surface. It was later clarified that in other models, like inflammatory bowel disease and cancer, the B cells producing IL-10 may have other

markers. For example, Olkhanud et al. [102] demonstrated that in breast cancer, regulatory B cells can be classified as CD19+CD25+B220+.

In humans, some of the cell phenotypes are the same as previously described mouse markers. In human chronic HBV and HCV infections, IL-10-producing B regulatory cells have the markers CD19, CD5, and CD1d (hi) [100, 101].

1.7.6 Regulatory B cells exercise function via IL-10

In vitro studies have shown that IL-10 produced by CD19+CD5+CD1d^{hi} cells modulate the function of microglia. For example, co-culturing of IL-10-producing B regulatory cells with microglia lead to suppression and significantly less production of TNFα 24 hours after infection with mouse cytomegalovirus [103]. Additionally, when these B cells were unable to produce IL-10, microglia showed increased expression of MHC Class II molecules [103].

In vitro studies have also shown that IL-10 produced by CD19+CD5+CD1d^{hi} cells is important for differentiation of regulatory T cells. Twenty four hours post-mCMV infection, naïve T cells differentiated into regulatory T cells when co-cultured with IL-10-producing regulatory B cells [103].

1.7.7 Overview of previous work leading to current hypothesis

Previous studies with mice deficient in IL-10 were associated with uncontrolled inflammatory responses and worse clinical outcomes because of development of spontaneous colitis. This uncontrolled inflammatory response was associated with increases in production of pro-inflammatory cytokines like IFNγ, TNFα, IL-1β, and IL-

12b as well as increased numbers of Th1 cells. Previous doctoral student Kulcsar had therefore hypothesized that IL-10 deficient mice infected with NSV would have worse clinical outcomes because of uncontrolled inflammatory responses in the CNS [104]. Surprisingly, there was only a select increase in levels of IL-17a mRNA, TH17 cells, double IL-17+IFN+ TH17 cells, and neutrophils [15, 17]. Not only were levels of other pro-inflammatory cytokines not increased, IFNγ, TNFα, IL-1β, and IL-12b mRNA were decreased in IL-10 deficient mice compared to WT control mice (data unpublished). This current study focused on why there was a select TH17-focused response in the absence of IL-10, while other pro-inflammatory cytokines were suppressed. Additionally, other strains of SINV were used in this study to allow for longer term evaluation of the rolw of IL-10 in the CNS during SINV infection.

1.8 HYPOTHESIS

In the absence of IL-10, TGFβ is upregulated (**Figure 1.9.11**). In a concentration dependent manner, TGFβ increases differentiation of TH17, suppresses TH1-related responses, suppresses Tregs, and decreases antibody and B cell responses. It is further hypothesized that infection with the NSV strain of SINV induces a high amount of TGFβ, the TE12 strain induces an intermediate amount of TGFβ, and TE strain induces the lowest concentration of TGFβ. Increased TGFβ3 leads to pathogenic TH17 cell differentiation and accelerated mortality. Increased TGFβ1 leads to suppressed B cell and antibody responses.

1.9 Figures and tables

Figure 1.9.1 Arboviral encephalitides are distributed worldwide

Figure 1.9.1 A Worldwide distribution of arboviral encephalitis, CDC

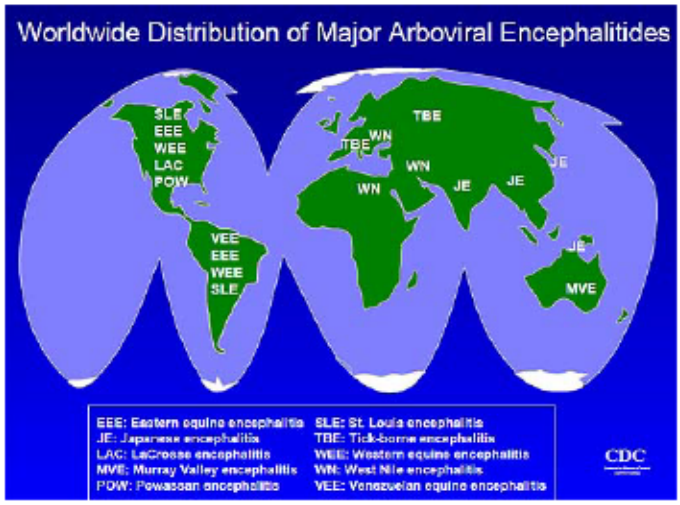

Mosquito-borne viruses are an important cause of encephalomyelitis worldwide. Alphaviruses are an important cause of these cases and include Eastern, Western, and Venezuelan Equine Encephalitis. Source: www.cdc.gov

Figure 1.9.1 B Cases of Eastern, Western Equine Encaphlitis by State, 2004-2009, CDC

Cases, Eastern Equine Encephalitis, 2004-2009

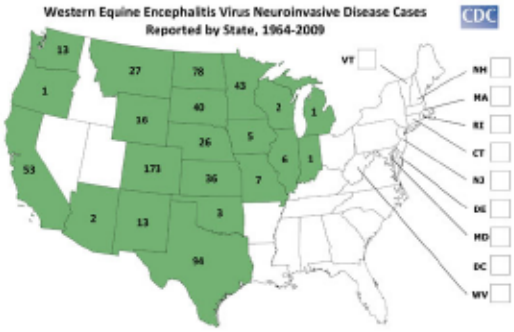

Cases of Western Equine Encephalitis, 1964-2009

EEEV is distributed along the Eastern Coast of the United States while WEEV is distributed in the Midwest and Western Coast of the United States. Although there are low numbers of cases, fatality rate is high, those who survive have neurological deficits, and there are no treatments available. Source: www.cdc.gov

Figure 1.9.1 C Distribution of CHIKV in the United States, 2015

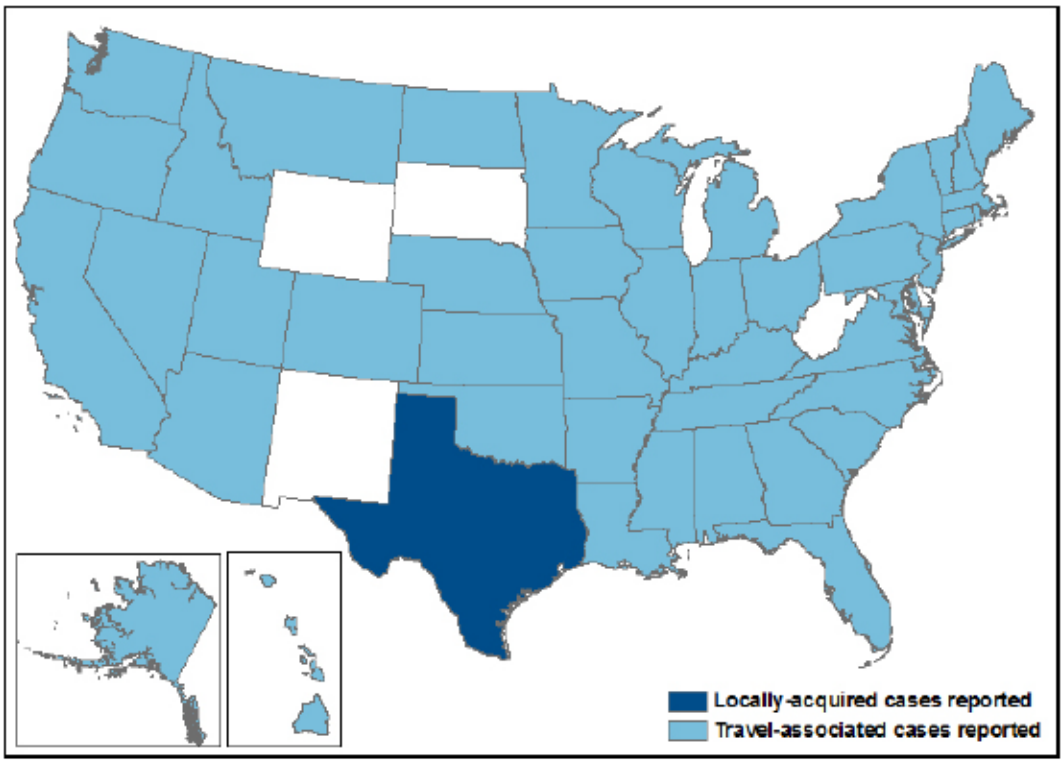

Most cases of CHIKV reported in the United States are acquired while traveling. Cases were reported in 2015 as being locally acquired and not travel associated in Texas.
Source: www.cdc.gov

Figure 1.9.2 Diagram of alphavirus replication

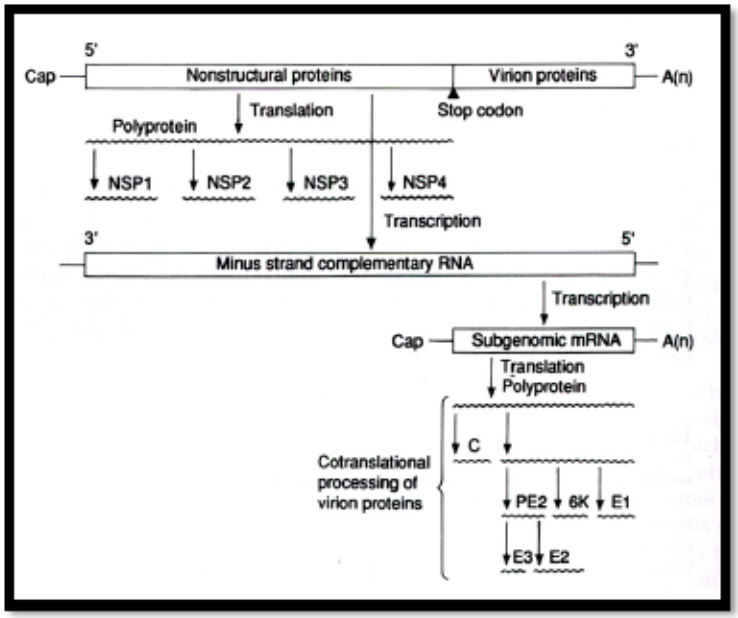

Source: https://web.stanford.edu/group/virus/1999/jchow/rep.html

Alphaviral replication begins with translation of the 5' two thirds of the genome into a large polyprotein (P1234) that cleaves itself and forms 4 nonstructural proteins (NSP1-4). These proteins are indispensable for the production of a complementary RNA strand. NSP4 is cleaved first and the P123/NSP4 complex is believed to initiate the synthesis of the complementary minus RNA strand. In Sindbis virus, a stop codon is present in front of the NSP4 sequence. A read-through mechanism translates through this codon followed by cleavage of NSP4. The complementary minus strand is used as a template for the production of a copy of the genomic RNA along with a subgenomic mRNA strand. The subgenomic message corresponds to the 3' end of the genome that contains the structural proteins (i.e. capsid proteins, envelope proteins, etc.). One template strand can yield multiple copies of structural proteins. The subgenomic message is then translated into another polyprotein which is also cleaved. Four or five structural proteins result from this cleavage: C-the nucleocapsid protein; E1, E2 (some species also contain E3)-the envelope glycoproteins, and 6K-a small transmembrane protein.

Figure 1.9.3 Sindbis Virus Strains

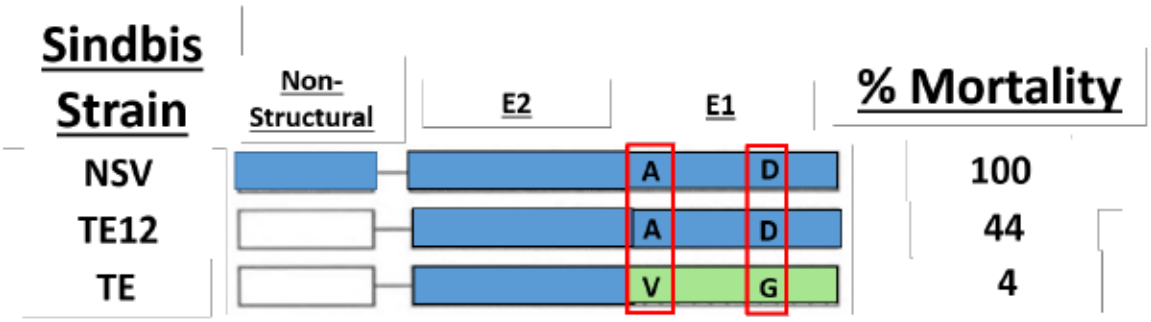

NSV, TE12, and TE are the three SINV strains used in this study. Shown is percent mortality in adult, C57Bl/6 mice. Adapted by Martin from [10].

Figure 1.9.4 Key components of SINV specific immune response that leads to survival or death

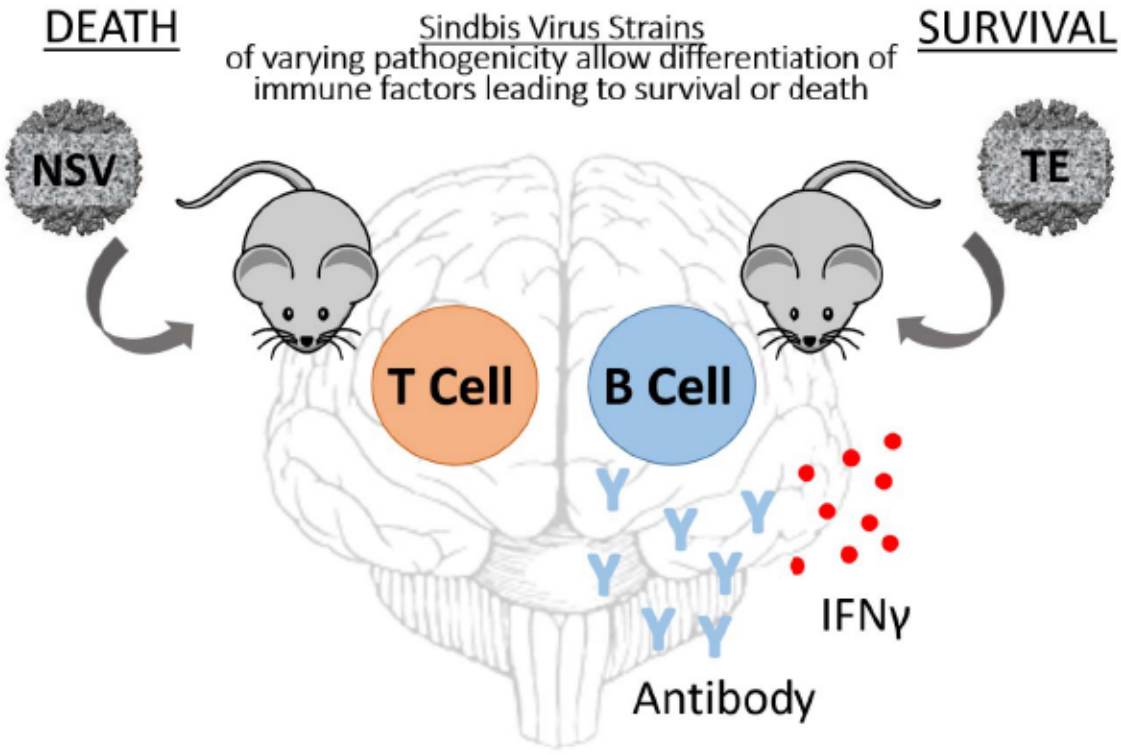

Framework of immune components that may contribute to survival or death of adult, C57Bl/6 mice. Antibody and IFNγ have been associated with viral clearance and survival. T cells have been implicated in immunopathology.

Figure 1.9.5 Innate Lymphoid Cell Classification

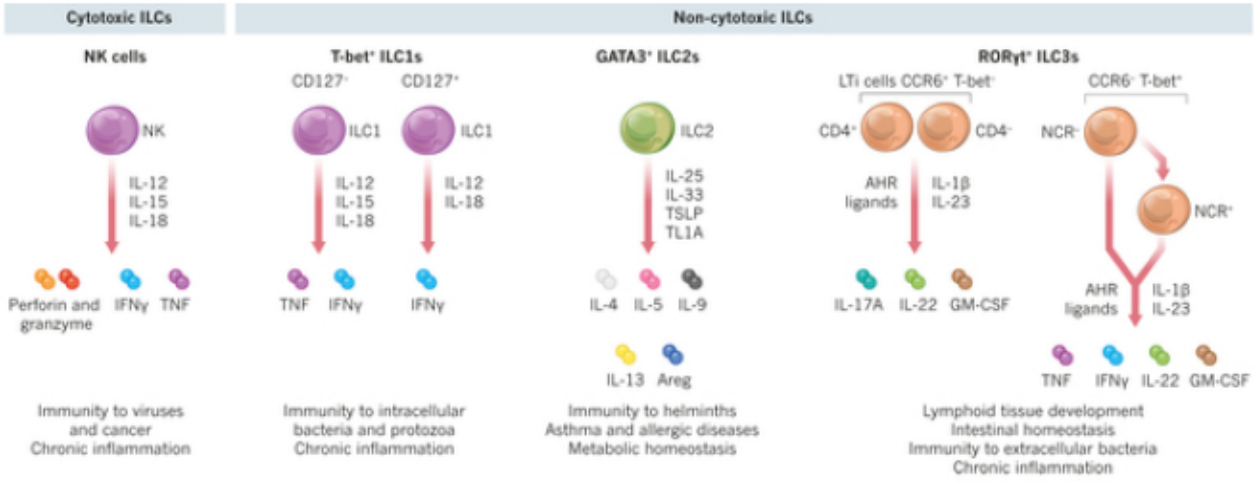

Source: http://www.nature.com/nature/journal/v517/n7534/full/nature14189.html

To date, there are three classes of non-cytotoxic Innate Lymphoid Cells (ILC1-3) and one class of cytotoxic ILCs (Natural Killer cells). Each class of cells can be identified by surface receptors, transcription factors, and production of cytokines and chemokines. For example, ILC2's can be classified as Lineage-, $CD127^{+}$, $IL\text{-}5^{+}$, $IL\text{-}13^{+}$, $GATA3^{+}$. IL-17-producing ILC3s can be distinguished as Lineage-, $CD127^{+}$, $ROR\gamma t^{+}$, $IL\text{-}17^{+}$.

Figure 1.9.6 Helper T Cell Differentiation

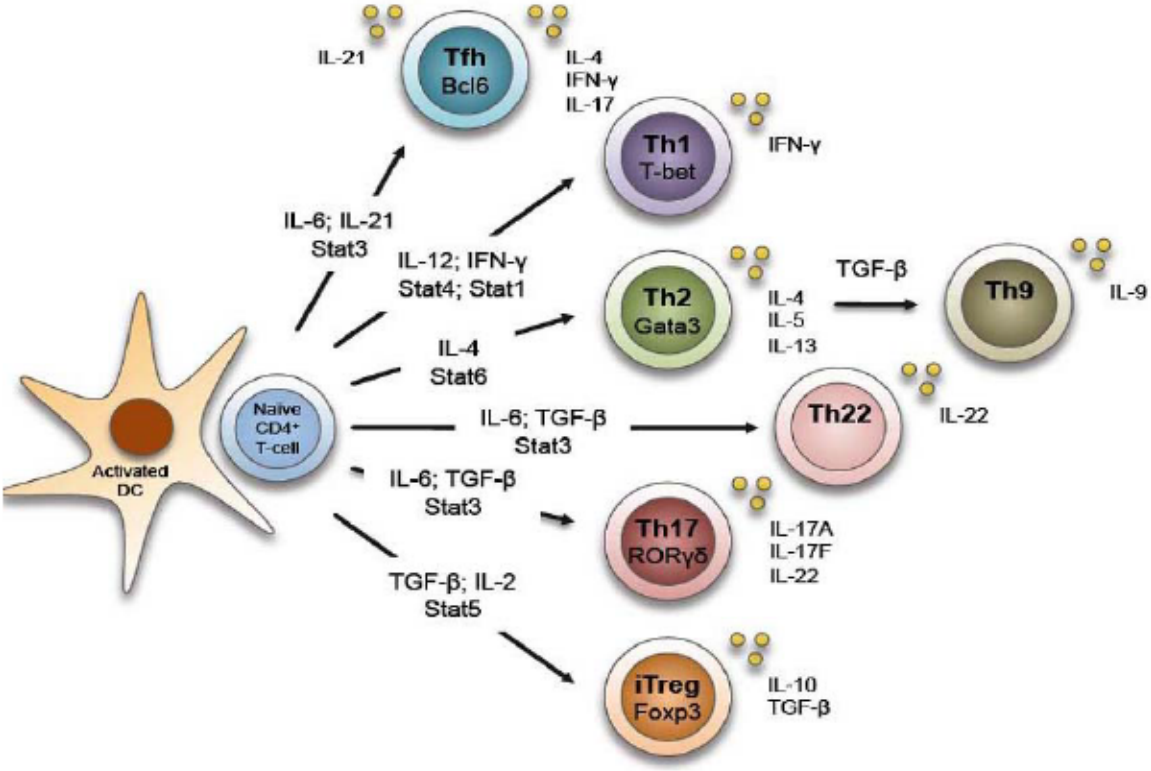

Naïve CD4+ T cells are activated by antigen presenting cells, i.e. activated dendritic cells. Depending on the concentration of cytokines and presence of transcription factors, helper T cells can differentiate into T follicular helper cells, helper T cells type 1 (TH1), helper T cells type 2 (TH2), helper T cells type 9 (TH9), helper T cells type 17 (TH17), helper T cells type 22 (TH22), or regulatory T cells (Treg). Each subtype is associated with specific cytokines and transcription factors as shown above.

Source:
https://www.erasmusmc.nl/content/3025942/3030149/thelper17subsetinpulmdiseases?lang=en

Figure 1.9.7 Processing of pro- to latent- to mature-TGFβ

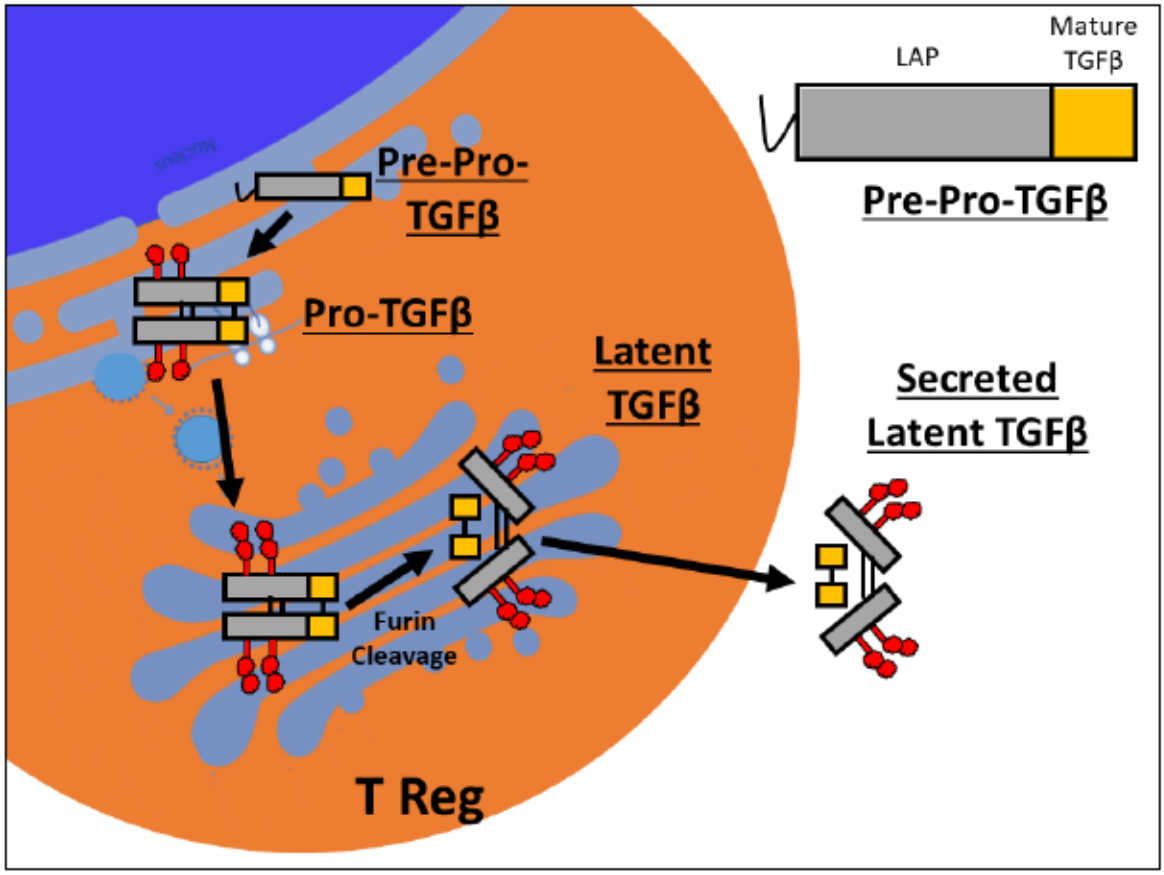

Source: Martin, NM, August 2017

TGFβ is first made as a polypeptide, Pre-pro-TGFβ, that includes LAP and mature TGFβ. In the endoplasmic reticulum, the pre-pro form is processed, glycosylated, and dimerized to become the pro-form. Further processing occurs in the Golgi Complex and pro-TGFβ becomes latent TGFβ. Golgi processing includes glycosylation and furin cleavage. Latent TGFβ is secreted. Mature TGFβ remain inactive until removal of LAP.

Figure 1.9.8 TGFβ signaling pathway

Figure 1.9.8.A Simplified example of TGFβ pathway in regulatory T cells

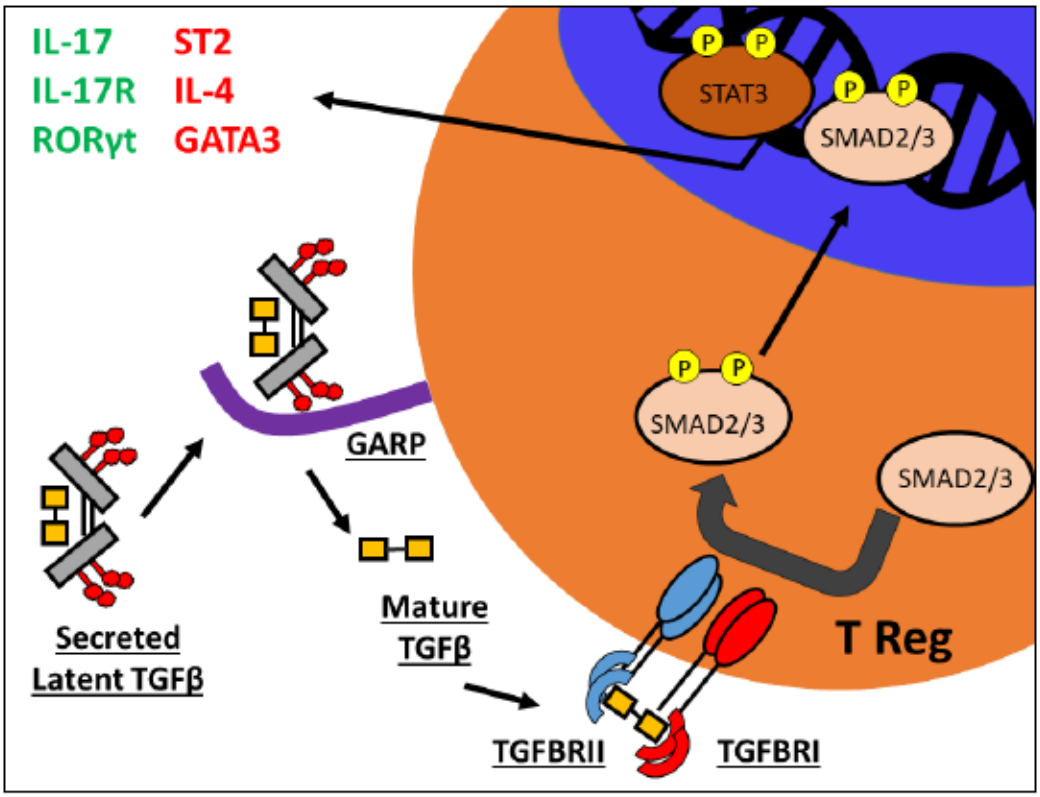

Secreted latent TGFβ will not be active until LAP has been cleave as well as release from surface glycoprotein GARP. Once released, mature TGFβ will bind to its cognate receptor, TGFBRII. Upon binding, TGFBRI will dimerize and signal transduction will proceed intracellularly. Activation of the intracellular TGFβ pathway begins with phosphorylation of SMAD2/3 (in this example) by the TGFBR. This ultimately leads to upregulation of TGFβ-regulated transcripts, i.e. TH17 related genes like RORγt, IL-17R, and IL-17. This can also, in certain circumstances, lead to the suppression of other gens like GATA3, IL-4, and ST2, which are important for Th2 related responses.

Figure 1.9.8.B Steps to TGFβ pathway activation

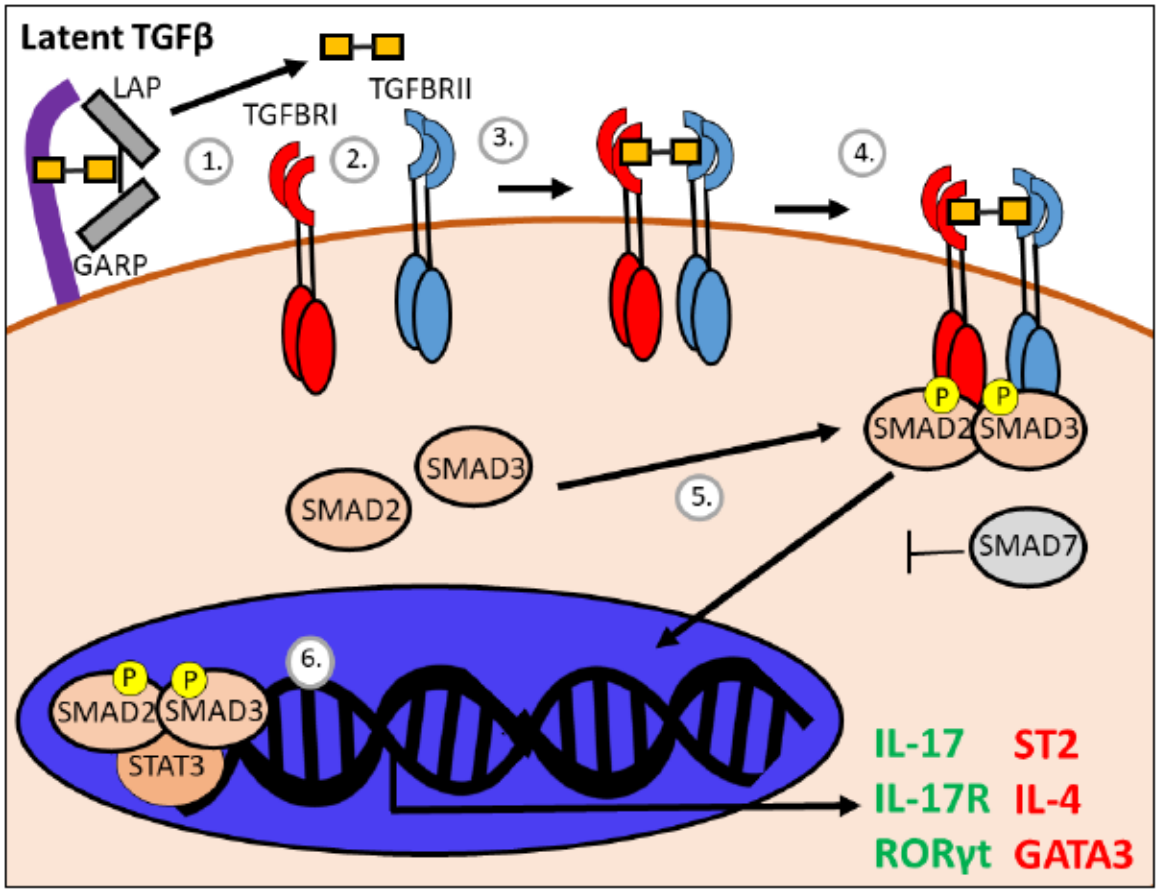

Source: Martin, 2017

Simplified overview of the TGFβ signaling pathway. Secreted latent TGFβ will not be active until LAP has been cleave as well as release from surface glycoprotein GARP. Once released, mature TGFβ will bind to its cognate receptor, TGFBRII. Upon binding, TGFBRI will dimerize and signal transduction will proceed intracellularly. Activation of the intracellular TGFβ pathway begins with phosphorylation of SMAD2/3 (in this example) by the TGFBR. This ultimately leads to upregulation of TGFβ-regulated transcripts, i.e. TH17 related genes like RORγt, IL-17R, and IL-17. This can also, in certain circumstances, lead to the suppression of other gens like GATA3, IL-4, and ST2, which are important for Th2 related responses.

Figure 1.9.9 Effects of TGFβ are concentration dependent

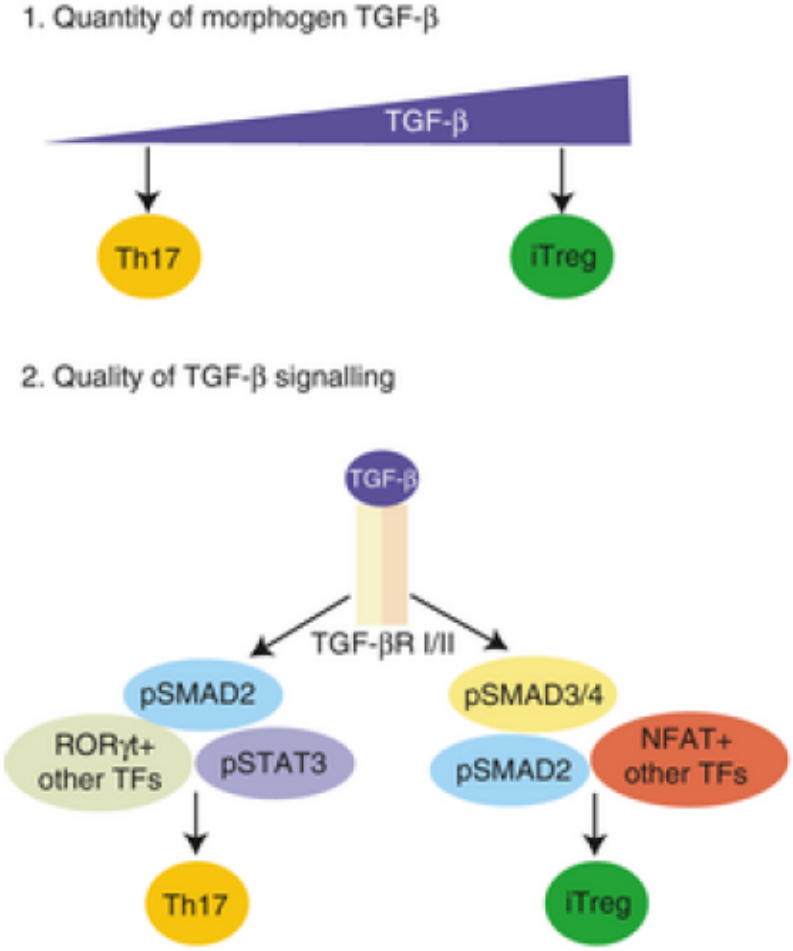

Part 1 shows that different doses of TGFβ can influence the differentiation of T cells into different subpopulations. For example, higher doses of TGFβ may induce TH17 cells whereas lower doses will induce Tregs. Part 2 shows that different combinations of SMAD proteins (as well as other TGFβ effectors) can also lead to different T cell differentiation outcomes. For example, when SMAD2/3 is phosphorylated by the TGFBR is in combination with RORγt and other transcription factors, T cells will be differentiated into TH17 cells. Conversely, when SMAD2 and SMAD3/4 are phosphorylated and found in combination with NFAT and other transcription factors, regulatory T cells will be induced.

Source: [75]

Figure 1.9.10 Upregulation of TGFβ in the absence of IL-10

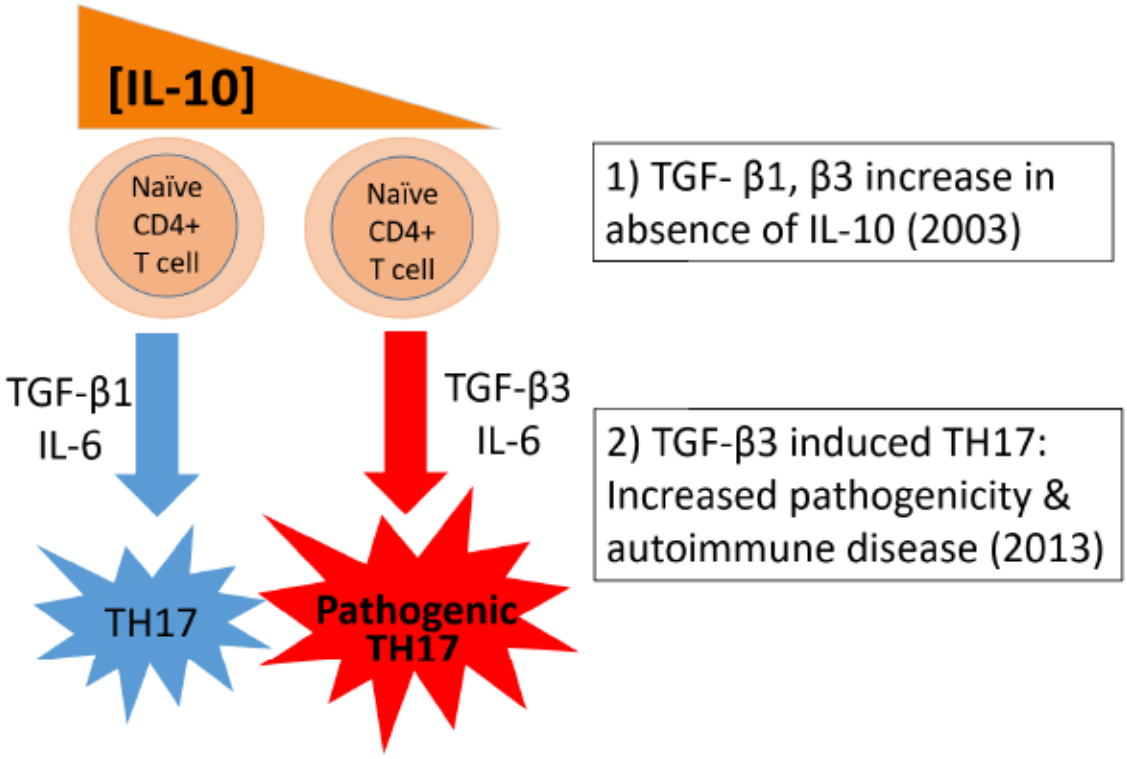

Source: Adapted by Martin, NM from [80]

Summary of evidence to support the hypothesis that, in the absence of IL-10, TGFβ will be upregulated. TGFβ3, and not TGFβ1, is hypothesized to induce pathogenic TH17 cells.

Figure 1.9.11 Hypothesis

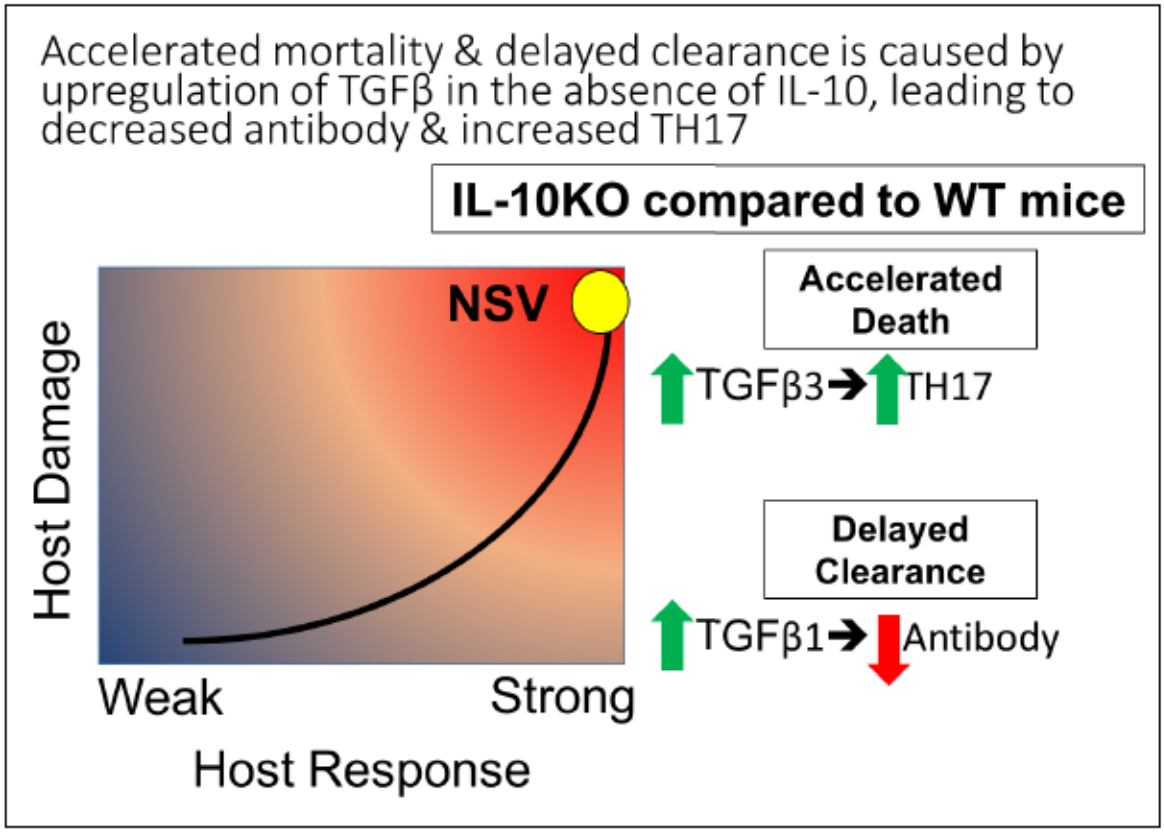

The graph to the left depicts the Host-Microbe Damage Response Framework, adapted from Casadevall and Petrovski, 2003. This framework states that microbial pathogenesis is caused by the interaction between the host and the microbe. Disease is when the damage from the microbe-host interaction exceeds a threshold. The damage can be caused by the microbe itself or the host's immune response. Adapting this framework to alphaviral encephalomyelitis, NSV-infection induces a strong host immune response and damage to host and death is caused by both damaging inflammatory responses in the CNS and viral replication. In the absence of IL-10, there is more damage inflicted to the host thus a more rapid course of morbidity and mortality. We hypothesize that in the absence of IL-10, TGFβ is upregulated. In a concentration dependent manner, TGFβ increases differentiation of TH17, suppresses TH1-related responses, suppresses Tregs, and decreases antibody and B cell responses. NSV infection induces a high amount of TGFβ1 post infection, TE12 induces an intermediate amount, and TE induces the lowest concentration. Increased TGFβ3 leads to pathogenic TH17 cell differentiation and accelerated mortality. Increased TGFβ1 leads to suppressed B cell and antibody responses.

CHAPTER 2

TGFβ Induction of Type 17 Responses and Suppression of Antibody in IL-10 Deficient Mice During Fatal Alphavirus Encephalomyelitis

Nina M. Martin[1] and Diane E. Griffin[1]

[1]W. Harry Feinstone Department of Molecular Microbiology and Immunology, Johns Hopkins Bloomberg School of Public Health, Baltimore, MD, 21205

ABSTRACT:

Sindbis virus (SINV) causes viral encephalitis in mice, with different SINV strains leading to varying degrees of morbidity and mortality. During infection with the fatal NSV strain, previous work showed that the cytokine IL-10 is an important modulator of IL-17 and TH17, whereas TH1-associated pro-inflammatory cytokines like IFNγ and TNFα were decreased in mice lacking IL-10. We examined the role of another regulatory cytokine, TGFβ, and showed that it was up-regulated in the absence of IL-10 and performed similar, yet divergent roles to IL-10 in the CNS. Mice lacking IL-10 infected with NSV had higher levels of TGFβ1 and TGFβ3 proteins, more production of TGFβ by T cells and innate lymphoid cells, lower levels of surface molecules that prevent cleavage of pro-TGFβ, and more activation of TGFβ down-stream SMAD effector molecules than NSV-infected WT mice. These differences were associated with more IL-17 production by ILC3s and more RORγt, PCKα, STAT3 and IL-17R expression by IL10KO mice. These results taken together show that TGFβ is an important compensatory mechanism in the absence of IL-10. Increased levels of TGFβ leads to suppression of inflammation but also increased IL-17 related responses with increased immunopathogenicity and higher fatality rates as well as delayed viral clearance.

2.1 INTRODUCTION

Viral encephalitis is life-threatening and an important cause of long-term disability worldwide, yet the mechanisms of neurocognitive damage remain poorly understood [105], making development of therapeutic intervention difficult. Many encephalitic viruses are arthropod-borne including the flaviviruses (e.g. West Nile virus and Japanese encephalitis virus) and the alphaviruses (e.g. Eastern Equine Encephalitis and Venezuelan Equine Encephalitis) [105]. Venezuelan equine encephalitis (VEE) and eastern equine encephalitis (EEE) viruses are important causes of seasonal disease in the Americas. EEEV has a mortality rate of about 35% and almost all survivors are left with neurological sequelae [3]. A recent outbreak of VEEV in Colombia and Venezuela resulted in an estimated 75,000 to 100,000 cases [106-108]. As the emergence and spread of these neurotropic viruses increases, the need to understand the mechanisms responsible for severe and fatal infections becomes more critical in order to develop effective interventions.

Sindbis virus (SINV) is the prototypic alphavirus [109] and although disease in humans is usually mild, the disease in mice parallels viral-induced encephalitis as seen in patients infected with EEEV or VEEV. Outcomes in mice to SINV are strain- and age-dependent and virus strains differ in virulence [10, 12, 19, 109-111]. A neuroadapted strain (NSV) causes lethal encephalitis in 4-6 week old C57Bl/6 mice.

T cells are implicated as sources of immunopathology, although the mechanism remains unclear [112, 113]. It has also been accepted that antibody to the E2 structural glycoprotein and production of IFNγ are necessary for noncytolytic viral clearance and survival [30, 33, 36, 39, 42, 45, 114].

Because of their putative role in immunopathogenesis, understanding how T cells are regulated is important. IL-10 is a Type II cytokine that suppresses helper T cells type I and type 17, dendritic cells, macrophages, and natural killer cells. Not only are these cells important for efficient viral clearance, but they can also contribute to immune pathology [115-117]. IL-10 also down modulates MHC Class II, rendering cells unable to present antigen, and suppresses production of pro-inflammatory cytokines and chemokines [47]. In models of gastrointestinal disease, mice lacking IL-10 develop spontaneous colitis due to a robust inflammatory response to commensal organisms that includes IFNγ [49, 118, 119]. In addition to regulating T cell function, Il-10 also has an impact on B cell development. IL-10 induces isotype switching from IgM to IgG by naïve human B lymphocytes [120] and up-regulates MHC Class II on B cells [121].

IL-10 is an important regulator of the immune response during SINV infection. In the absence of IL-10, adult, NSV-infected B6 mice display accelerated morbidity and mortality and a selective increase in pathogenic TH17 cells and neutrophils and the transcription of the genes encoding IL-17 and GM-CSF [15], but not of other pro-inflammatory cytokines such as IFNγ, TNFα, IL-12, and IL-1β. Levels of these mRNA transcripts were lower in the CNS of mice lacking IL-10 compared to WT mice. The results were surprising as it was expected that a general increase in inflammation would be observed in the absence of IL-10, as observed in models of colitis.

Viral clearance was delayed in IL-10KO animals, while peak titers remained the same. As mentioned previously, clearance of SINV from neurons is dependent on the combined effects of antibody to the E2 surface glycoprotein produced by B cells and IFNγ produced by T cells entering the CNS in response to infection. Taking the data

together, it appeared that another factor was functioning in the place of IL-10 to suppress these pro-inflammatory cytokines (IFNγ, TNFα, IL-1β, IL-12b) but also to promote TH17 responses.

A candidate factor is transforming growth factor beta (TGFβ), which has overlapping suppressive functions with those of IL-10 and has been reported to suppress production of IFNγ, TNFα, and other pro-inflammatory cytokines [122, 123]. TGFβ also induces the differentiation of either TH17 or regulatory T cells, depending on the conditions. For example, at lower doses, TGFβ can induce naïve helper T cells to become regulatory T cells whereas at higher doses, TH17 cells can be induced [75]. Moreover, this multifunctional activity depends on the cocktail of other cytokines present. For instance, TGFβ and IL-6 cooperate to drive towards TH17 differentiation [124, 125]. Finally, IL-10 activates B cell responses, while TGFβ suppresses B cell activation, maturation, and antibody production. For instance, TGFβ induced regulatory T cells suppress B cells in a noncytolytic manner [126]

Activation of the TGFβ pathway can be difficult to assess as TGFβ levels are regulated post-transcriptionally. It is produced in a pro-form that must be cleaved to be activated (Figure 2.5.1). It is tethered to the surface of a cell in its pro-form via the latency-associated peptide (LAP) and the surface glycoprotein, glycoprotein A repetitions predominant (GARP), until all are cleaved by proteolytic enzymes or environmental conditions like pH to release active TGFβ. TGFβ binding to its cognate receptors, TGFbRI and TGFbRII, activates a signal transduction pathway that results in phosphorylation of SMAD2/3. Phospho-SMAD2/3 up-regulates immune response genes like IL-17, while suppressing other inflammatory genes like IFNγ, TNFα, and IL-12. This

pathway also inhibits MHC Class II expression on B cells and blocks the production of antibody. Thus TGFβ has overlapping suppressive functions with IL-10, but it differs in that it promotes TH17 cell differentiation and suppresses B cell activation.

It has been reported that in the absence of IL-10, TGFβ will compensate and lead to worse clinical outcomes [80]. For example, Lee et al. observed that increased TGFβ leads to the development of pathogenic TH17 cells that were key to inducing autoimmunity [127]. The isoform of TGFβ may also influence TH17 cell function. Though still controversial, some studies have shown that TGFβ3, but not TGFβ1 induces pathogenic TH17 cells leading to autoimmunity [80].

To determine the role of TGFβ in the response to NSV infection, we have analyzed the immune response in the CNS of IL-10KO mice in comparison to WT mice and show that an elevated TGFβ pathway activation leads to accelerated mortality and morbidity via increased IL-17 related responses.

2.2 MATERIALS AND METHODS

2.2.1 Animals and Infection

The NSV strain of SINV was grown and assayed by plaque formation in BHK-21 ells and administered intranasally at 10^5 pfu in PBS. C57BL/6J WT and B6.129P2-Il10tm1Cgn/J (C57BL/6J IL10KO mice were purchased from Jackson Laboratories (Bar Harbor, ME) and bred in house. All mice were sex and age (4-6 weeks-old) matched. Morbidity and mortality was scored as previously described in [15]. Briefly, the scoring system was: 0, no signs of disease; 1, abnormal hind-limb and tail posture, ruffled fur, and/or hunched back; 2, unilateral hind-limb paralysis; 3, bilateral hind-limb paralysis or full-body paralysis; 4, dead. For collection of cervical lymph nodes, brain, or spinal cords, mice were anesthetized with isoflurane, perfused with ice-cold PBS, and tissues collected were used fresh or snap frozen and stored at −80 °C. All experiments were performed according to guidelines approved by the Johns Hopkins University Institutional Animal Care and Use Committee.

2.2.2 Virus Assays

20% weight per volume homogenates of brain and spinal cord tissues were made in PBS and clarified by centrifugation. Infectious virus was assayed by plaque formation on BHK-21 cells. Data are plotted as the mean of the $\log_{10}$ value of plaque forming units (pfu) ± SEM. For statistical analysis, samples in which no virus was detected at a 1:10 dilution were assigned a value halfway between zero and the limit of detection.

2.2.3 EIA

Enzyme immunoassays (EIA) were performed to measure SINV-specific antibody: 96-well Maxisorp plates (Nalgene Nunc) were coated with 10^6 PFU/well of polyethylene glycol (PEG)-precipitated NSV in 50 mM $NaHCO_3$ (pH 9.6) at 4°C overnight. Blocking buffer (10% FBS and 0.05% Tween 20 in PBS) was added for 2 hours at 37°C. Brain homogenates (10%, wt/vol) diluted 1:2 in blocking buffer were incubated at 4°C overnight. Bound antibodies were detected using HRP-conjugated goat anti-mouse IgM or IgG (Southern Biotech) diluted 1:1,000 in blocking buffer and incubated at room temperature for 2 hours. Plates were developed using the BD OptEIA TMB Substrate Reagent kit with H_2SO_4 as a stop solution. Absorbance was read at 450 nm. Average optical density (OD) values for brains from uninfected mice were subtracted from the OD values of brains from infected mice.

Active TGFβ1 and TGFβ3 levels (TGFβ homodimers that were not bound to LAP or GARP) were measured by EIA (R & D Systems ELISA [enzyme-linked immunosorbent assay] kits) according to the manufacturer's instructions. Brain homogenates (10%, wt/vol) were tested in duplicate.

2.2.4 Mononuclear Cell Isolation

Mononuclear cells were isolated from brains and cervical lymph nodes collected from 10 WT or IL10KO mice at 7 and 10 (unless otherwise noted) days post-infection. Cervical lymph nodes were pooled from 10 mice per group in 10 mL of RPMI+1% FBS and homogenized in C tubes using the GentleMACS system (Miltenyi) spleen program 1 for two cycles. Brain tissue was collected from 10 mice per group in ice cold HBSS.

After tissue collection, two brains were pooled per C tube containing 4 mL of enzyme digest mix made up of RPMI + 1% FBS, 1 mg/mL collagenase (Roche), and 0.1 mg/mL DNase (Roche) and dissociated with scissors. Further dissociation was performed via GentleMACS (Miltenyi) brain program 3 (total of 5x with 2, 15 minute 37°C incubations with gentle rocking). All suspensions were filtered through 70 µm cell strainers and centrifuged. Red blood cells were lysed using 2 mL of red blood cell lysis buffer (Sigma #R-7757) for 3 minutes and then washed with PBS.

To remove debris, pellets were suspended in 30% percoll, underlayed with 70% percoll for a 30/70% gradient and centrifuged for 30 minutes at 850xg at 4°C. The top debris layer was aspirated off and mononuclear cells at the interface were collected and washed with PBS + 2 mM EDTA. Pellets were suspended in PBS + 2 mM EDTA and live cells were counted using trypan blue exclusion.

2.2.5 Flow Cytometry

Approximately 1×10^6 cells were stained with the violet Live/Dead Fixable Cell Stain Kit (Invitrogen) in PBS + 2 mM EDTA, blocked with rat anti-mouse CD16/CD32 (BD Pharmingen), diluted in PBS + 2 mM EDTA + 0.5% BSA, surface-stained for 30 minutes on ice, fixed, and suspended in FACS buffer. All antibodies were from BD Pharmingen or eBioscience: CD45-FITC, CD3-APC, CD4-PerCP-Cy5.5, GARP-PE, Lineage-FITC, IL-7Ra-PE Cy7, CD19-PerCPCy5.5, IgM-FITC, CD5-APC, CD1d-PECy7. Cell types were defined as follows: T cells (CD45+CD3+), CD4 T cells (CD45+CD3+CD4+), ILC (Lin^- IL-7Ra+), B cells (CD19+), regulatory B cells (CD19+CD5+$CD1d^{hi}$IgM+).

2.2.6 Transcription factor staining via flow cytometry.

For determination of T cell differentiation, transcription factors were assayed using Foxp3 Buffer Set (eBiosciences). After surface staining, cells were fixed, permeablized, and stained for RORγt or GATA3. Cells were defined as follows: ILC3 (LIN-, IL-7Ra+RORγt+), ILC2 (LIN-, IL-7Ra+, GATA3+), TH2 (CD45+, CD3+, CD4+, GATA3+).

2.2.7 Intracellular cytokine staining via flow cytometry.

To determine cytokine production by T cells, B cells, and ILCs, 2–3 × 10^6 cells were stimulated in RPMI + 1% FBS containing 50 ng/mL of phorbol-12-myristate 13-acetate (PMA) and 1 μg/mL ionomycin in the presence of GolgiPlug-brefeldin A (BD Pharmingen) for 4 hours. After surface staining, cells were fixed and permeabilized using either the CytoFix/CytoPerm kit (BD Pharmingen). Intracellular markers were stained for 30 minutes on ice and suspended in 500 μL of FACS Buffer. All antibodies were from BD Pharmingen or eBioscience: IL-4-PE, IL-17-PE, LAP-PE, TGFb1-PE, TGFb3-Biotin, anti-Biotin-PE. Data were acquired with a BD FACS Canto II using FACS Diva software (version 6.0) and analyzed using FlowJo version 10.3.0.

2.2.8 Measurement of SMAD2/3 phosphorylation via flow cytometry.

To determine the activation of SMAD2/3 within T cells, ILC3, and B cells, PhosphoFlow (BD) was performed. 2–3 × 10^6 cells were stimulated in RPMI + 1% FBS containing 50 ng/mL of phorbol-12-myristate 13-acetate (PMA) and 1 μg/mL ionomycin

in the presence of GolgiPlug-brefeldin A (BD Pharmingen) for 4 hours. After surface staining, cells were fixed and permeabilized using the PhosphoFlow kit (BD Pharmingen). Cells were stained p-SMAD2/3 for 30 minutes at 4°C and suspended in FAC Buffer. Data were acquired with a BD FACS Canto II flow cytometer using FACS Diva software (version 6.0) and analyzed using FlowJo (v 10.3.0.).

2.2.9 Gene Expression Analysis Using Real-Time PCR

RNA was isolated from frozen tissue using the RNeasy Lipid Mini RNA Isolation Kit (Qiagen). RNA was quantified using a nanodrop spectrophotometer, and cDNA was prepared with the High Capacity cDNA Reverse Transcription Kit (Life Technologies) using 0.5–2.5 µg RNA. Quantitative real-time PCR was performed using 2.5 µL cDNA, TaqMan gene expression arrays (pkca, tgfb1, tgfb3, smad2, smad3), and 2× Universal PCR Mastermix (Applied Biosystems). Gapdh mRNA levels were determined using the rodent primer and probe set (Applied Biosystems). All reactions were run on the Applied Biosystems 7500 real-time PCR machine with the following conditions: 50°C for 2 minutes, 95°C for 10 minutes, 95°C for 15 seconds, and 60°C for 1 minute for 50 cycles. Transcript levels were determined by normalizing the target gene Ct value to the Ct value of Gapdh. This normalized value was used to calculate the fold change relative to the average of the uninfected control (ΔΔCt method).

2.2.10 Statistical Analysis

Data from two to four independent experiments with 6-10 mice per group were used. Differences between groups during the course of infection were determined using

two-way ANOVA employing Bonferroni posttests. Differences between groups at a single time point were determined using an unpaired, two-tailed Student t test with a 95% confidence interval. All statistical analyses were calculated in GraphPad Prism 5 (v5.01).

2.3 RESULTS

2.3.1 IL-10 deficiency leads to increased TGF-beta 1 and 3 protein

To determine if IL-10 deficiency leads to changes in mRNA expression of TGFβ1 or TGFβ3, we performed RT-qPCR on RNA isolated from brains of WT or IL10KO mice infected with NSV. On day 5 post-infection, there was a significant increase in mRNA transcripts of TGFβ1 but not TGFβ3 (Figure 2.5.2 A & B).

Protein levels of TGFβ1 & TGFβ3 were next quantitated to determine if IL-10 deficiency altered the response. Brains from IL10KO mice had significantly higher amounts of active TGFβ1 protein (greatest difference at 7 days post-infection in brain, 75.70 versus 2,272 pg/mL, $p < .001$) & TGFβ3 protein (greatest difference at 5days post-infection, 33.89 versus 134.8 pg/mL, $p < .001$) (Figure 2.5.2 C, E). Spinal cords from IL-10 deficient mice also had more active TGFβ1 and TGFβ3 compared to WT mice. TGFβ1 was increased on day 7 and TGFβ3 was increased on both days 5 and 7 post-infection (Figure 2.5.2 D, F). Increases in TGFβ1 and TGFβ3 protein levels in brains were also confirmed via Western Blot (Figure 2.5.2 G).

2.3.2 IL-10 deficiency leads to increased TGFβ production by Innate Lymphoid Cells Type 3

To determine which cell types were producing TGFβ, first we analyzed innate lymphoid type 3 cells (ILC3) because higher levels of TGFβ1 and TGFβ3 protein were observed as early as day 3 post-infection. Production of TGFβ1 post-NSV infection was

measured via intracellular cytokine staining and flow cytometry (Figure 2.5.3). On day 3 post-infection, there was a higher percent of cells producing TGFβ1, but not number (Figure 2.5.3, B). Day 5 post-infection, there was a significantly higher number and percent of ILC3's producing TGFβ1 (Figure 2.5.3, B). There were no differences in the percent or the number of ILC3s in CLN (Figure 2.5.3, C).

2.3.3 IL-10 deficiency leads to increased TGFβ production by T cells

T cells are major producers of TGFβ. To quantitate the number of T cells producing TGFβ1, intracellular cytokine staining and flow cytometry was performed on cells from the brains of WT and IL10KO mice. While the numbers of CD3+ T cells were similar, IL-10 deficient mice had higher numbers and percentages of CD3+ T cells producing TGFβ1 (Figure 2.5.4, B). To differentiate between the two major classes of T cells, we compared production of TGFβ by CD3+CD4+ helper T cells and CD3+CD8+ T cells. There were no differences in the numbers of either CD4+ or CD8+ T cells. However, a higher percentage of CD4+ T cells produced TGFβ1 in IL-10 deficient mice compared to WT (Figure 2.5.4, C, right). There were no significant differences in percent or number of CD8+ T cells producing TGFβ1 (Figure 2.5.4, D). There were no significant differences in TGFβ1-producing CD4+ or CD8+ T cells in CLNs. As reported previously in [15], IL-10 deficiency did not impact the recruitment of either CD4+ or CD8+ T cells into the CNS, but altered T cell differentiation and production of cytokines like TGFβ and IL-17.

2.3.4 IL-10 deficiency leads to changes in TGFβ-related surface proteins.

To evaluate TGFβ pathway activation, the proteins GARP and TGFβRII were quantified. Inactive, pro-TGFβ is tethered to the cell membrane by surface glycoprotein, GARP (Figure 2.5.1) before it can bind its receptor TGFβRII. GARP is cleaved when the TGFβ pathway is activated [128]. We quantitated the number and percent of GARP+ cells in brains and CLN via flow cytometry (Figure 2.5.5, A). Lymphocytes isolated from IL10KO mice had significantly fewer numbers of GARP+ cells. Taken together with the increased levels of TGFβ1 and TGFβ3 protein, this data supports the observation that more active TGFβ is being produced.

We next performed flow cytometry to assess the impact of IL-10 deficiency on TGFβRII expression by lymphocytes isolated from brains of WT or IL10KO mice (Figure 2.5.6). Cerebral lymphocytes from IL-10KO mice had higher numbers and percentages of live cells that express TGFβRII compared to WT controls on both day 3 and 5 post-infection (Figure 2.5.6, A). There were no significant differences in numbers or percentages of TGFβRII-positive cells in CLN (Figure 2.5.6, B).

These data taken together support the hypothesis that IL-10 deficiency leads to lower expression of inactive TGFβ pathway components compared to WT, i.e. GARP, and potentially higher pathway activation via TGFβRII. Next, we determined if the downstream TGFβ effector molecules were also impacted by IL-10 deficiency.

2.3.5 IL-10 deficiency leads to increased mRNA transcripts, phosphorylation, and ultimately activation of SMAD2/3.

To study the activation of the TGFβ pathway, we measured TGFβ's signal transduction molecultes, SMAD2 and SMAD3. Upon binding of TGFβ to its receptors, SMAD2 and SMAD3 are phosphorylated and are therefore considered direct indicators of TGFβ pathway activation. First, via qPCR, we quantitated relative SMAD2 & SMAD3 mRNA expression 7 days post-infection since this is the peak of T cell number and activation in the CNS post-NSV infection (Figure 2.5.7, A). SMAD2 and SMAD3 mRNA expression was increased in IL10KO brains (Smad2 mRNA ddCT values of 50.53 versus 70.56, $p < .001$; Smad3 mRNA ddCT values of 14.17 versus 18.38, $p < .05$) compared to brains from WT mice.

To determine the relative amounts of SMAD2/3 phosphorylation, we isolated and pooled lymphocytes from WT or IL10KO mice post-NSV infection (Figure 2.5.7, B-D). Following isolation, SMAD2/3 phosphorylation events in total cells were measured via PhosphoFlow, an application of flow cytometry to measure intracellular phosphorylation events. There was a greater number and percentage of live cells that were positive for phosphorylated SMAD2/3 in IL10KO mice compared to WT mice on day 3 post-NSV infection (Figure 2.5.7, B). There were no significant differences in percentages or numbers of phosphorylation events in cells isolated from CLN (Figure 2.5.7, C).

2.3.6 IL10 deficiency leads to decreased inhibitory SMAD7 protein.

To determine if the inhibitor of the TGFβ pathway, SMAD7, is altered in the absence of IL-10, we harvested six WT and IL10KO brains at different times post-NSV

infection, purified protein, and performed a Western Blot. Analysis showed that SMAD7 is down-regulated in IL10KO mouse brains on day 3, 5, and 7 post-NSV infection compared to WT mice (Figure 2.5.7, E). This result indicated that the pathway is likely less inhibited in mice lacking IL-10. These results taken together show that there is more active TGFβ protein being produced, there is less inhibition of the TGFβ pathways, and, indirectly at least, there is less pro-TGFβ due to the fact that there is less GARP.

2.3.7 IL10 deficiency and TGFβ up-regulation lead to increased Type 17 activity through increased PKCα, RORγt, STAT3, and IL-17R

TGFβ-dependent up-regulation of STAT3/IL-17 and suppression of pro-inflammatory cytokines are mediated via protein kinase C alpha (PKCα) [129]. At 7 days post-NSV infection, the peak of T cell activation in the CNS, IL10KO mice displayed elevated PKCα mRNA expression in brain compared to WT controls (ddCT values of 64.70 versus 71.62, $p < .05$) (Figure 2.5.8, A).

Next considered was another transcription factor important in the regulation of the IL-17, RORγt [79, 130]. Because RORγt's regulation of IL-17 is common to many cell types including T cells, neutrophils, and ILCs, RORγt expression was measured in total isolated lymphocytes from the CNS and CLN (Figure 2.5.8, B-E). Numbers and percentages of live lymphocytes positive for RORγt were higher in brains of IL10KO mice compared to WT (Figure 2.5.8, C). In CLN, there was a significantly higher percent and number of RORγt+ cells on day 5, but not day 3 post-infection (Figure 2.5.8, D).

The transcription factor STAT3 up-regulates IL-17a gene expression [124]. This can be activated via the TGFβ pathway [76, 129]. We measured the presence of STAT3 via western blot (Figure 2.5.8, E). IL10KO mice had higher levels of STAT3, even on day 0 — meaning that the baseline level is higher in the absence of IL-10.

Another downstream consequence of TGFβ activation is up-regulation of the receptor for IL-17, IL-17R. Employing immunostained Western Blots, we demonstrate that the protein levels of IL-17R (includes both IL17RA and IL17RC) are elevated in IL10KO mice compared to WT (Figure 2.5.8, F). Not only is there more IL-17 mRNA and protein as previously shown, but also an increase in expression of its cognate receptor in IL10KO mice compared to WT.

2.3.8 IL10 deficiency and TGFβ upregulation consequently leads to increased IL-17a producing ILC3s.

Previous studies [15] showed that *IL17a* mRNA was elevated in brains of IL10KO mice on day 3 post-NSV infection, proceeding T cell recruitment to the CNS. This study did not determined which cell type was an early producer of IL-17 (neutrophil depletion had no effect on disease outcomes). ILC3s are early producers of IL-17A [131-133]. To determine if IL-10 deficiency impacted IL-17A production by ILC3s, intracellular staining and flow cytometry was performed on lymphocytes isolated from brains and CLN (Figure 2.5.9, A). At both day 3 and 5 post-infection in brains, there were a higher percentage and number of ILC3 that produced IL-17A in IL-10 deficient mice (Figure 2.5.9, B). Also, the number and percentages of live cells that were ILC3s were increased in IL10KO mice compared to WT controls (data not shown). In CLN,

there were elevated numbers and percentages of IL-17A producing ILC3 cells in IL10KO mice on day 3, but not day 5 post-infection (Figure 2.5.9, C).

2.3.9 IL-10 deficiency impairs ILC2 recruitment to the CNS

Innate lymphoid cells type 2 were first described in 2010 as a small, but potent regulator of type 2 immune responses, similar to function of helper T cells type 2 (TH2) [134]. These are early responders to infection and activators of the B cell response via direct activation and inhibition of helper T cells as well as release of IL-5 and IL-13. Studies in the CNS are limited to date, but a protective role in EAE/MS and cerebral malaria for ILC2's have been implicated [135-138]. To study the impact of IL-10 deficiency on ILC2 recruitment, flow cytometry was performed on lymphocytes isolated from the brain and CLN post-NSV infection (Figure 2.5.10, A and B). There were lower percentages of ILC2s (Lineage-IL-7Ra+GATA3+ cells) in brain on both day 3 and 5 post-infection (Figure 2.5.11, B). The numbers of cells were significantly higher on day 5, but not 3 post-infection. Similar percentages and numbers of ILC2s were present in CLN as in the brain with lower numbers and percentages of ILC2s on both 3and 5 days post-infection (Figure 2.5.11, C).

2.3.10 IL-10 deficiency impairs ST2 expression on TH2 cells

Previous studies showed that IL-4 production by TH2 cells (CD4+ GATA3+ T cells) was not different in the brains of IL10KO compared to WT mice. Other markers may be more indicative of TH2 activation than production of IL-4. ST2 is a receptor found on ILC2s, TH2, and Treg cells that binds the alarmin IL-33. On Th2 cells, ST2 is

important for Th2 effector functions and is implicated in recruitment and activation of B cells and the antibody response [139-142]. To assess if ST2 expression on the surface of TH2 cells was altered in IL-10 deficient mice, we performed flow cytometry on lymphocytes isolated from brains and CLN post infection (Figure 2.5.12, A). ST2 was expressed at a lower level on fewer CD4+ T cells in IL-10 deficient mice compared to WT after NSV infection.

2.3.11 IL-10 deficiency impairs antibody production

To assess the impact of IL-10 deficiency on SINV-specific antibody production, EIA was used to measured antibody in the CNS in homogenates from pooled brains from six WT or IL10KO animals. Brains from IL-10-deficient mice had significantly less SINV-specific IgG1 and IgM on days 5 and 7 post-infection compared to WT mice (Figure 2.5.13, A & B). Virus-specific IgG2 and IgG4 levels were similar in the WT and IL10KO strains (data not shown).

2.3.12 IL-10 deficiency impairs CD19+ B cell recruitment

To test the impact of IL-10 deficiency on CD19+ B cell recruitment into the CNS during infection, flow cytometry was performed on lymphocytes isolated from brain and CLN (Figure 2.4.14, A). In the brain, the percentages of live cells that were CD19+ were higher in WT mice on days 3 and 7, but not day 5 post-infection compared to IL10KO mice (Figure 2.5.14, B). The numbers of CD19+ B cells in the brain were only significantly higher on day 7 post-infection. In CLN, CD19+ cells were more abundant in WT mice on days 3, 5 and 7 post-NSV infection compared to IL10KO mice. The

numbers of CD19+ cells were significantly higher only on days 5 and 7 post-infection (Figure 2.5.14, C). These results indicate that B cell generation in CLN as well as recruitment to the CNS is impaired by IL-10 deficiency.

2.3.13 IL-10 deficiency impairs regulatory B cell recruitment to the CNS

Regulatory B cells are important suppressors of inflammation as well as activators of B cells and regulatory T Cells with subpopulations that produce IL-10 and TGFβ. Both the number and percentage of regulatory B cells were lower in the brains of IL10KO mice at 3 and 5 days post-infection (Figure 2.5.15). These data, along with the aforementioned increased TGFβ production, show that IL10KO mice have fewer regulatory B cells but are producing more TGFβ and more phosphorylation of SMAD2/3.

2.4 DISCUSSION

Balance between inflammatory helper and regulatory T cells is crucial for survival from inflammatory diseases like viral encephalitis. In the center of this balance are IL-10 and TGFβ, two cytokines that govern inflammation and suppression. Understanding how these two cytokines work in partnership is key to understanding neuroprotection and clearance versus fatality. From EAE and other inflammatory disease models, it is known that TGFβ and IL-10 work in tandem to strike a balance between TH17 and regulatory T cells; changes in levels of TGF and IL-10 mRNA and protein can determine survival versus fatality [57, 143, 144]. Innate lymphoid cells type 3 have also been recently been reported to be important sources IL-17 and their dysregulation can lead to worse clinical outcomes [145]. Conversely, lack of ILC3's inhibits recruitment of helper T cells to the CNS during EAE [131]. The role of these cells and their modulation by IL-10 or TGFβ during viral encephalitis was previously unknown.

It has been reported that IL-10 is an important modulator of IL-17 and TH17 cells during fatal SINV infection, whereas pro-inflammatory cytokines like IFNγ and TNF were decreased in mice lacking IL-10 [15]. We report that another cytokine, TGFβ, is also up-regulated in the absence of IL-10 and that TGFβ performs similar, yet distinct roles from IL-10. We found that mice infected with NSV lacking IL-10 had increased TGFβ1 and TGFβ3 protein production, increased production of TGFβ by ILCs and T cells, decreased expression of surface molecules that prevent cleavage of pro-TGFβ, and increased activation of the TGFβ signal transduction pathway. These increases were associated with increased IL-17 production by ILC3s, increased RORγt, PCKα, and IL-

17R expression. These results taken together suggest an important compensatory mechanism for TGFβ in the absence of IL-10 that leads not only to a suppression of inflammation, but also to an increase in IL-17 related responses. These alterations lead to increased immunopathogenicity and higher fatality rates as well as delayed viral clearance.

Ongoing work considers that the mechanism of increased IL-17 response due to TGFβ may be concentration dependent. This is not a new hypothesis; *in vitro* and *in vivo* studies have shown that higher doses of TGFβ, in conjunction with other cytokines, induces TH17 cell differentiation whereas lower doses induce regulatory T cells [79, 127]. Current work demonstrates that virulent, intermediate virulent, and avirulent strains of SINV induce differing amounts of TGFβ. TGFβ has the lowest level of induction after non-fatal TE infection in WT and IL10KO mice, intermediate virulent TE12 induces a medium concentration and NSV infection induces the highest amount of TGFβ. These increasing doses of TGFβ are associated with different impacts on the IL-17 related response, the Th1 response, as well as the antibody response.

Understanding the interactions between IL-10 and TGFβ signaling is important for success of immunotherapies that target these cytokines. The results reported here have demonstrated that TGFβ likely represents a partially redundant cytokine that becomes regulated in a different way in the absence of IL-10.

2.5 FIGURES AND TABLES

Figure 2.5.1 The TGF-beta pathway

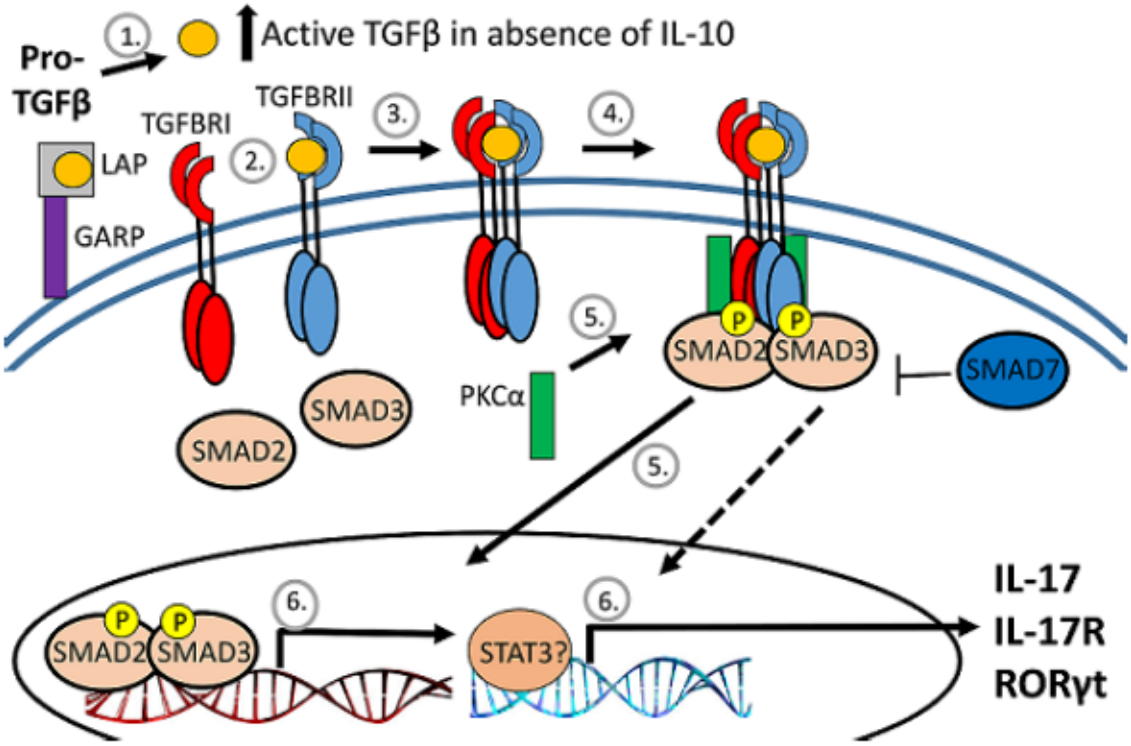

Activation of the TGFβ pathway. Inactive TGFβ is tethered to the surface of cells in its pro-form by LAP and GARP. Cleavage of the pro-form into its active form is triggered by proteases, changes in pH, or other protein interactions. Once cleaved, TGFβ binds to TGFbRII. This binding allows for the recruitment of TGFBR1, dimerization, and phosphorylation of intracellular kinase domains. This phosphorylation induces a signal transduction cascade and phosphorylation of downstream SMAD effectors. There are seven different SMAD proteins and the combination of proteins that are phosphorylated determines the cellular outcomes. Above is pictured the combination of SMAD2 and SMAD3 that when phosphorylated translocate into the nucleus and upregulates the expression of immune genes like IL-17. Conversely, SMAD7 typically acts as an inhibitor of the pathway.

Figure 2.5.2 TGFβ1 and TGFβ3 are elevated in IL-10 deficient mice

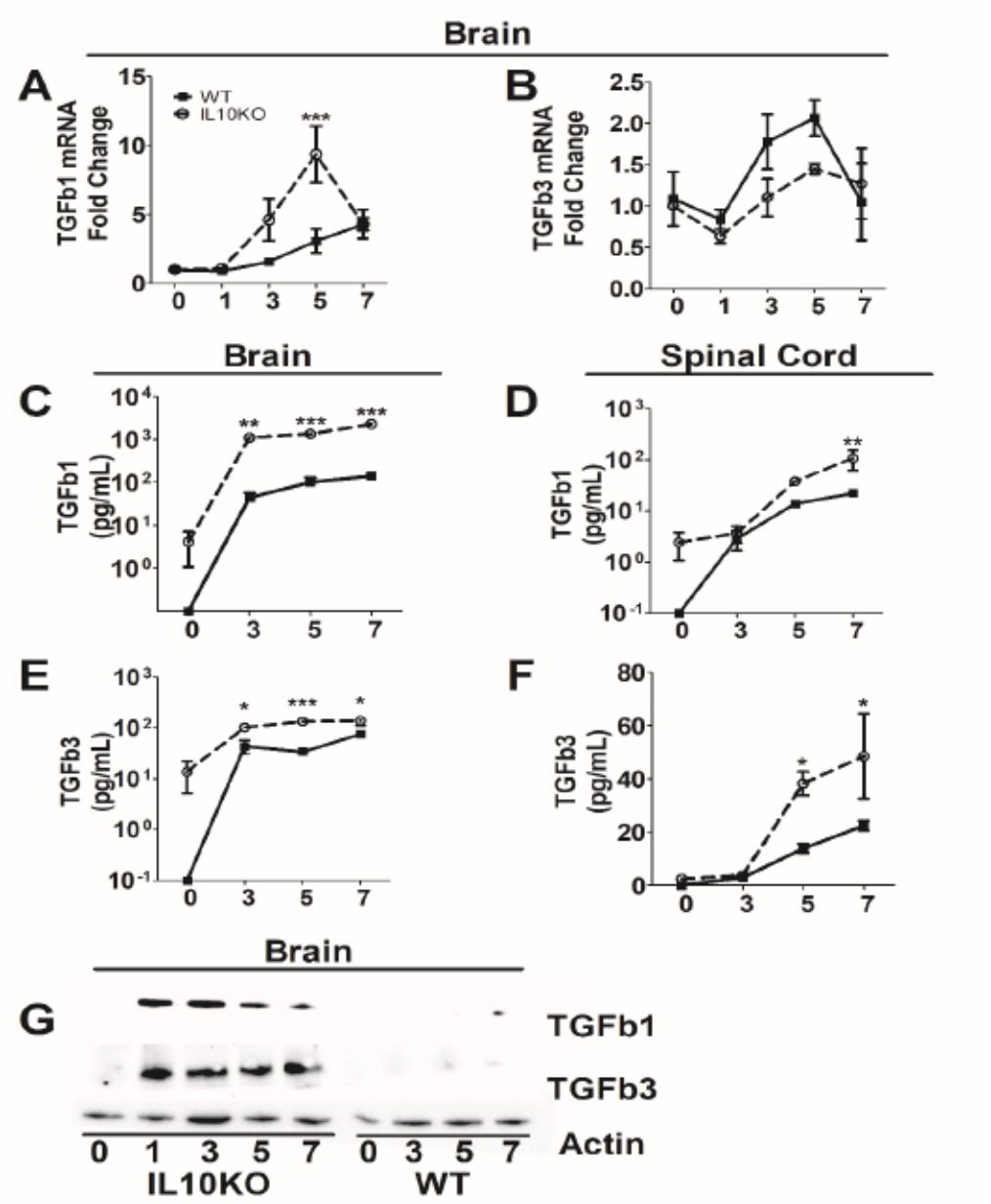

Analysis of TGFβ1 (A) and TGFβ3 (B) mRNAs in the brains of WT (filled square, solid line) and IL-10KO (open circle, dashed line) mice during NSV infection. Gene Ct values were normalized to GAPDH, and fold change was calculated relative to uninfected controls (ΔΔCt). Data are pooled from two independent experiments and presented as the mean ± SEM from 6 mice at each time point; ***$p < 0.001$. Protein levels of TGFβ1 and TGFβ3 were measured in brain (B & E) and spinal cord (C & F) tissues via EIA. Data were pooled from 2 independent experiments and represent the means ± SEM for 8 mice at each time point; *$p < 0.05$; **$p < .01$; ***$p < 0.001$. Secondary validation was performed via western blot in (G) which shows TGFβ1 and TGFβ3 protein in 5 pooled brain tissues per time point post NSV infection.

Figure 2.5.3 IL-10 deficiency leads to increased TGFβ production by ILC3s

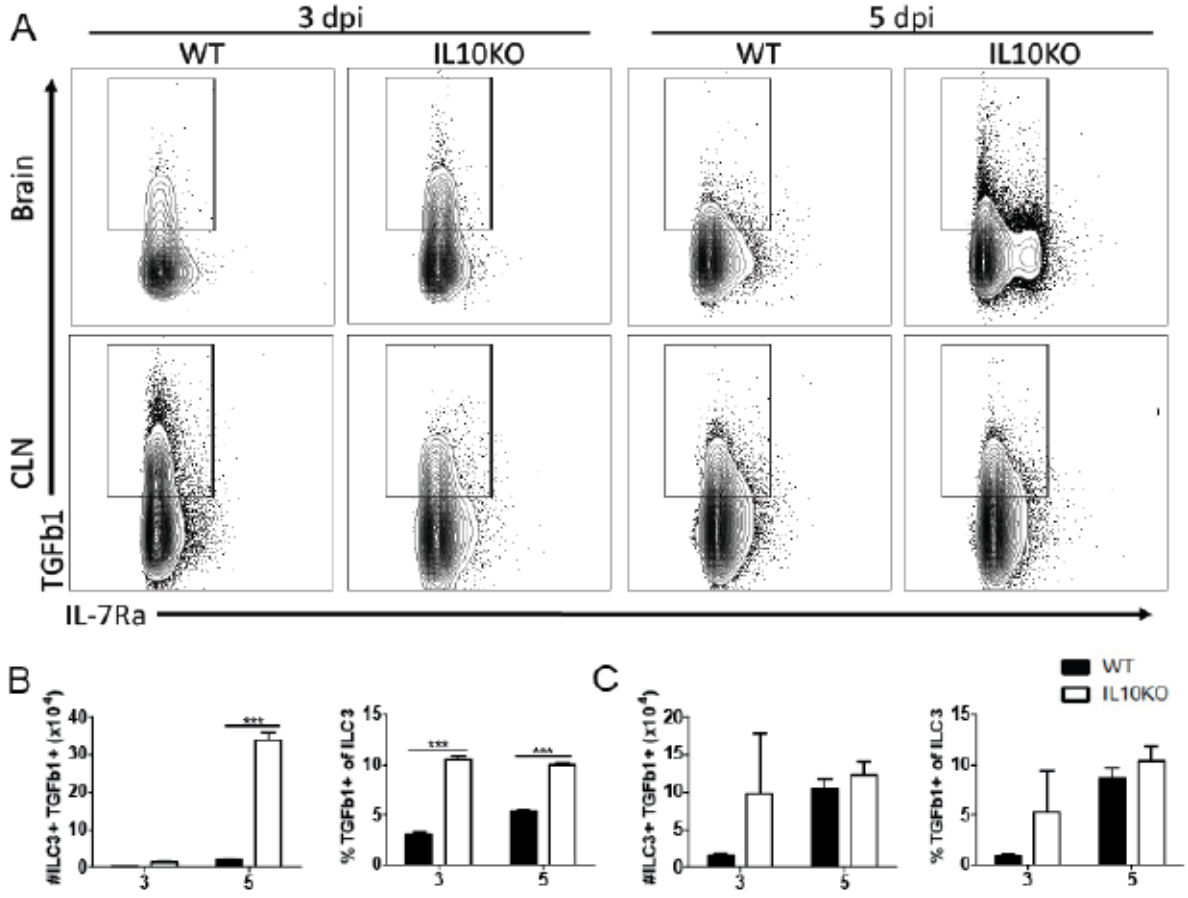

IL-10 deficiency increases TGFβ1 production by ILC3s. To assess the impact of IL-10 deficiency on TGFβ1 production by ILC3s, intracellular cytokine staining and flow cytometry were performed on brains and CLN from WT (black bars) or IL10KO (white bars) mice. Representative flow cytometry plots are shown in (A). ILC3s were identified as Lineage-IL-7Ra+RORgt+ cells. Percent and number of ILC3's producing TGFβ1 were measured in brain (B) and CLN (C). Bars represent mean ± SEM from 10 mice per group; ***p < .001.

Figure 2.5.4 IL-10 deficiency leads to increased TGFβ production by T cells

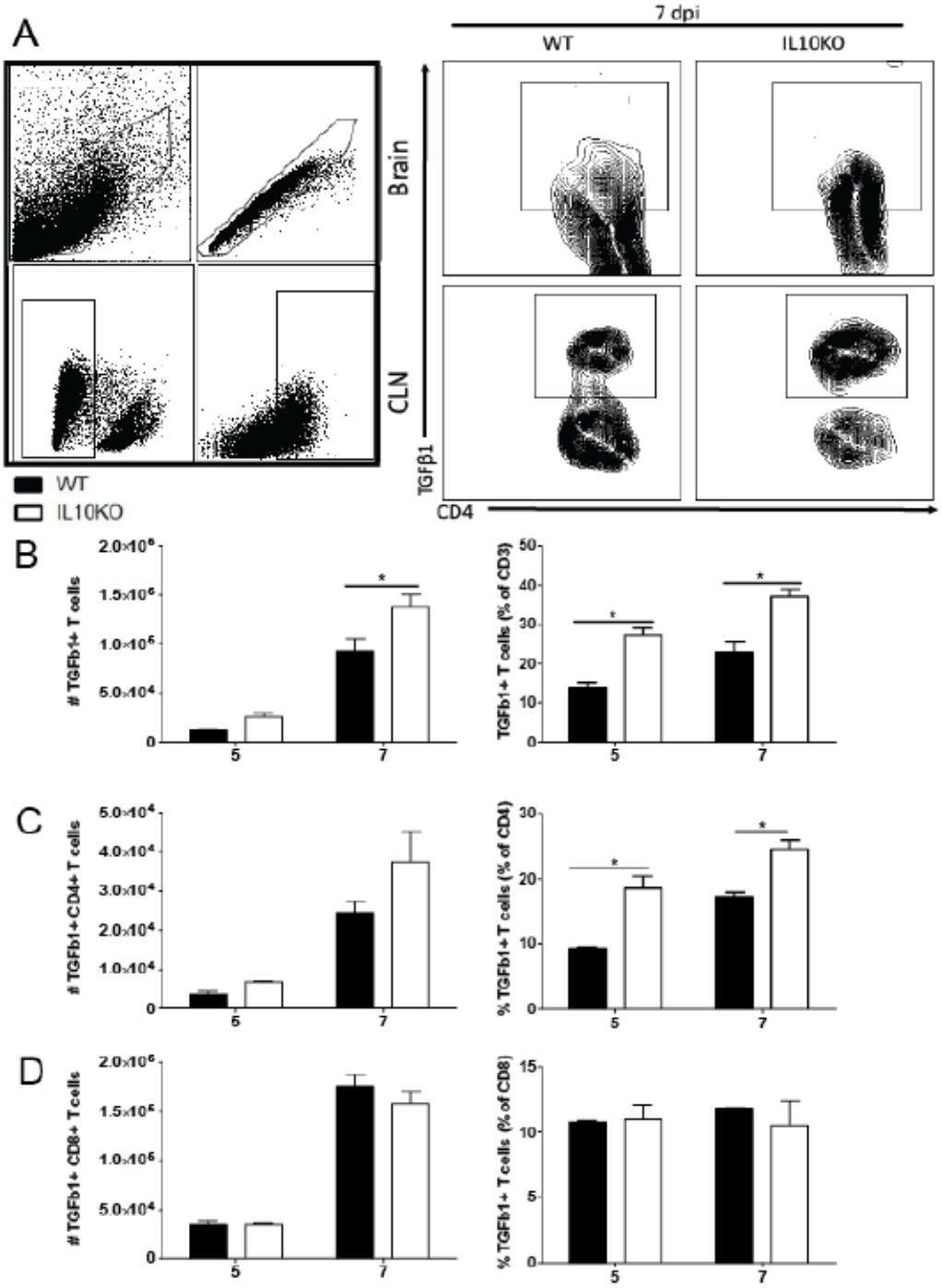

IL-10 deficiency alters production of TGFb1 by CD4+, but not CD8+ T cells. T cells were isolated from brains of WT (black bars) or IL10KO (white bars) mice. Representative flow cytometry plots are shown in (A). Total CD3+ T cell numbers were not different. (B) CD3+ T cells producing TGFβ1 in brains were measured as percent and number of live cells. (C) Helper T cells were measured in brains as a percent and number of CD3+ T cells. (D) CD8+ T cells were measured in brains as percent and number of CD3+ T cells. Bars represent mean ± SEM from 10 mice per group; *p < .05.

Figure 2.5.5 IL-10 deficiency leads to changes in TGFβ-pathway membrane proteins (GARP)

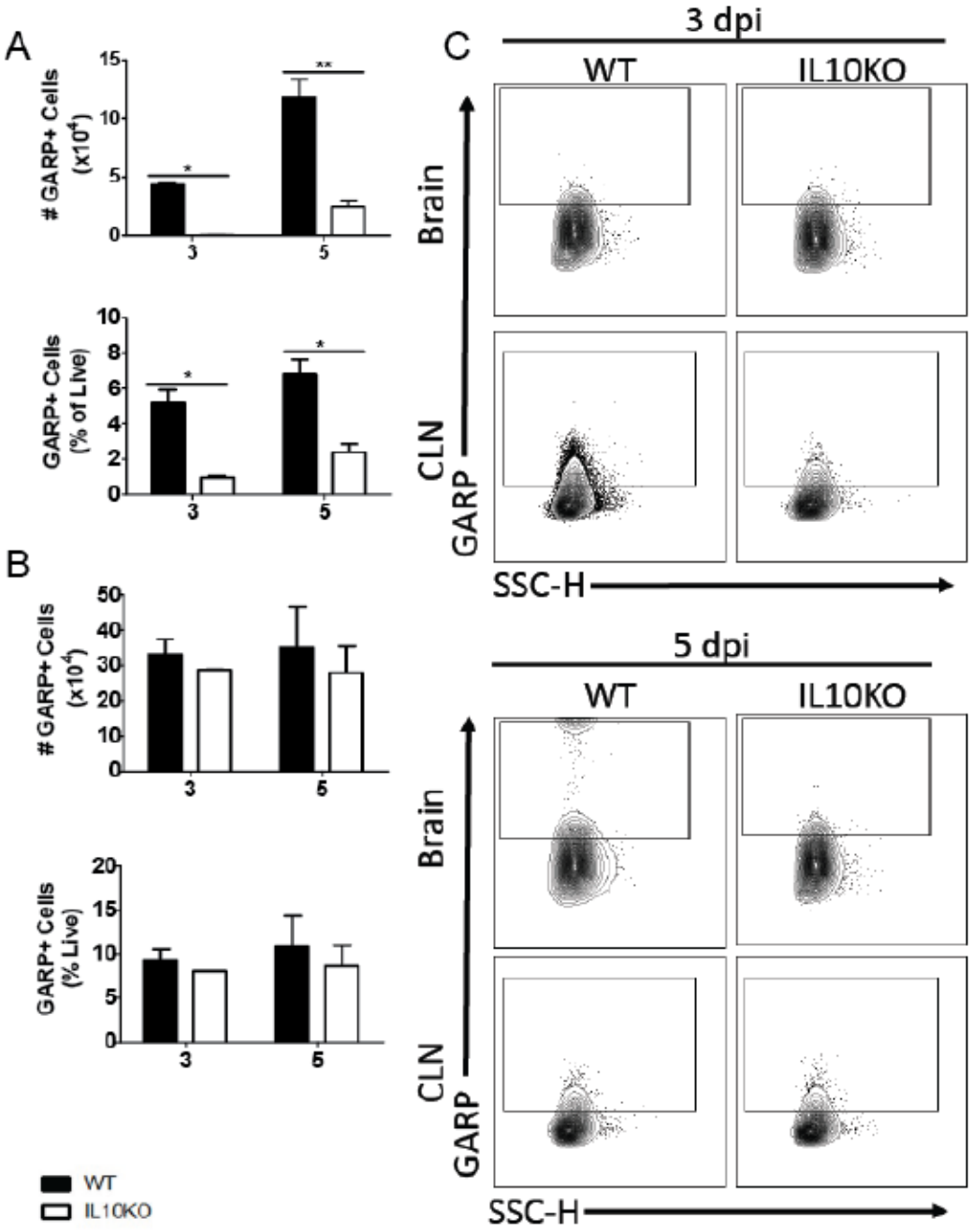

(A-C) Flow cytometric analysis of isolated cells pooled from the brains (n = 10) of WT (black bars) or IL10KO (white bars) mice at 5 and 7 days post infection. Total GARP+, cells were measured as percentage (A, left) and number (A, right). Helper T cells expressing GARP were measured as percentage (B, left) and number (B, right). CD8+ T cells expressing GARP, LAP, or TGFbRII were measured as percentage (C, left) and frequency (C, right). Representative flow cytometry plots are shown in (D). The data represent the mean ± SEM from three independent experiments; *p <.05, **p < .01.

Figure 2.5.6 IL-10 deficiency leads to changes in TGFβ-pathway membrane proteins (TGFbRII)

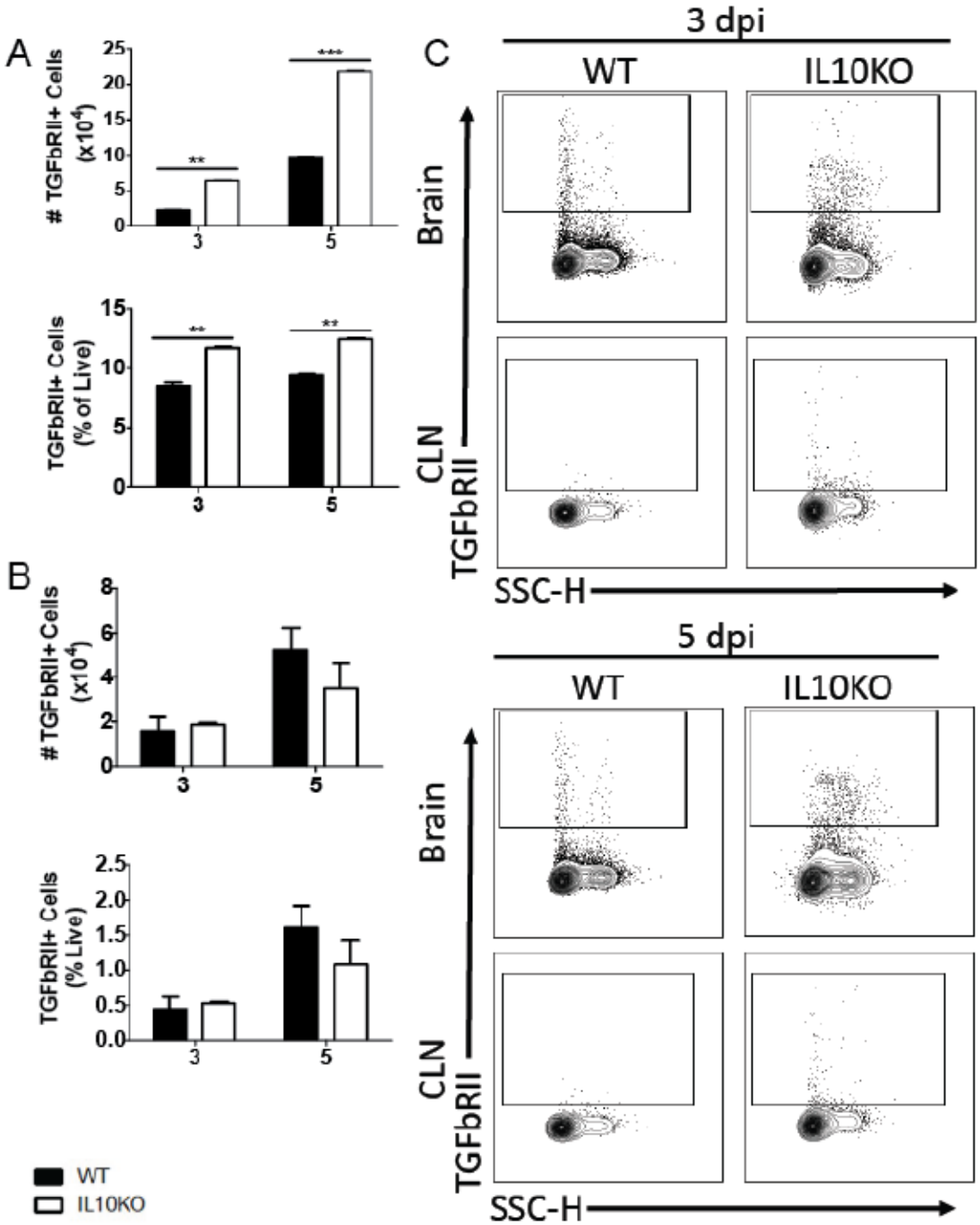

(A-C) Flow cytometric analysis of isolated cells pooled from the brains (n = 10) of WT (black bars) or IL10KO (white bars) mice at 3 and 5 days post infection. Total TGFbRII+ cells were measured as percentage and number in brains (A) and CLN (B). Representative flow cytometry plots are shown in (C). The data represent the mean ± SEM from three independent experiments; **p < .05, ***p < 0.001.

Figure 2.5.7 IL-10 deficiency leads to increased downstream TGFβ pathway effector activation (SMAD2/3, pSMAD2/3, SMAD4, SMAD7)

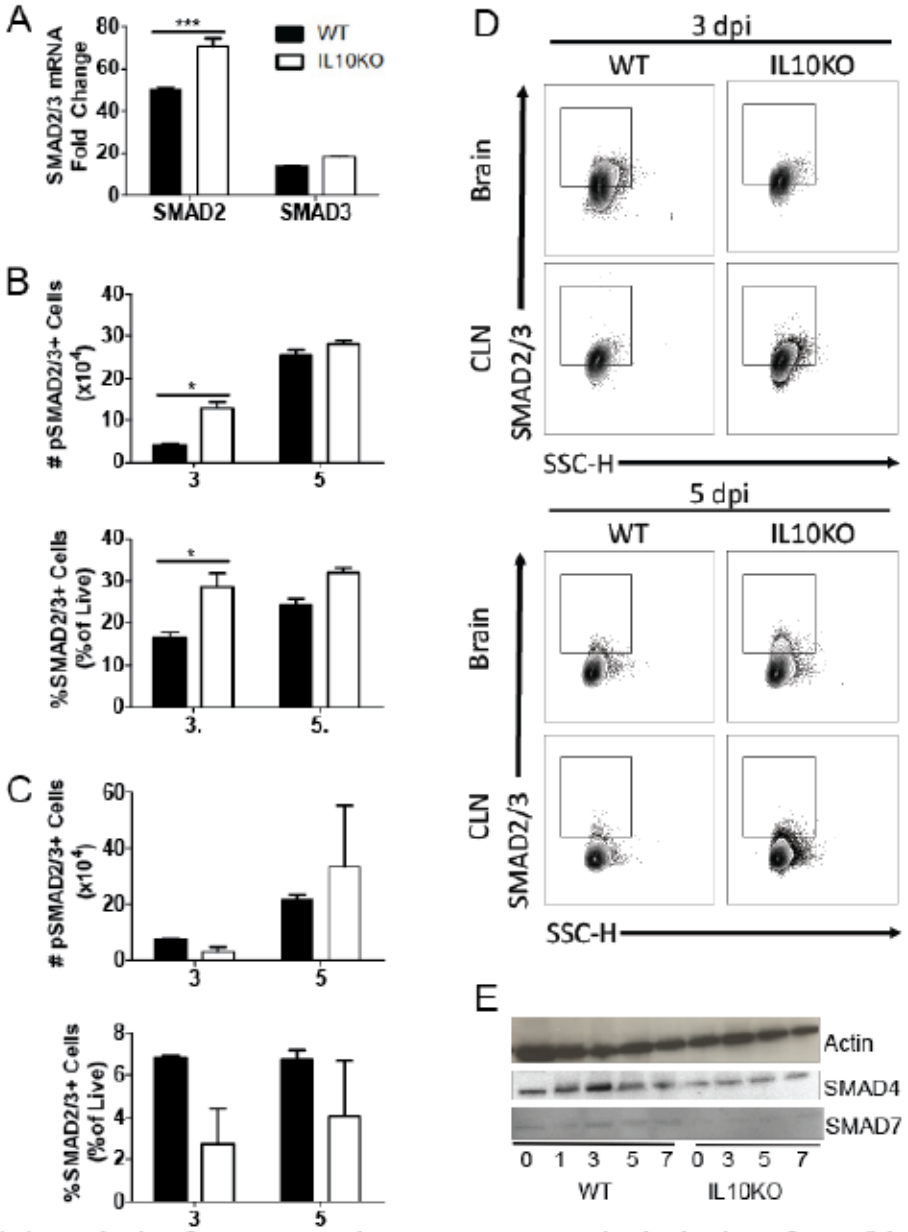

(A) Analysis of SMAD2 and SMAD3 mRNAs in the brains of WT (black bar) and IL-10KO (white bar) mice on day 7 post infection. Gene Ct values were normalized to GAPDH, and fold change was calculated relative to uninfected controls (ΔΔCt). Data are pooled from two independent experiments and presented as the mean ± SEM from 6 mice in each group; ***$p < 0.001$. Flow cytometric analysis of p-SMAD2/3 phosphorylation events in brains (B) and CLIN (C) as a number and percent of live cells. 10 mice per group were pooled. Experiment repeated 3x, representative plot shown. Data are presented as the mean ± SEM; *$p < 0.05$. (E) Western blot protein analysis of SMAD4, SMAD7 and actin in WT or IL10KO brains following NSV infection. Pooled 5 mice per time point.

Figure 2.5.8 IL-10 deficiency leads to changes in TGFβ/IL-17 related effectors

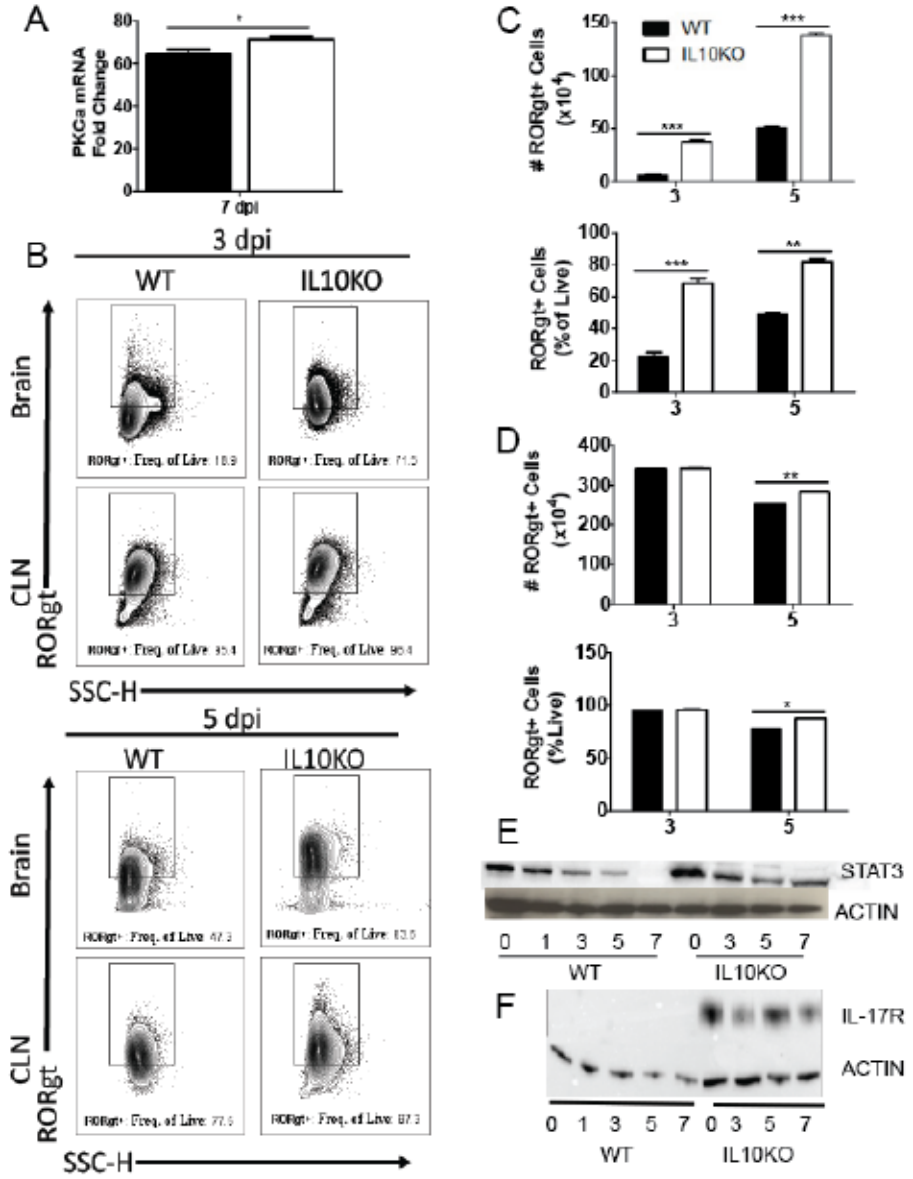

IL-17 related genes and proteins were altered in the absence of IL-10. (A) Analysis of PKCα mRNAs in the brains of WT (black bar) and IL-10KO (white bar) mice during NSV infection. Gene Ct values were normalized to GAPDH, and fold change was calculated relative to uninfected controls (ΔΔCt). Data are pooled from two independent experiments and presented as the mean ± SEM from 6 mice in each group; *$p < 0.05$. (B-D) Flow cytometric analysis of cells expressing RORgt in WT (black bars) and IL10KO (white bars) mice. Representative flow cytometry plots are shown in (B). Number and percent of live in brains (C) and CLN (D) were measured. Data are pooled from two independent experiments and presented as the mean ± SEM from 10 mice per time point; *$p < 0.05$, **$p < 0.01$, ***$p < 0.001$. Protein levels of STAT3 (E) and IL-17R (F) in brains of WT or IL10KO mice were measured via western blot. 5 mice per time point per group were pooled. Experiment repeated 3x, representative blots shown.

Figure 2.5.9 IL-10 deficiency leads to increased IL-17 production by ILC3s

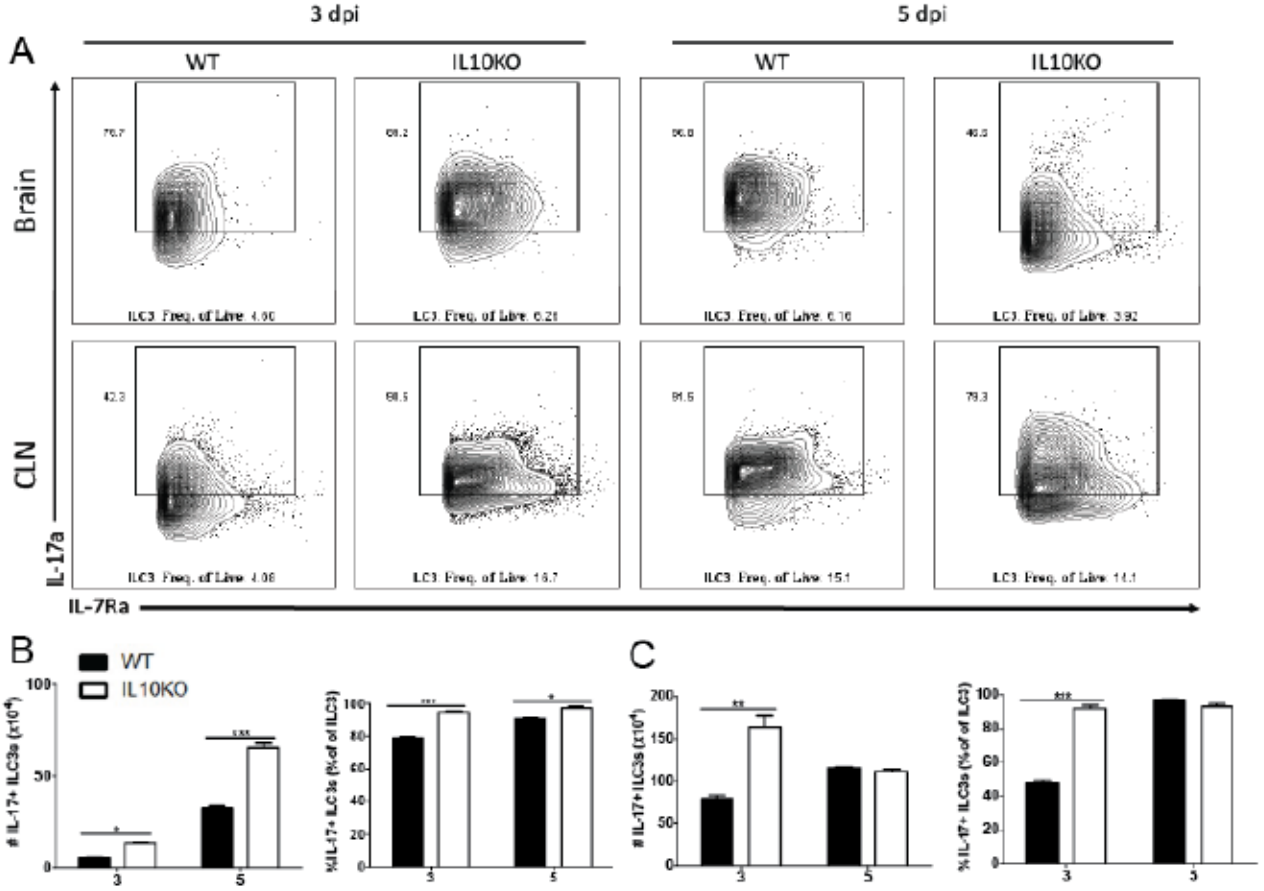

(A-C) Flow cytometric analysis of IL-17 production by ILC3s isolated and pooled from the brains and CLN (n = 10) of WT (black bars) or IL10KO (white bars) mice at 3 and 5 days post infection. Representative flow cytometry plots are shown in (A). IL-17 production in brains (B) and CLN (C) was measured as percentage and number of ILC3+ cells. The data represent the mean ± SEM from three independent experiments; *p < .05, **p < .01, ***p < 0.001.

Figure 2.5.10 Example of ILC2 flow cytometry gating strategy

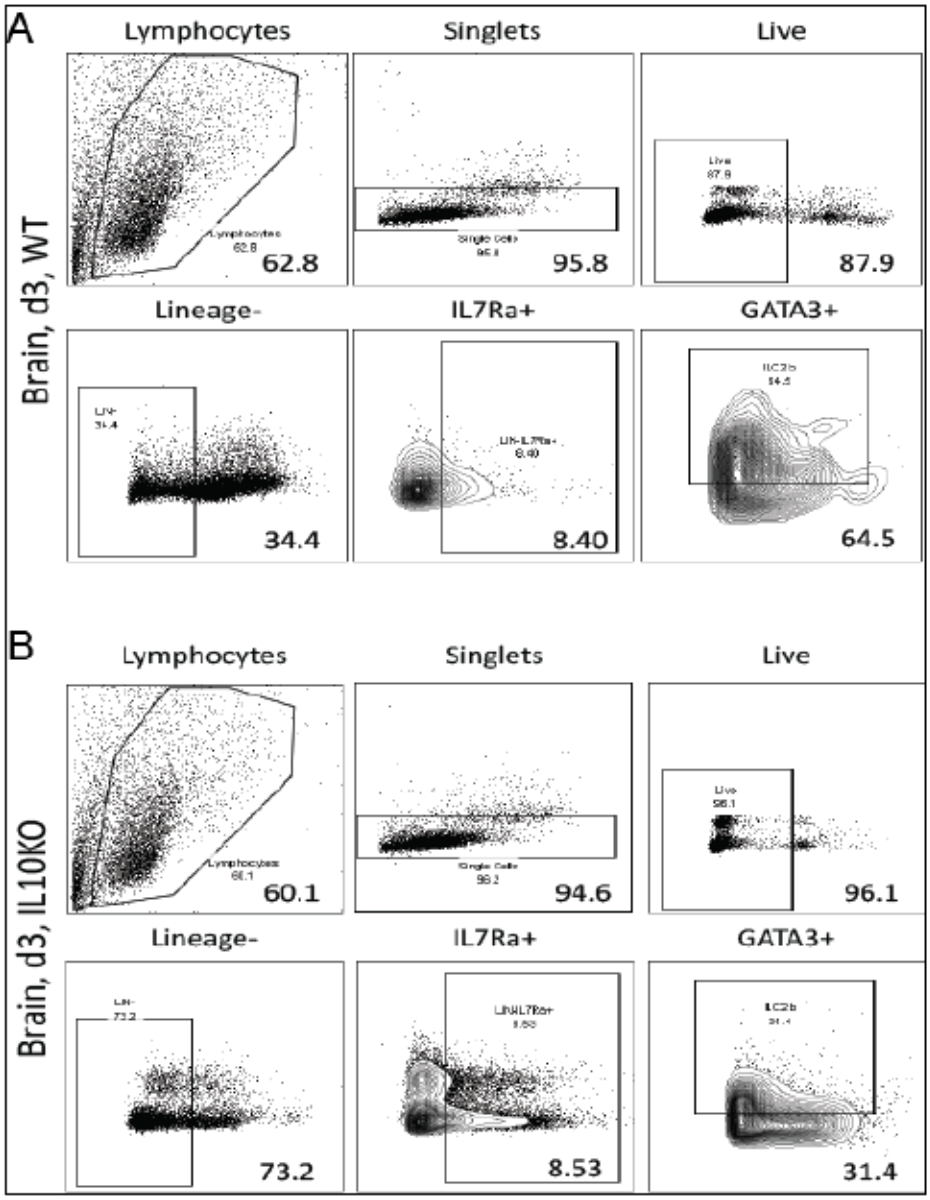

To assess the impact of IL-10 deficiency on ILC2 recruitment to the CNS from the CLNs, surface staining, transcription factor staining, and flow cytometry was performed on lymphocytes isolated brains and CLN from WT (black bars) or IL10KO (white bars) mice. Representative flow cytometry plots from three days post infection of WT (A) and IL10KO (B) brains are shown. ILC2s were defined as Lineage- IL-7Ra+ GATA3+.

Figure 2.5.11 IL-10 deficiency decreases ILC2s in CNS

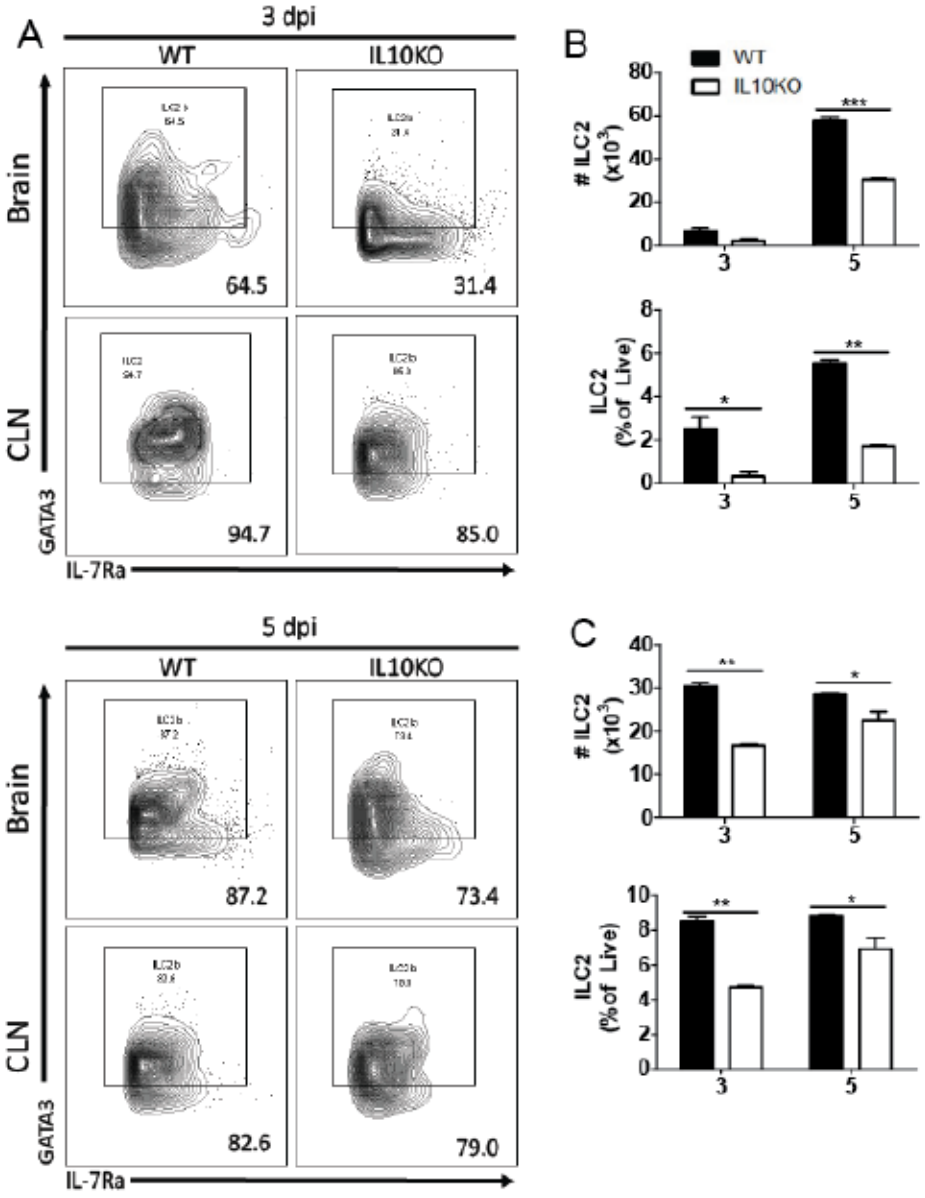

To assess the impact of IL-10 deficiency on ILC2 recruitment to the CNS from the CLNs, surface staining, transcription factor staining, and flow cytometry was performed on lymphocytes isolated brains and CLN from WT (black bars) or IL10KO (white bars) mice. Representative flow cytometry plots are shown in (A). ILC2s were defined as Lineage- IL-7Ra+ GATA3+. Percent and number of ILC2s were measured in brain (B) and CLN (C). Bars represent mean ± SEM from 10 mice per group; *p < .05, **p < .01.

Figure 2.5.12 IL-10 deficiency decreases ST2 expression on TH2 response in CNS

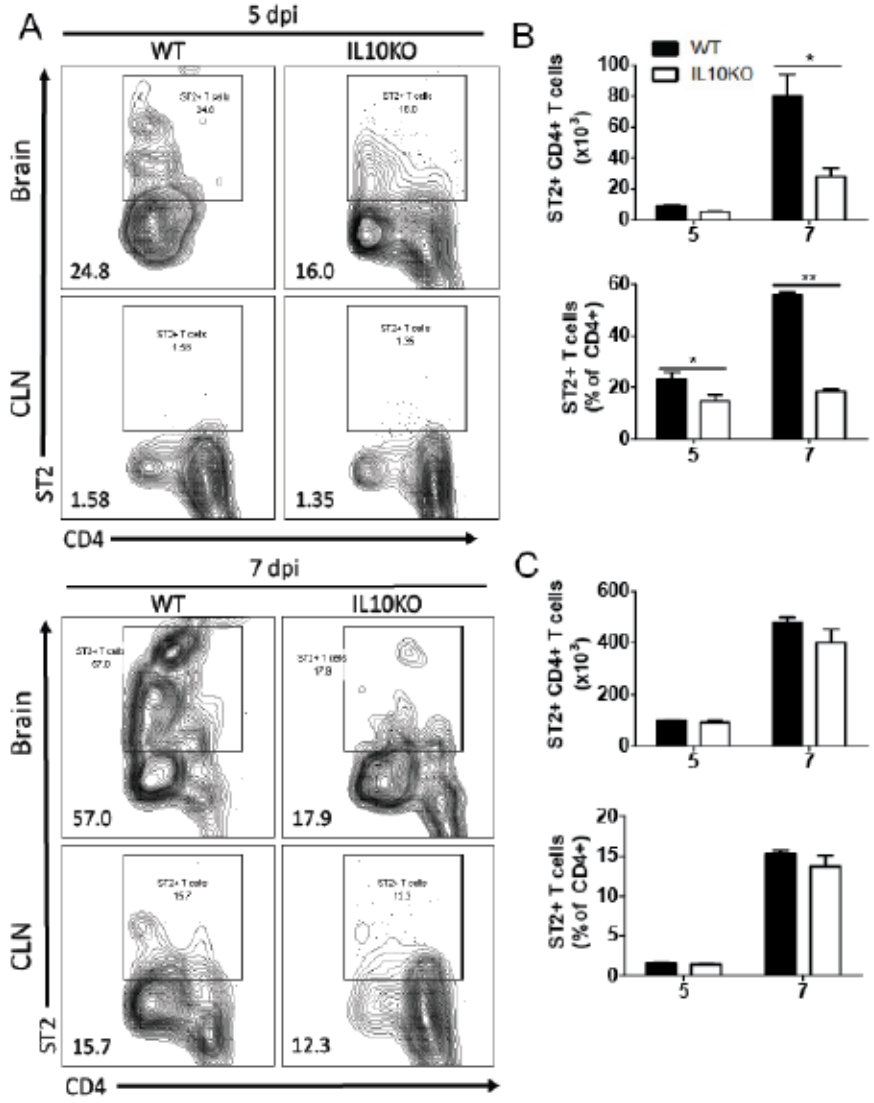

To assess the impact of IL-10 deficiency on ST2 expression on TH2 cells, surface staining, transcription factor staining, and flow cytometry was performed on lymphocytes isolated brains and CLN from WT (black bars) or IL10KO (white bars) mice. Representative flow cytometry plots are shown in (A). TH2 cells were defined as CD45hi CD3+ CD4+ GATA3+. Percent and number of TH2 ST2+ ells were measured in brain (B) and CLN (C). Bars represent mean ± SEM from 10 mice per group; *$p < .05$, **$p < .01$.

Figure 2.5.13 IL-10 deficiency impacts quantity of SINV-specific IgG1 and IgM

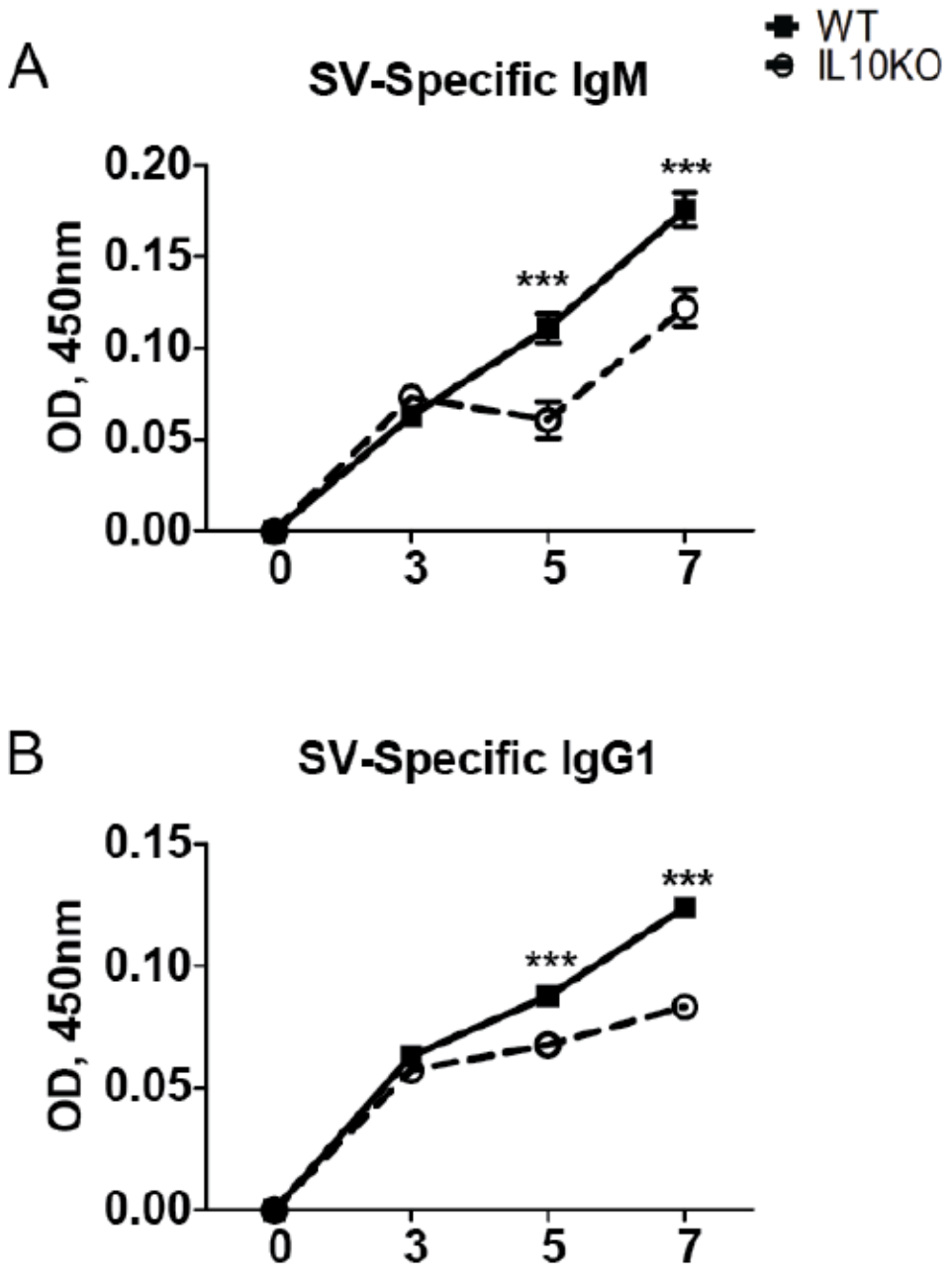

(A-B) Analysis of SINV specific IgG and IgM antibodies via EIA. Data were pooled from 2 independent experiments and represent the means ± SEM for 6 mice at each time point; ***$p < 0.001$.

Figure 2.5.14 IL-10 deficiency leads to decreased CD19+ B cells

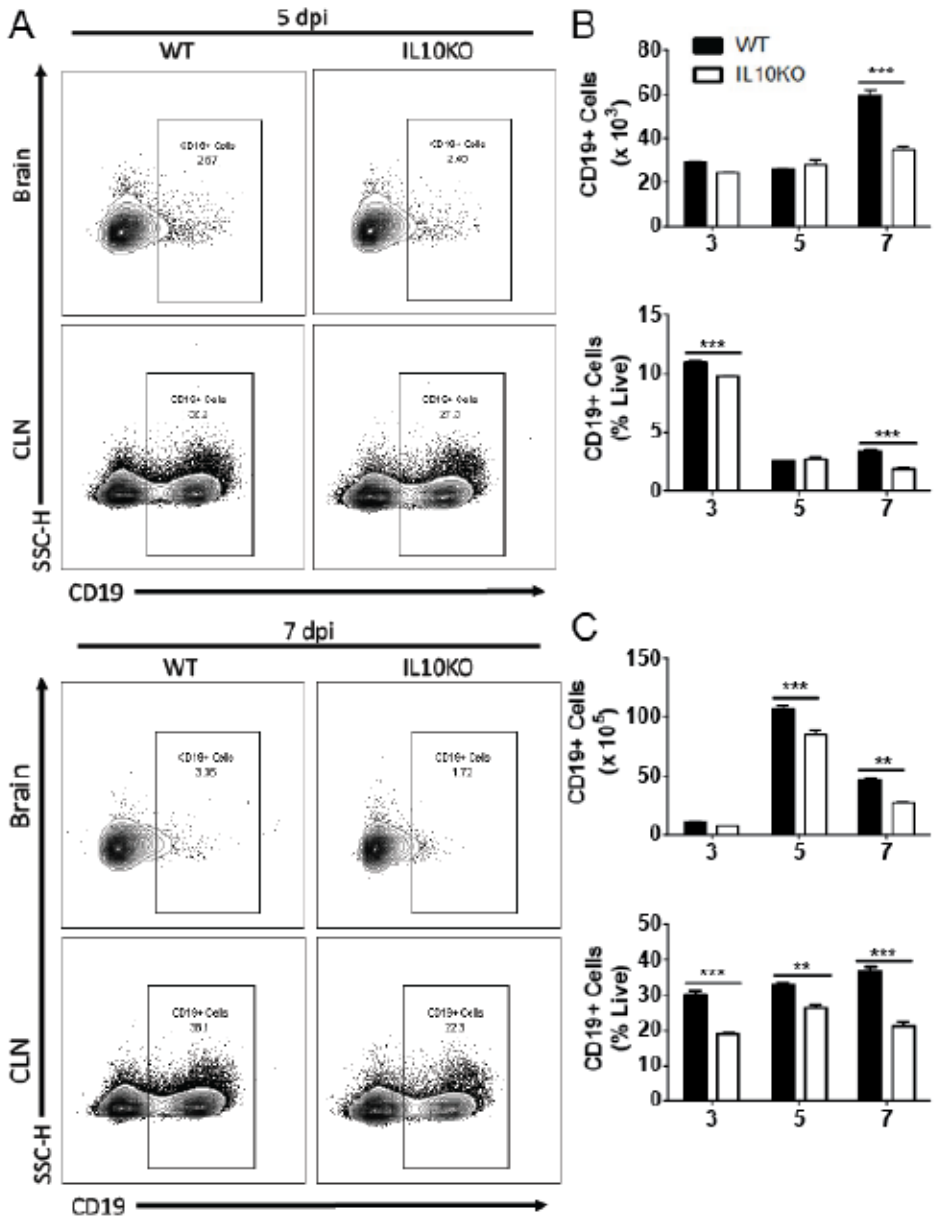

To assess the impact of IL-10 deficiency on CD19+ B cells flow cytometry was performed on brains and CLN from WT (black bars) or IL10KO (white bars) mice. Representative flow cytometry plots are shown in (A). Percent and number of CD19+ B cells were measured in brain (B) and CLN (C). Bars represent mean ± SEM from 10 mice per group; **p < .01, ***p < .001.

Figure 2.5.15 IL-10 deficiency decreases Regulatory B cells

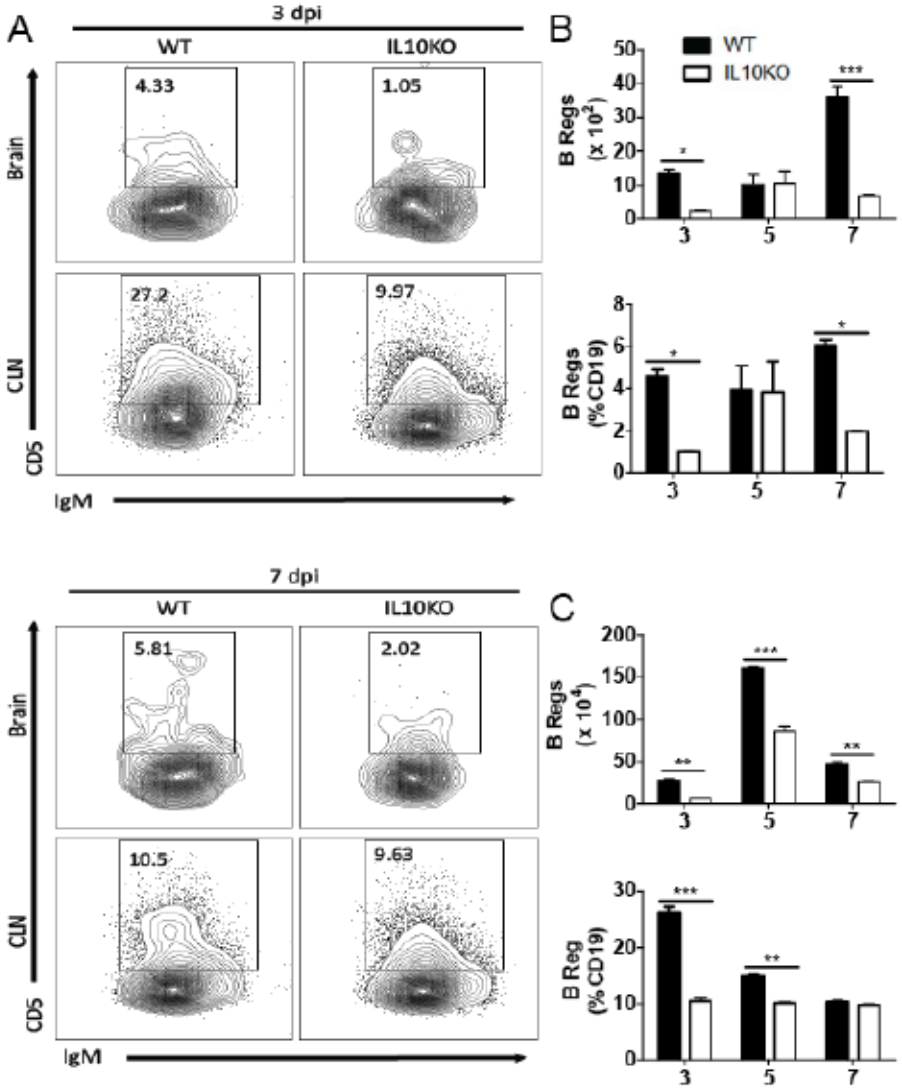

To assess the impact of IL-10 deficiency on regulatory B cells, surface staining and flow cytometry was performed on brains and CLN from WT (black bars) or IL10KO (white bars) mice. Representative flow cytometry plots are shown in (A). Regulatory B cells were defined as CD19+ CD1dhi CD5+ IgM+. Percent and number of regulatory B cells were measured in brain (B) and CLN (C). Bars represent mean ± SEM from 10 mice per group; *p < .05, **p < .01, ***p < .001.

CHAPTER 3:

TGFβ MODULATION OF VIRUS CLEARANCE OF INTERMEDIATE VIRULENT SINDBIS VIRUS IN IL-10 DEFICIENT MICE

Nina M. Martin & Diane E. Griffin

ABSTRACT

Alphaviruses, like Sindbis virus (SINV), are an important cause of mosquito borne outbreaks of arthritis, rash and encephalomyelitis. Studies with recombinant SINV strains in mice have implicated T cells in pathogenesis of disease. Previous work with fatal NSV infection in IL-10 deficient mice was limited by the rapid onset of morbidity and mortality in B6 mice. The TE12 SINV strain of intermediate virulence allows for longer term study of IL-10 deficient mice and better elucidation of the mechanisms leading to death versus clearance and survival. We show the modulatory impacts of IL-10 during intermediate virulent infection with the TE12 recombinant strain on CD4+ Helper T cell differentiation in the CNS and associated clinical outcomes. We show that the absence of IL-10 during TE12 infection leads to prolonged morbidity, increased mortality, increased weight loss, and delayed viral clearance. These clinical manifestations are associated with decreased regulatory T cells and Helper T cells Type 2 in the absence of IL-10. There was no impact on TH17 responses. This implicates a different role for IL-10 during intermediate virulent SINV infection than in the previously observed fatal infection model.

3.1 INTRODUCTION

Outbreaks of mosquito-borne viral diseases are on the rise, with recent extensions to new geographic regions causing rash, arthritis and encephalomyelitis [146, 147]. Alphaviruses, including chikungunya, eastern equine encephalitis, and Venezuelan equine encephalitis viruses, are important causes of mosquito borne disease [106, 108, 148-151]. The latter two viruses cause encephalomyelitis, an inflammatory disease of the central nervous system with high fatality rates and long-term neurological deficits in survivors.

Sindbis virus (SINV), the prototypical alphavirus, is the most widespread alphavirus. It causes rash and arthritis in humans. In mice, SINV causes encephalomyelitis, the severity of which depends on the particular virus strain and a number of host factors, including age and genetic background[10-12, 19]. SINV strains that cause varying degrees of pathogenicity have been developed by serial passaging and by construction of recombinant viruses. This has resulted in the development of a neuroadapted SINV (NSV). This virulent strain was generated by passaging the original AR339 isolate through the mouse brains to generate a virus that causes fatal encephalomyelitis in suckling and adult C57Bl/6 mice [12, 109]. Another strain, TOTO1101, generated by recombination, causes little disease even in suckling mice. A third strain, TE12, is a recombinant SINV strain that has the E1 and E2 envelope glycoproteins from NSV on the TOTO1101 background. Infection of mice with the TE12 virus causes intermediate virulence, with approximately sixty percent fatality rate in adult C57Bl/6 mice [10]. Strains with intermediate virulence factors associated with

outcome allow for longer term study of mechanisms leading to death versus neuroprotection and facilitate the study of clearance and immunopathogenesis [19, 152].

Previous studies have shown that the immune response has both positive and negative effects on mouse survival and virus clearance. Both antibody and IFNγ contribute to noncytolytic viral clearance from neurons [9, 33, 36, 45, 114] while T cells are implicated in immunopathogenesis and fatal encephalomyelitis. The evidence for T cell-mediated disease is based on studies of immune compromised and knock out mice [38, 113]. In particular, TH17 cells are associated with accelerated morbidity and mortality in NSV-infected IL-10-deficient mice. IL-10 is an important regulator of T cell function and SINV-induced immunopathology [15, 16]. IL-10 dysregulation has been implicated in adverse inflammatory outcomes during influenza and CMV infection [57, 153]. Regulatory T cells are major producers of IL-10 post-SINV infection [15, 16] and many cell types are regulated by IL-10, including DCs, macrophages, NK cells, and lymphocytes [154].

Data from NSV-infected mice suggested delayed viral clearance in IL-10-deficient animals, however, the rapid death of the IL-10-deficient hosts has made the mechanism of death difficult to analyze. To determine whether IL-10 plays a role in the pathogenesis of alphaviral encephalomyelitis during infection with a virus of intermediate virulence, we have studied TE12 infection of IL-10-deficient C57Bl/6 mice. IL-10-deficient mice had higher fatality rates, prolonged morbidity, and delayed viral clearance compared to wild type controls. These outcomes are associated with decreased T cells, with a particular negative impact on TH2 and regulatory T cells and increased TH1-related factors such as increased levels of IFNγ protein. These data demonstrate an

important role of IL-10 in regulating pathogenesis during intermediate virulent SINV infection.

3.2 MATERIALS AND METHODS

3.2.1 Animals and virus

C57Bl/6J wild-type (WT) and B6.129P2-Il10tm1Cgn/J (C57Bl/6J IL10 KO) mice were purchased from Jackson Laboratories and bred in house at Johns Hopkins University. Mice in all experiments were sex (equal numbers of males and females were used in every experiment) and age (4-6 weeks old) matched. The TE12 strain of SINV was grown and assayed by plaque formation in BHK cells [10] and infected intranasally at $1x10^5$ PFU TE12 in 1x PBS. Morbidity and mortality experiments were done as previously described in [15] using the scoring system: 0) no clinical symptoms observed, 1) abnormal hind-limb and tail posture, ruffled fur, and/or hunched back, 2) unilateral hind-limb paralysis, 3) bilateral hind-limb paralysis or full-body paralysis, and 4) dead. For collection of cervical lymph nodes, brains, and spinal cords, mice were anesthetized with isoflurane, perfused with ice cold PBS, followed by tissue collection. Tissues were used fresh or snap frozen and stored at -80°C. All experiments were performed according to guidelines and protocols approved by the Johns Hopkins University Institutional Animal Care and Use Committee.

3.2.2 Quantification of infectious virus and viral RNA

20% weight per volume brain and spinal cord tissue homogenates were made by thawing snap frozen tissues and homogenizing in PBS. Homogenates were serially-diluted in DMEM+1% FBS and plated on BHK-21 cell monolayers, incubated for 1 hour, overlaid with 1.2% bactoagar, and incubated at 37°C with 5% CO_2 for 48 hours. Cells

were stained with neutral red and plaques were counted. Each time point represents the geometric mean of the $\log_{10}$ value of plaque forming units per gram ± SEM. Samples in which no virus was detected at a 1:10 dilution were given a value of midway between the lower limit of detection and zero for statistical analyses.

For absolute quantification of viral RNA in brain and spinal cords, total RNA was extracted from snap frozen tissues using the RNeasy Lipid Mini RNA Isolation Kit (Qiagen). After quantification via nanodrop, 500 ng of RNA was used to synthesize cDNA via High Capacity cDNA Reverse Transcription Kit (Life Technologies). Quantitative real-time PCR was performed using 2.5 µl of cDNA and TaqMan gene expression arrays in 2x Universal PCR Mastermix (Applied Biosystems). Absolute quantification of SINV E2 copies/10^6 genome copies was measured by comparing values to standard curve of Gapdh mRNA levels using the rodent primer and probe set (Applied Biosystems). All reactions were run on the Applied Biosystems 7500 Real-time PCR machine.

3.2.3 Mononuclear cell isolation

Mononuclear cells were isolated from brains and cervical lymph nodes collected from WT and IL10KO mice at 5, 7 and 10 days post-infection. Cervical lymph nodes were pooled from 6-10 mice per group per time point in 10 mL of RPMI+1% FBS and homogenized in C tubes using the GentleMACS system (Miltenyi) spleen program 1 for two cycles. Brain tissue was collected from 6-10 mice per group per time point in ice cold Hanks Balanced Salt Solution. For cell isolation, two brains were pooled per C tube containing 4 mL of enzyme digest mix made up of RPMI + 1% FBS, 1 mg/mL

collagenase (Roche), and 0.1 mg/mL DNase and dissociated with scissors. Further dissociation was performed via GentleMACS (Miltenyi) brain program 3 (total of 5x with 2, 15 minute 37° C incubations with gentle rocking). All suspensions were filtered through 70 μm cell strainers and centrifuged. Red blood cells were lysed using 2 mL of red blood cell lysis buffer for 3 minutes and then washed with PBS.

To remove debris, pellets were suspended in 30% percoll, underlaid with 70% percoll for a 30/70% gradient and centrifuged for 30 minutes at 850xg at 4° C. The top debris layer was aspirated off and mononuclear cells at the interface were collected and washed with PBS + 2mM EDTA. Pellets were resuspended in PBS + 2 mM EDTA and live cells were counted using trypan blue exclusion.

3.2.4 Identification of cells by flow cytometry

To determine the number and type of infiltrating cells, ~$1x10^6$ cells were used for each panel. The cells were stained with a violet live/dead stain (Invitrogen #L345955), blocked with rat anti-mouse CD16/CD32 Block (BD #553142), surface stained for phenotyping, and then fixed using 1:1 dilution of 4% paraformaldehyde and FACS buffer, and data acquired.

The surface marker antibodies used were anti-CD45-FITC (BD), CD3-APC (BD), CD4-PerCpCy5.5 (BD), CD8-PECy7 (BD), CD25-PE (BD), Lineage-Fitc (eBiosciences), IL-7Ra-PECy7 (eBiosciences), CD19-PerCP-Cy5.5 (eBiosciences), CD5-PECy7 (eBiosciences), CD1d-APC (eBiosciences), IgM-FITC (eBiosciences). Cell types were defined as follows: T cells (CD3+), CD4 T cells (CD3+CD4+), CD8 T cells (CD3+CD8+), regulatory B cells (CD19+CD5+CD1dhiIgM+), ILC2 (Lin-IL-

7Ra+GATA3+). Data are acquired using the BD FACS Canto II flow cytometer and FACS Diva software, and analyzed using FlowJo (v10.3.0).

3.2.5 Transcription factor staining by flow cytometry

For determination of T cell differentiation, transcription factors were assayed using Foxp3 Buffer Set (eBiosciences). After surface staining, cells were fixed, permeablized, and stained for GATA3, foxP3, RORgt, or Tbet. Cells were defined as follows: regulatory T cells (CD3+CD4+CD25+foxp3+), TH17 cells (CD3+CD4+RORgt+), TH1 cells (CD3+CD4+Tbet+), and TH2 cells (CD3+CD4+GATA3+). Innate lymphoid cells type 2 were also quantitated (Lineage-, IL-7Ra+, GATA3+).

3.2.6 Intracellular cytokine staining by flow cytometry

For determination of T cell cytokine production, 2-3x10^6 cells were stimulated with RPMI + 1% FBS containing 50 ng/mL of phorbol-12-myristate 13-acetate (PMA) and 1µg/mL of ionomycin in the presence of GolgiPlug (BD #555029) for 4 hours. Cells were then washed and stained with the violet live/dead marker (Invitrogen #L345955), blocked with rat anti-mouse CD16/CD32 Block (BD #553142), and then stained for the surface markers for Helper T cells (CD3-APC and CD4-FITC). After surface staining, cells were fixed and permeabilzed using the BD CytoFix/CytoPerm kit (BD #554714). In CD4+ T cells, cytokine staining was performed either by itself or in conjunction with transcription factor staining. Cells were stained for IFNγ-PE, IL-4-PE, or IL-17a-PE.

Cells were washed, suspended in FACS buffer and acquired using the BD FACS Canto II and FACS Diva, and analyzed using FlowJo software (v10.3.0).

3.2.7 Gene expression analysis using real-time PCR

RNA was extracted from snap frozen tissues using the RNeasy Lipid Mini RNA Isolation Kit (Qiagen). After quantification via nanodrop, 500 ng of RNA was used to synthesize cDNA via High Capacity cDNA Reverse Transcription Kit (Life Technologies). Quantitative real-time PCR was performed using 2.5 µl of cDNA and TaqMan gene expression arrays in 2x Universal PCR Mastermix (Applied Biosystems, #4304437). The TaqMan gene expression arrays used were Ifnγ, IL-2, IL-10, IL-17a, IL-4, gata3, and foxp3. Gapdh mRNA levels were determined using the rodent primer and probe set (Applied Biosystems). All reactions were run on the Applied Biosystems 7500 Real-time PCR machine. Transcript levels were determined by normalizing the target gene Ct value to the Ct value of the endogenous housekeeping gene Gapdh. This normalized value was used to calculate the fold-change relative to the average of the uninfected control (ΔΔCt method).

3.2.8 Quantification of protein via EIA

Enzyme immunoassays (EIA) were performed to measure IFNγ protein levels in brains harvested from WT or IL10KO mice infected with TE12. IFNγ EIA kits were used (R & D Systems ELISA [enzyme-linked immunosorbent assay] kits) according to the manufacturer's instructions. Brain homogenates (10%, wt/vol) from n=6 mice per time point were pooled and tested in duplicate.

EIA was also used to quantitate SINV-specific IgG (total) and IgM antibody in brains and spinal cords harvested from WT or IL10KO mice infected with TE12. 96-well Maxisorp plates (Nalgene Nunc) were coated with 10^6 PFU/well of polyethylene glycol (PEG)-precipitated TE12 in 50 mM NaHCO3 (pH 9.6) at 4°C overnight. Blocking buffer (10% FBS and 0.05% Tween 20 in PBS) was added for 2 hours at 37°C. Brain homogenates (10%, wt/vol) diluted 1:2 in blocking buffer were incubated at 4°C overnight. Bound antibodies were detected using HRP-conjugated goat anti-mouse IgM or IgG (Southern Biotech) diluted 1:1,000 in blocking buffer and incubated at room temperature for 2 hours. Plates were developed using the BD OptEIA TMB Substrate Reagent kit with H2SO4 as a stop solution. Absorbance was read at 450 nm. Average optical density (OD) values for brains from uninfected mice were subtracted from the OD values of brains from infected mice.

3.2.9 Statistical analysis

Data from three independent experiments or at least 6 mice per group are used. All statistical analysis was done using GraphPad Prism 5 (v5.01). Survival was calculated using Kaplan-Meier survival curves [Log rank (Mantel Cox) Test]. Differences between groups during the course of infection were determined using a 2-way ANOVA and Bonferroni post-tests to compare the difference between groups at each time point (morbidity, cellular infiltrates, cytokine analysis, and viral titers).

3.3 RESULTS

3.3.1 IL-10 is up-regulated in response to TE12 infection

To determine if IL-10 is up-regulated after TE12 infection, mRNA expression was measured at timed intervals from the brains and spinal cords of C57Bl/6 mice and compared to age-matched, uninfected controls. In the brain and spinal cord, *Il10* gene expression was elevated by day three, peaked at day ten, and remained above baseline at twenty one days post infection (Figure 3.5.1, A, B).

3.3.2 IL-10 deficiency leads to prolonged morbidity and increased mortality

To determine the effect of IL-10 deficiency on morbidity and mortality resulting from TE12 infection, 4-6 week old C57Bl/6 WT and IL10KO mice were infected intranasally and evaluated daily. The mean time to death was similar for the WT and KO animals, but IL-10-deficient mice had higher mortality (62.5%) than wild type mice (35.0%) (Figure 3.5.2, A; $p = .0356$). Mice lacking IL-10 also showed signs of encephalomyelitis earlier (day 4) than WT mice and those that survived were slower to recover from infection compared to wild type controls (Figure 3.5.2, B). IL-10-deficient mice also lost more weight and surviving mice recovered weight at a slower rate than wild type controls (Figure 3.5.2, C). These clinical manifestations of disease indicate an important role for IL-10 in survival and recovery from TE12 infection.

3.3.3 IL-10 deficiency leads to delayed viral clearance and increased viral RNA

To assess the impact of IL-10 deficiency on virus replication and clearance, plaque assays were performed on brain (Figure 3.5.3, A) and spinal cord (Figure 3.5.3, B) tissues from TE12-infected WT or IL10KO mice. Amounts of infectious virus peaked at days 3 and 5 post-infection in both WT and IL10KO mice in brain and spinal cord tissues. Viral clearance was delayed in IL-10-deficient mice compared to WT controls in both brain and spinal cord tissues. While infectious virus was completely cleared by day 21 post-infection in WT mice, viable virus persisted in some, but not all IL10KO mice.

The amount of viral RNA was also quantitated in brain (Figure 3.5.3, C) and spinal cord (Figure 3.5.3, D) tissues. SINV-specific RNA was detected at day 3 post-infection in brains of both WT and IL10KO mice. Viral RNA peaked on day 5 in brain and on day 7 in spinal cord in both WT and IL10KO mice. SINV-specific RNA persisted in TE12-infected brains and spinal cords in those animals that survived and recovered from clinical manifestations of disease [9]. However, IL-10-deficient mice had higher viral RNA levels on days 10 and 14 post-infection in brain and on day 10 in spinal cord compared to WT controls. There were no significant differences at day 21 post-infection. A significant increase in viral RNA in IL10KO spinal cords was observed on 10 days post-infection. These results suggest an important role of IL-10 in viral clearance in both brain and spinal cord tissues,

3.3.4 IL-10 deficiency leads to TGFβ1, but not TGFβ3, elevation post-TE12 infection

To determine if the absence of IL-10 impacted the expression of TGFβ1 and TGFβ3 protein, EIA was performed. TGFβ1 was elevated in IL10KO mice compared to

WT controls in brain and spinal cords (Figure 3.5.4A, B). While TGFβ3 protein increased during infection, there were no significant differences between WT and IL10KO (Figure 3.5.4C, D). These results are different from those observed during NSV infection where both isoforms were elevated in IL10KO mice (see Chapter 2).

3.3.5 IL-10 deficiency increases recruitment of CD3+ T cells into the CNS

IL-10 is important for T cell differentiation, activation and suppression during inflammatory disease. To assess the impact of IL-10 deficiency on T cell responses to TE12 infection, flow cytometry was performed on lymphocytes isolated from CLN and brain tissues from IL10KO and WT mice on days 5, 7 and 10 post-infection (Figure 3.5.5, A). IL-10 deficiency did not impact the total number of cells isolated from brain or CLN (Figure 3.5.5, B & E). However, IL-10 deficiency did increase numbers and percentages of CD3+ T cells into the brain, but not in the CLN (Figure 3.5.5, C, F). Mice lacking IL-10 had increased percentages of CD3+ T cells in the brain on 5, 7, and 10 days post-infection (Figure 3.5.5, D). Numbers of CD3+ T cells were increased in IL10KO mice on days 7 and 10 (Figure 3.5.5, C).

3.3.6 IL-10 deficiency increases recruitment of CD4+ T cells into the CNS

Next, helper T cells were quantitated using flow cytometry on lymphocytes isolated from brains and CLN from WT and IL10KO mice on days 5, 7, and 10 post-infection (Figure 3.5.6, A). On days 7 and 10 post-infection, higher numbers of CD4+ T cells were isolated from brains of IL-10 deficient mice (Figure 3.5.6, B). There were no differences in numbers or percent of CD4+ T cells in CLNs (Figure 3.5.6, D, E).

3.3.7 IL-10 deficiency minimally impacts recruitment of CD8+ T cells into the CNS

To measure the impact of IL-10 deficiency on CD8+ T cell responses, flow cytometry was performed on lymphocytes isolated from brain and CLN tissues from WT and IL10KO mice (Figure 3.5.7 A). The only measured difference was a higher number of CD8+ T cells in the brains of IL10KO mice on 7 and 10 days post-infection (Figure 3.5.7, B, top). There were no significant changes in the percent of CD8+ T cells (Figure 3.5.7, B, bottom) or in number or percent of CD8+ T cells in the CLN (Figure 3.5.7, C).

3.3.8 IL-10 deficiency leads to decreased regulatory T cells

To determine the impact of IL-10 deficiency on regulatory T cells, we first measured levels of *foxp3* mRNA in the brain (Figure 3.5.8, A). *Foxp3* mRNA levels were lower in IL10KO mice from day 5 continuously to day 21 post-infection.

Flow cytometry was performed on lymphocytes isolated from CLN and brain tissues of TE12-infected IL10KO or WT mice on days 7 and 10 post-infection (Figure 3.5.8, B). Regulatory T cells, identified as CD3+CD4+CD25+foxP3+, were present in lower numbers and percentages in brain tissues from IL10KO than WT mice on days 7 and 10 post-TE12 infection (Figure 3.5.8, C). There were similar numbers and percentages of regulatory T cells in CLN tissues (Figure 3.5.8, D). This, along with previous work in [17], suggests that IL-10 is important in infected tissue to maintain regulatory populations within the CNS, but not necessarily for activation within CLNs.

3.3.9 IL-10 deficiency impacts TH1 related cytokines and minimally impacts TH1 cells

Because helper T cells type 1 (TH1) are important for viral clearance, but can also drive pathological changes, the TH1 response was assessed (Figure 3.5.9). To determine the impact of IL-10 deficiency on TH1 related cytokine production, RT-qPCR was performed on cDNA from brains from IL10KO or WT mice. Levels of mRNA for the pro-inflammatory cytokines IL-2 (Figure 3.5.9, A) and IFNγ (Figure 3.5.9, B) are elevated in IL10KO compared to WT mice post-infection. IFNγ protein levels were also quantitated via EIA after TE12 infection (Figure 3.5.9, C). Compared to WT mice, IL-10-deficient mice had decreased IFNγ protein on days 5 and 7 post-infection while levels were increased on days 10 and 14.

To quantitate the number of TH1 cells during TE12 infection, isolated lymphocytes were stained with CD3, CD4, and T-bet, the master transcription factor important for the differentiation and activation of TH1 cells (Figure 3.5.9, D). There were more TH1 cells 7 days post-infection in brains of IL10KO than WT mice (Figure 3.5.9, E, F). There were no significant differences in numbers and percentages in the CLN (Figure 3.5.9, G, H).

3.3.10 IL-10 deficiency does not lead to an increased type 17 response

Because IL10KO mice had accelerated production of IL-17a mRNA and TH17 cells after NSV infection (Chapter 2), we assessed TH17 responses post-TE12 infection. First, *Il17a* mRNA was quantified via RT-qPCR in IL10KO or WT mouse brain and spinal cord tissues compared to uninfected controls (Figure 3.5.10, A). No differences in

Il17a mRNA were observed in brain or spinal cord tissues of IL10KO and WT mice. Using flow cytometry, we next assessed the number and percentage of IL-17A-producing CD4+ T cells in TE12-infected IL10KO and WT mice (Figure 3.5.10, B). On day 7 and 10 post-infection, there were no differences in the percentages of IL-17A-producing CD4+ T cells in the brain (Figure 3.5.10, C) or CLN (Figure 3.5.10, D).

These results taken together demonstrate that *Il17a* mRNA levels and TH17 cells are present in the CNS of both WT and IL-10KO mice during TE12 infection, but that IL-10 deficiency did not impact this response.

3.3.11 IL-10 deficiency decreases TH2 cell responses

Because helper T cells type 2 (TH2) are important for activation of B cells, differentiation into antibody secreting cells, and ultimate production of antibody, the TH2 related response was assessed (Figure 3.5.11). To determine the impact of IL-10 deficiency on TH2 related factors, RT-qPCR was performed on cDNA from brain and spinal cord tissues from IL10KO or WT mice. GATA3, a transcription factor important for the differentiation and activation of TH2 cells, was first assessed. *GATA3* mRNA was lower in brains of IL10KO mice than WT mice from 5 to 21 days post-infection (Figure 3.5.11, A). This decrease coincides with the recruitment of the adaptive immune response in the CNS at 5 days post-infection. mRNA levels for *Il4*, a cytokine produced by TH2 cells, were also measured (Figure 3.5.11, B). Levels of *Ii4* mRNA did not increase in response to infection in either IL10KO or WT mice. Because *Il4* mRNA is post-transcriptionally regulated [155], we next examined protein production by T cells.

TH2 cell frequency in CNS tissues was measured via flow cytometry by quantitating CD4+ T cells that produce IL-4 and express GATA3 (Figure 3.5.11, C). Mice deficient in IL-10 had lower numbers and percentages of CD4+ T cells producing IL-4 on days 7 and 10 post-infection compared to WT mice (Figure 3.5.11, D). There were no differences in numbers or percentages in CLN (Figure 3.5.11, E).

3.3.12 IL-10 deficiency leads to decreased ILC2 numbers in the CNS

Because IL-10 deficiency had an impact on TH2 responses, innate lymphoid cell type 2 (ILC2) numbers were examined via flow cytometry (Figure 3.5.12, A). ILC2s are innate activators of the TH2 and B cell responses and important sources of IL-5 and IL-13. Mice deficient in IL-10 had lower numbers and percentages of ILC2s on day 10 post-infection compared to WT mice (Figure 3.5.12, B, C). In CLN, IL-10-deficient mice had lower numbers and percentages of ILC2 compared to WT control mice (Figure 3.5.12, D, E).

3.3.13 IL-10 deficiency leads to decreased antibody production in the CNS

To determine the impact of IL-10 deficiency on antibody production, SINV-specific IgG (total) and IgM antibody were quantitated via EIA. Lower concentrations of SINV-specific IgG were measured on days 10 and 14 post-infection in brains (Figure 3.5.13, A) and spinal cords (Figure 3.5.13, B) of IL-10 deficient mice. On days 7 and 10 post-infection, a lower amount of SINV specific IgM antibody was produced in brains (Figure 3.5.13, C) of IL-10-deficient mice. In spinal cords (Figure 3.5.13, D), IL-10

deficient mice produced less SINV-specific IgM antibody on days 10 and 14 post-infection.

IL-10 deficiency leads to decreased B cell numbers in the CNS

Given lower levels of both IgG and IgM antibodies in the CNS of IL-10-deficient mice, CD19+ B cells were quantitated via flow cytometry (Figure 3.5.14, A). Mice deficient in IL-10 had lower numbers and percentages of CD19+ B cells in both brains (Figure 3.5.14, B & C) and CLN (Figure 3.5.14, D & E).

IL-10 deficiency leads to decreased regulatory B cell numbers in the CNS

Regulatory B cells produce IL-10 and down-regulate TH1 and TH17 responses. To test if IL-10 deficiency impacted numbers of regulatory B cells in the CNS, flow cytometry was performed (Figure 3.5.15, A). IL-10-deficient mice had lower numbers and percentages of regulatory B cells in brains compared to WT control mice on days 10 post-infection (Figure 3.5.15, B & C). In CLN, IL-10 deficient mice had lower numbers of regulatory B cells compared to WT mice 10 days post-infection (Figure 3.5.15, D & E).

3.4 DISCUSSION

Studies with the intermediately virulent TE12 strain of SINV provide the opportunity to study the mechanisms leading to neuroprotection and viral clearance versus immunopathogenesis during alphaviral encephalomyelitis. We have demonstrated an important role of IL-10 in regulating T cells, with a particular focus on subsets of CD4+ T cells. IL-10 deficiency led to prolonged morbidity, increased mortality, increased weight loss, and delayed viral clearance associated with increased numbers of CD3+ cells and TH1 cells, as well as decreased regulatory T cells and TH2 cells, without a difference in TH17 cells. Therefore, in contrast to studies with the highly neurovirulent NSV strain, IL-10 deficiency affected outcomes by a combination of delaying viral clearance and increased TH1-mediated immunopathogenesis rather than TH17-mediated pathogenesis.

While the role of IL-10 in chronic viral infections of the CNS has been well studied [156, 157], its role during acute viral infections has received limited attention. The major producers of IL-10 during viral infections in the CNS are Regulatory T cells. In both NSV and TE12-induced encephalomyelitis, IL-10 deficiency and worse outcomes were associated with lower numbers of regulatory T cells in the CNS. This has also been observed in experimental autoimmune encephalitis, the mouse model of multiple sclerosis, as well as experimental autoimmune neuritis, a mouse model for Guillain-Barre Syndrome [82, 90, 158]. During SINV infection, it is assumed that CD4+ helper T cells are recruited from the local CLN, but do not differentiate until they reach the CNS. Because IL-10 deficiency did not affect regulatory T cell numbers in the CLN, it is likely

that IL-10 deficiency affects either recruitment to the CNS or differentiation inside the CNS.

Regulatory T cells play a major role in decreasing the TH1 response in other infection models and does so by down-regulating MHC Type II on APCs and suppressing pro-inflammatory cytokines (IFNγ, TNF) and chemokines [159]. Increased inflammation due to IL-10 deficiency has been associated with detrimental outcomes. For example, impairment of regulatory T cell production of IL-10 can promote an overall increase in inflammation and worse clinical outcomes during acute encephalitis caused by tick borne viral encephalitis and Japanese encephalitis in mice and humans [56, 160, 161], as well as pediatric influenza and herpes simplex virus in mice [55, 59, 162]. Early in TE12 and NSV infection, IFNγ was decreased in IL10KO mice compared to WT. Because we were able to observe later time points after TE12 infection, we observed increased TH1 cells and *Ifng* mRNA and protein later in infection. This suggests innate factors suppress IFNγ in the absence of IL-10 until the arrival of T cells and other adaptive immune components. Non-CD4 sources of IFNγ have been characterized and scan be regulated by TGFβ. Natural killer cells are a major source of IFNγ in acute viral infections [163-165] and can be suppressed by TGFβ during, for example, MCMV infection [166].

A major difference between TE12- and NSV-induced pathogenesis in IL-10 deficient mice is the impact on TH2 response. During NSV infection, there was no impact in IL-10 deficient mice, while TE12 infection resulted in lower numbers of TH2 cells and higher numbers of TH1 cells in IL-10KO mice compared to WT. Antibody is essential to both mouse survival and viral clearance during alphaviral encephalomyelitis and perturbations in these immune factors will lead to worse clinical outcomes [9, 33, 36,

45, 114]. Because IFNγ is known to suppress TH2 cells and production of IL-4, the increased IFNγ in IL10KO mice after TE12 infection could lead to suppression of TH2 responses. Since it is possible to induce a fully functional, isotype-appropriate antibody response without TH2 cell activation, the IL-10 deficient mice were able to clear virus, but at a slower rate than WT control mice.

Another difference between NSV- and TE12-induced immunopathogenesis involved the increased expression of IL-17 and TH17 cells in NSV-, but not TE12-infected IL-10-deficient mice. NSV-infected mice had higher numbers of TH17 cells in the CNS and lower levels of pro-inflammatory cytokine mRNA (IFNα, IL-2, IL-12b, TNF) [15]. We postulate that the differences in TE12- and NSV-induced immunopathogenesis in IL-10 deficient mice are associated increases of TGFβ1 or 3 in the absence of IL-10. TGFβ performs similar yet different functions to IL-10 and can suppress inflammatory cytokines. In certain contexts, TGFβ can also induce the differentiation of TH17 or Tregs [77, 80, 123, 125, 167]. The ability of TGFβ to induce TH17 or Tregs is dose dependent, as well as other environmental factors (i.e. availability of other cytokines, like IL-6, IL-23, and IL-10, and transcription factors, like STAT3 or STAT6) [75]. TGFβ is also known to directly suppress B cell responses via a non-cytolyic mechanism [126].

IL-10 immune therapy remains the focus of many clinical trials for the treatment of inflammatory diseases [168-171]. Since there remains to be zero therapeutic interventions for viral encephalomyelitis, understanding the potential of using IL-10 as a therapeutic agent remains of high importance.

3.5 FIGURES AND TABLES

Figure 3.5.1 IL-10 is upregulated in response to TE12 infection in brain and spinal cords

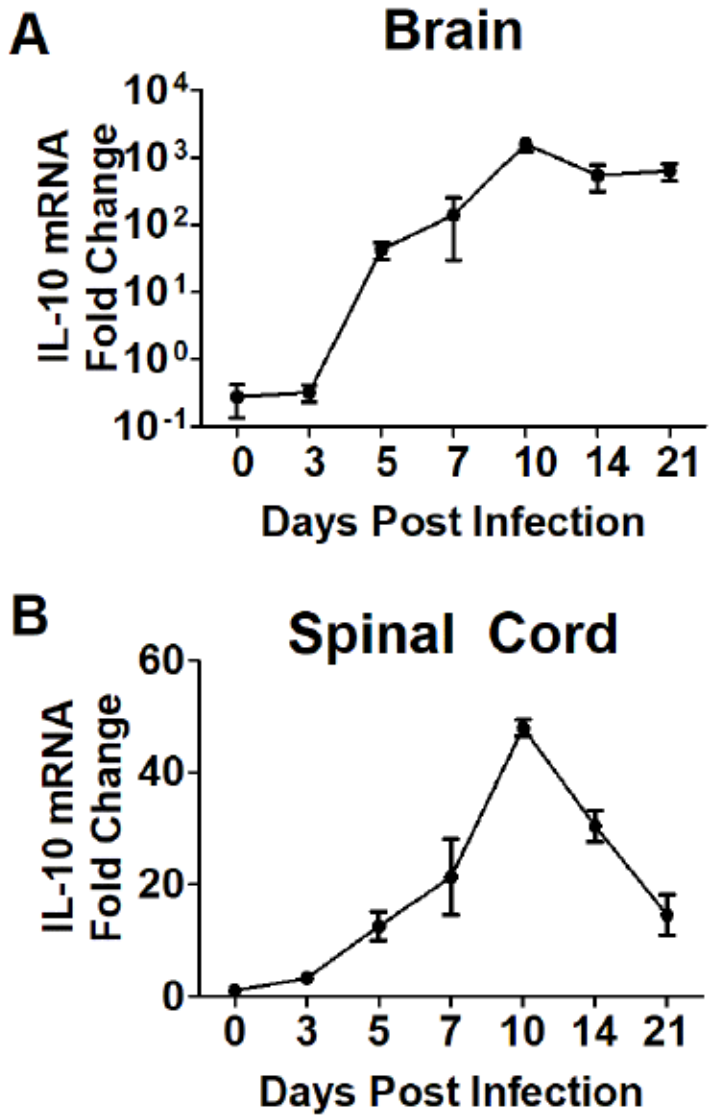

IL-10 mRNA is upregulated during TE12 infection. WT mice were intranasally infected with 10^5 pfu TE12. (A) Il10 mRNA expression measured by quantitative real-time PCR in the brains (A) and spinal cords (B) of TE12-infected WT mice. Ct values were normalized to GAPDH. Ct values and fold change were calculated relative to uninfected controls ($\Delta\Delta$Ct). Data are pooled from two independent experiments and represent the mean ± SEM of 6 mice at each time point.

Figure 3.5.2 IL-10 deficiency causes prolonged morbidity, increased and prolonged weight loss, and increased mortality

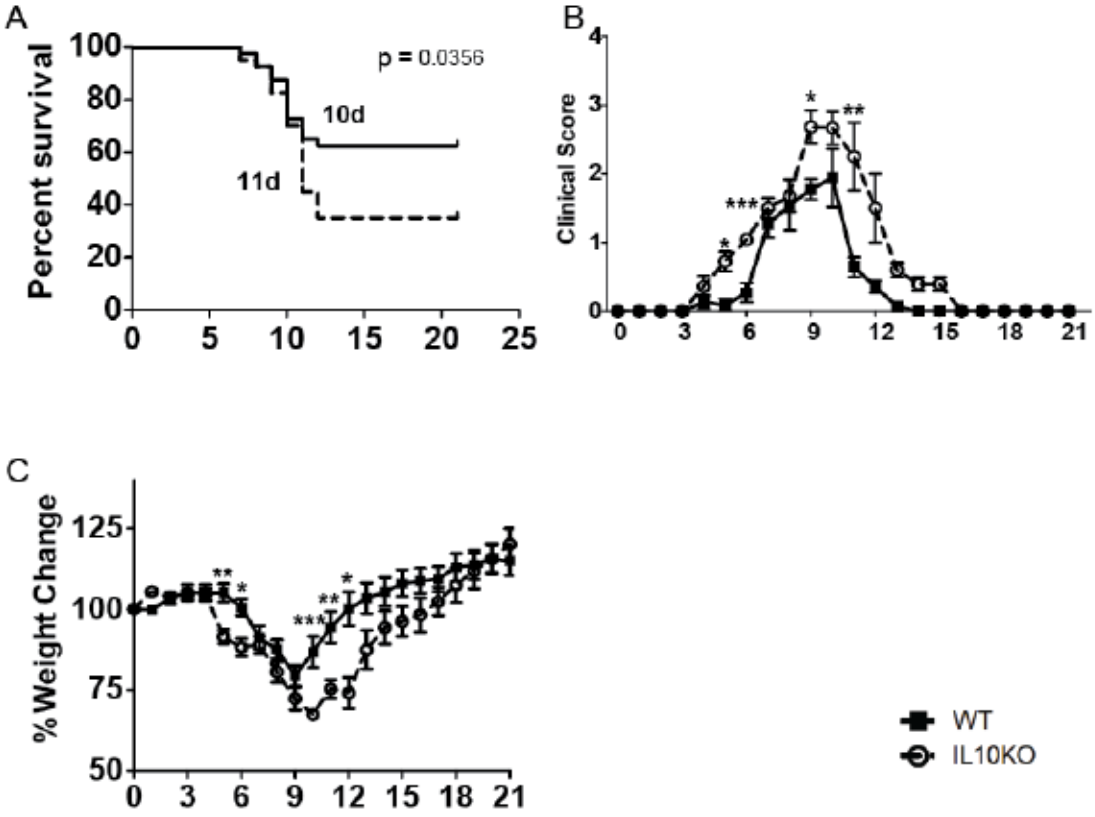

IL-10 is important in regulating disease progression. (A) Survival was assessed using a Kaplan–Meier curve and log-rank (Mantel Cox) test. Median day of survival was calculated for WT (10 dpi) and IL10KO (11 dpi) mice. Data are pooled from three independent experiments to achieve a total of n = 40 for each group. p = .0356 (log rank test). (B) Signs of disease in WT and IL10KO mice infected with TE12 were monitored daily. The clinical score scale was as follows: 0, no symptoms; 1, abnormal hind-limb and tail posture, ruffled fur, and/or hunched back; 2, unilateral hind-limb paralysis; 3, bilateral hind-limb paralysis and/or moribund; 4, dead. (C) Percent weight change was assessed by comparing daily measured weights to original weight of individual mice. Data are pooled from three independent experiments for a total of n = 40 for both groups and presented as the mean ± SEM; *p < .05, **p < .01, ***p < 0.001.

Figure 3.5.3 IL-10 deficiency delays viral clearance and increases viral RNA in brain and spinal cord tissues

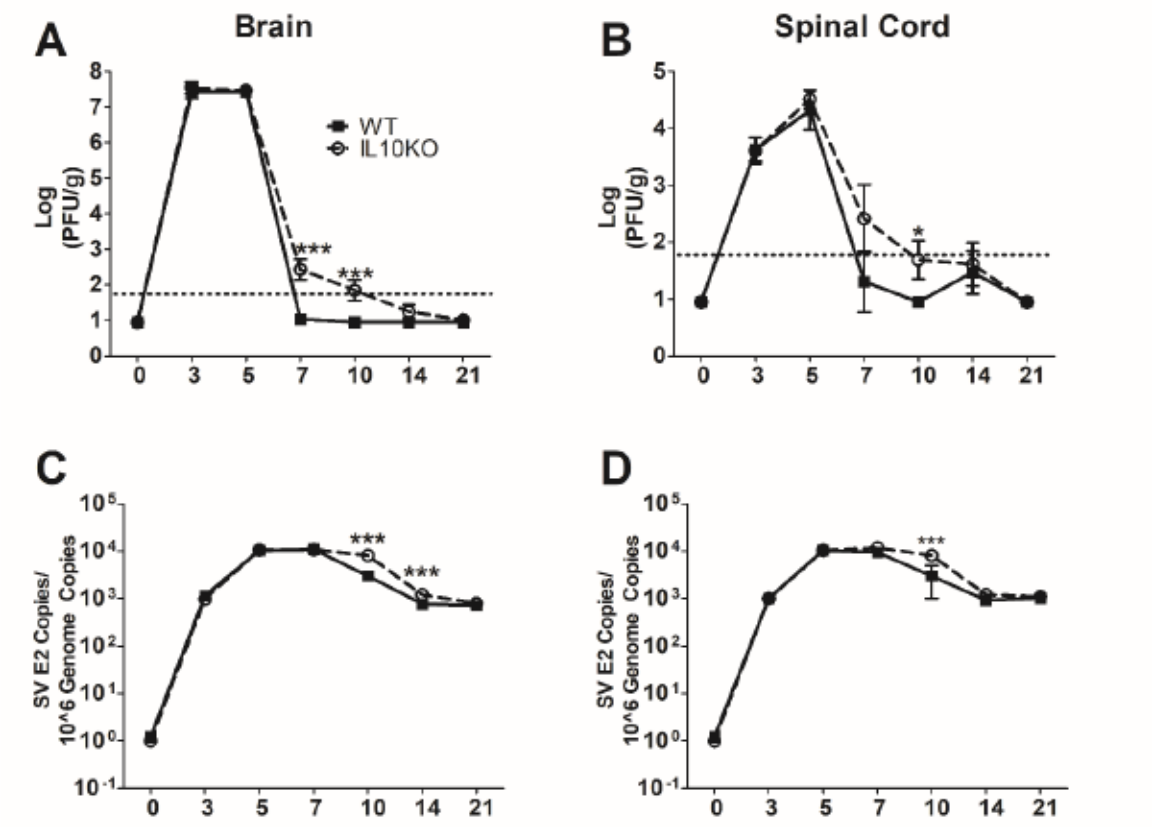

IL-10 is important in viral replication and clearance. (A and B) Virus titers were determined using brain (A) or spinal cord (B) homogenates prepared from WT (filled square, solid line) and IL10KO (open circle, dashed line) mice. Data are pooled from three independent experiments and presented as the mean ± SEM of 6 mice at each time point; * $p < .05$, ** $p < 0.01$, *** $p < .001$. The limit of detection was calculated and displayed as the horizontal dotted line. Some data points are below the limit detection because for that time point, some mice had no plaque growth while others had plaque growth. For statistical analysis, mice with 0 plaque growth were recalculated and entered as a number midway between the limit of detection and zero. (C and D) Viral RNA copy numbers were determined via PCR of RNA isolated from brain (C) or spinal cord (D) tissues. Data are pooled from three independent experiments and presented as the mean ± SEM of 6 mice at each time point; ** $p < 0.01$, *** $p < .001$.

Figure 3.5.4 IL-10 deficiency impacts TGFβ1 but not TGFβ3 protein expression

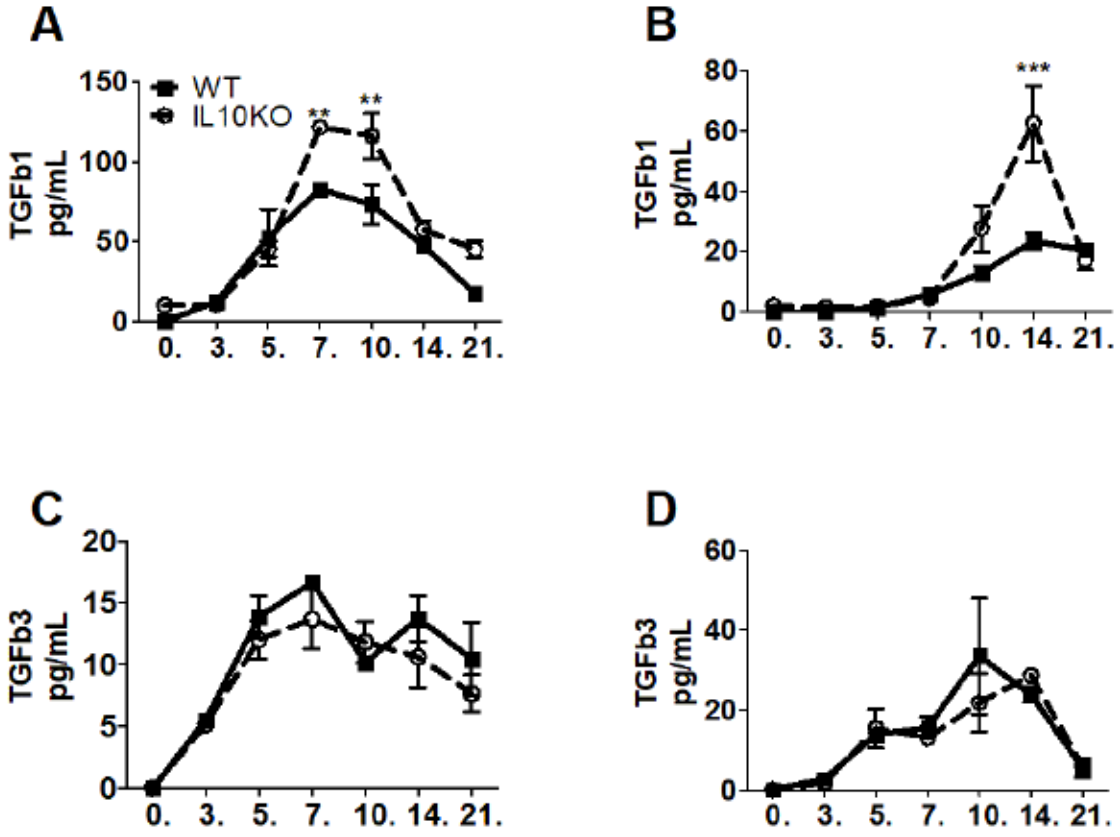

In the absence of IL-10, more TGFβ1 and TGFβ3 proteins are produced. (A-B) Protein levels of TGFβ1 and TGFβ3 were measured in brain (A & C) and spinal cord (B & D) tissues via EIA. Data were pooled from 2 independent experiments and represent the means ± SEM for 6 mice at each time point; *$p < 0.05$, **$p < .01$, ***$p < 0.001$

Figure 3.5.5 IL-10 deficiency alters number of CD3 T cells in CNS

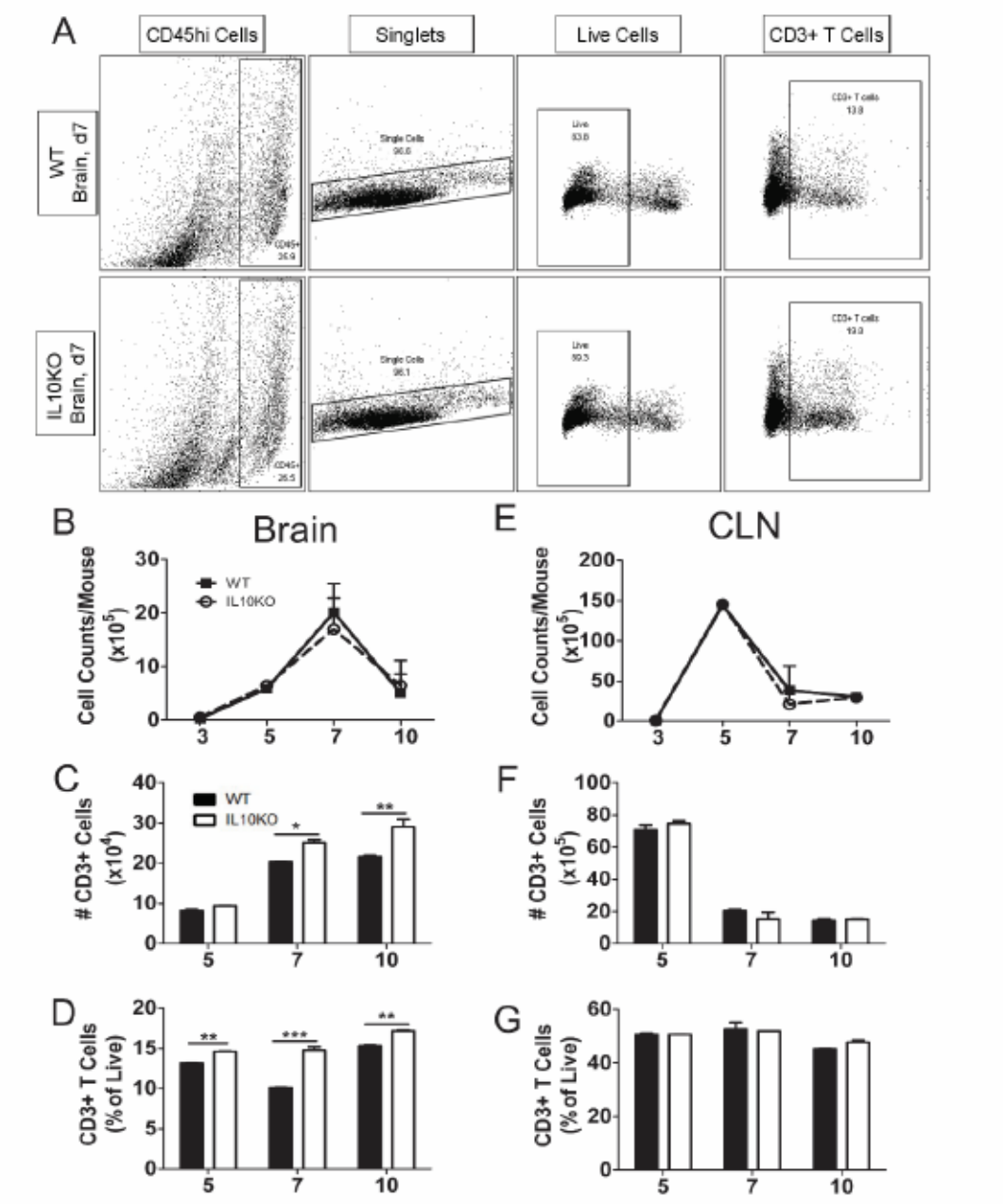

(A-G) Flow cytometric analysis of isolated cells pooled from the brains (n = 10) of WT (black bars) or IL10KO (white bars) mice at 5 (n = 6), 7 (n = 10), and 10 (n = 10) days post infection. Representative flow cytometry plots of cells isolated from WT or IL10KO are shown in (A). Total numbers of cells isolated from brains of WT and IL10KO mice were not different in brain (B) or CLN (E). Number (C) and percent (D) of CD3+ T cells were increased in IL10KO mice. In CLN, number (F0 and percent (G) CD3+ T cells were not different. The data represent the mean ± SEM from three independent experiments; *p <.05, **p < .01, ***p < 0.001.

Figure 3.5.6 IL-10 deficiency increased numbers of CD4+ helper T cells in the CNS

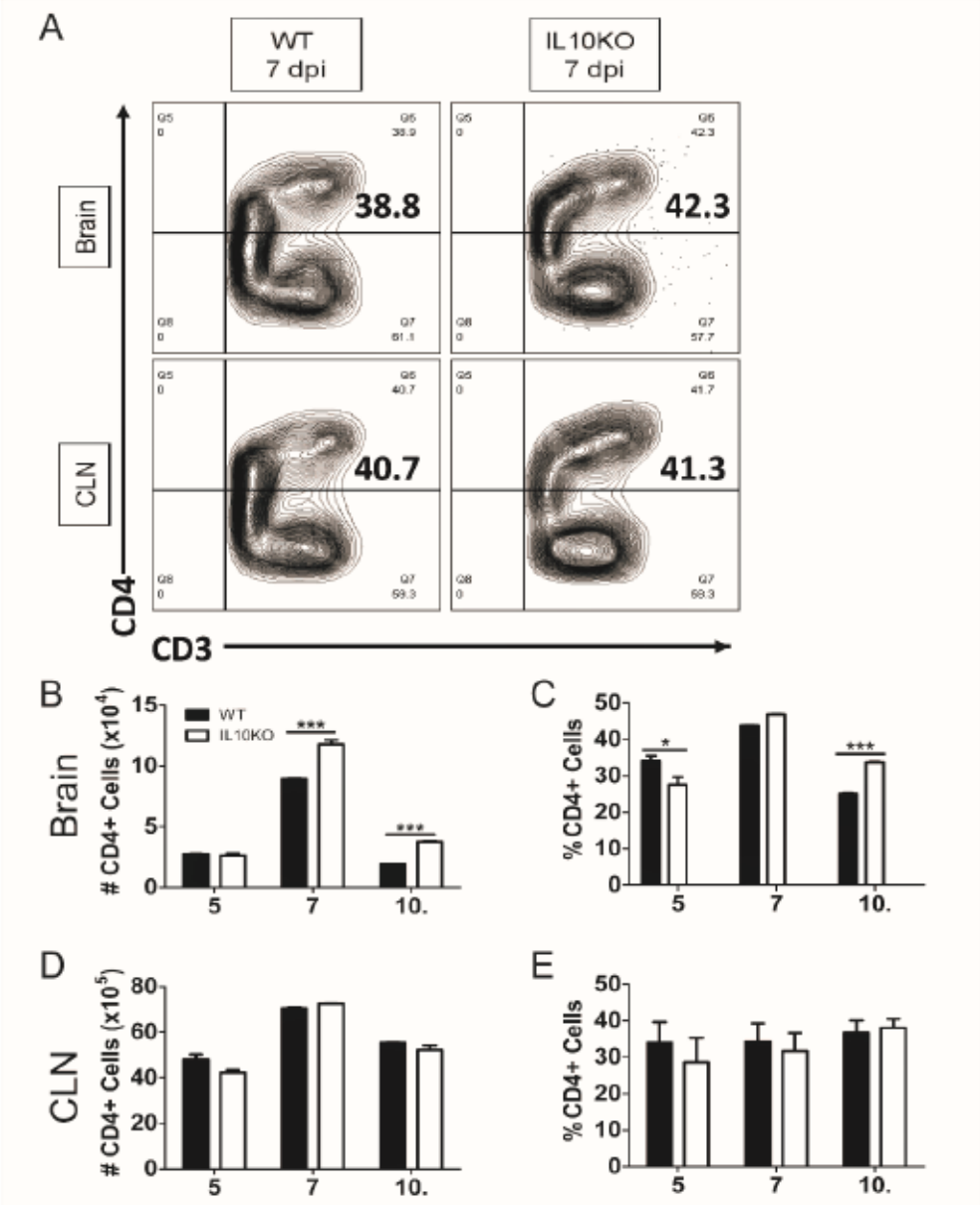

IL-10 deficiency impacts number of CD4+ T cells in the CNS. (A-E) Flow cytometric analysis of isolated cells pooled from the brains (n = 10) of WT (black bars) or IL10KO (white bars) mice at 5 (n = 6), 7 (n = 10), and 10 (n = 10) days post infection. Representative flow cytometry plots of cells isolated from WT or IL10KO are shown in (A). In brain, CD4+ T cell number (B) and percent (C) of CD3+ cells were increased in IL10KO mice. In CLN, CD4+ T cell number (D) and percent of CD3+ T cells (E) were not different. The data represent the mean ± SEM from three independent experiments; *p <.05, **p < .01, ***p < 0.001.

Figure 3.5.7 IL-10 deficiency increases numbers, but not percent of CD8+ T cells in the CNS

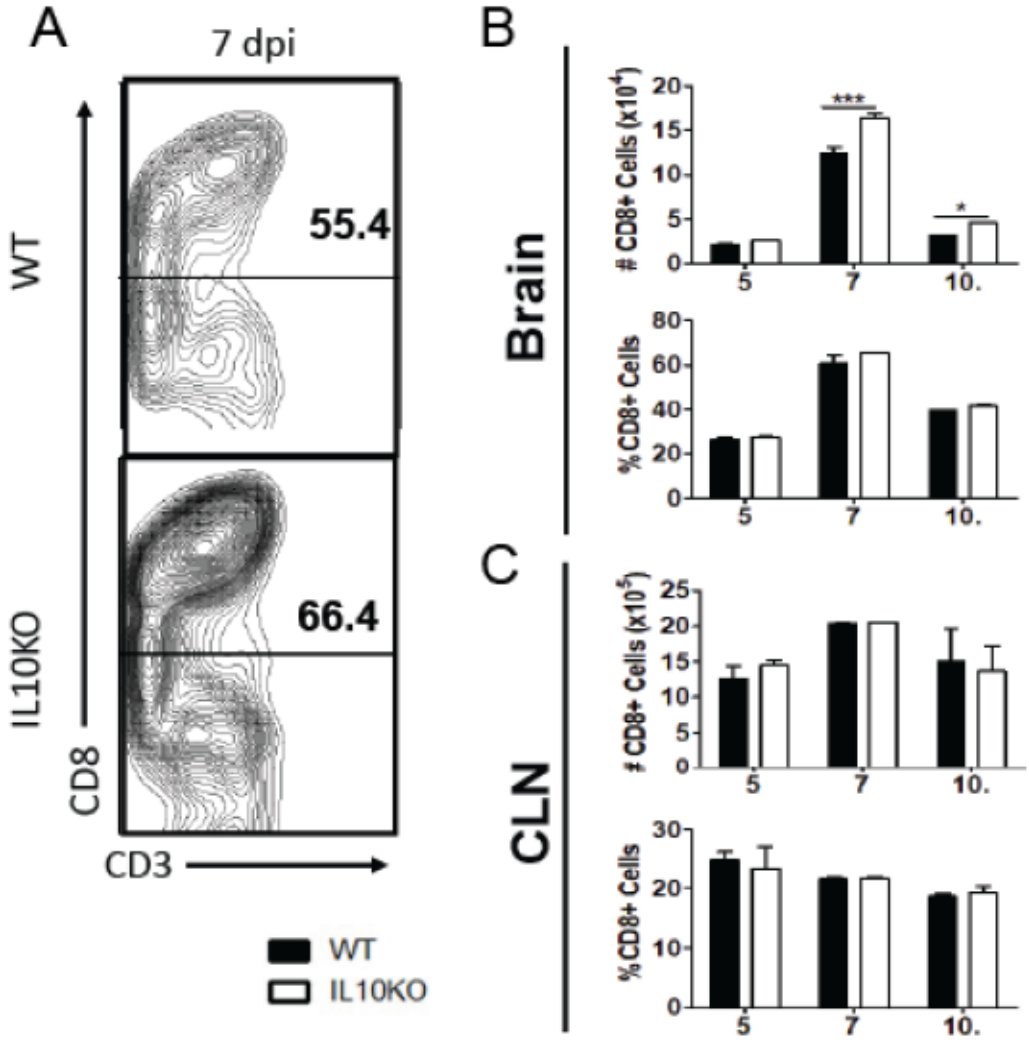

IL-10 deficiency alters recruitment of CD8+ T cells from CLN into CNS. (A-F) Flow cytometric analysis of isolated cells pooled from the brains of WT (black bars) or IL10KO (white bars) mice at 5 (n = 6), 7 (n = 10), and 10 (n = 10) days post infection. Representative flow cytometry plots of cells isolated from WT or IL10KO are shown (A). Number (B, top), but not percent (B, bottom) of CD8+ cells were altered. The number (C, top) and percent (C, bottom) of CD8+ T cells in CLN were not different. The data represent the mean ± SEM from three independent experiments; *p <.05, **p < .01, ***p < 0.001.

Figure 3.5.8 IL-10 deficiency decreases regulatory T cell response in CLN and brain tissues from TE12 infected mice

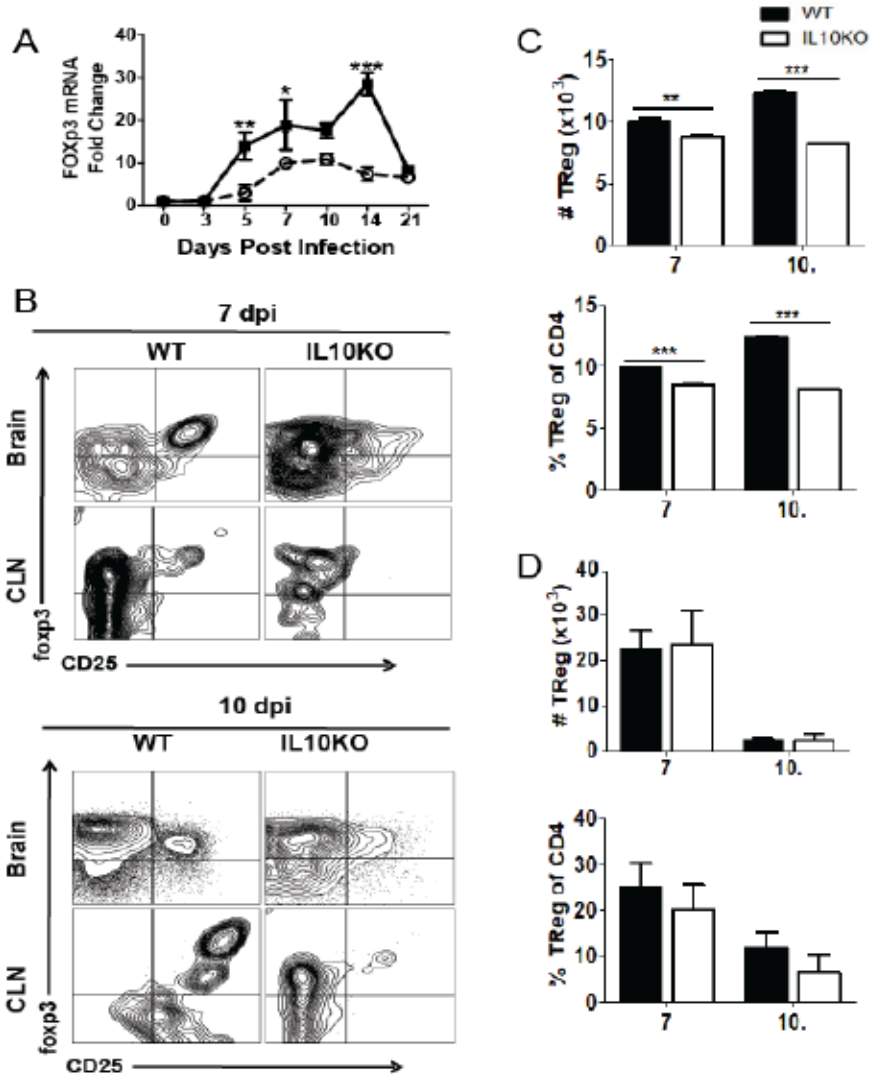

IL-10 deficiency impairs the regulatory T cell response. (A) Analysis of foxP3 mRNA expression in the brains of WT (filled square, solid line) and IL-10KO (open circle, dashed line) mice during TE12 infection. Gene Ct values were normalized to GAPDH, and fold change was calculated relative to uninfected controls (ΔΔCt). Data are pooled from two independent experiments and presented as the mean ± SEM from 6 mice at each time point; *p < .05, **p < .01, ***p < 0.001. (B-D) Flow cytometric analysis of isolated cells pooled from the brains (n = 10) of WT (black bars) or IL10KO (white bars) mice at 7 and 10 days post infection. Regulatory T cells were defined as CD3+CD4+CD25+foxP3+ cells. Representative flow cytometry plots are shown in (B). The frequency and percent of CD4+ cells were determined in brain (C) and CLN (D). The data represent the mean ± SEM from three independent experiments; **p < .01, ***P < 0.001.

Figure 3.5.9 IL-10 deficiency impacts the TH1 related response

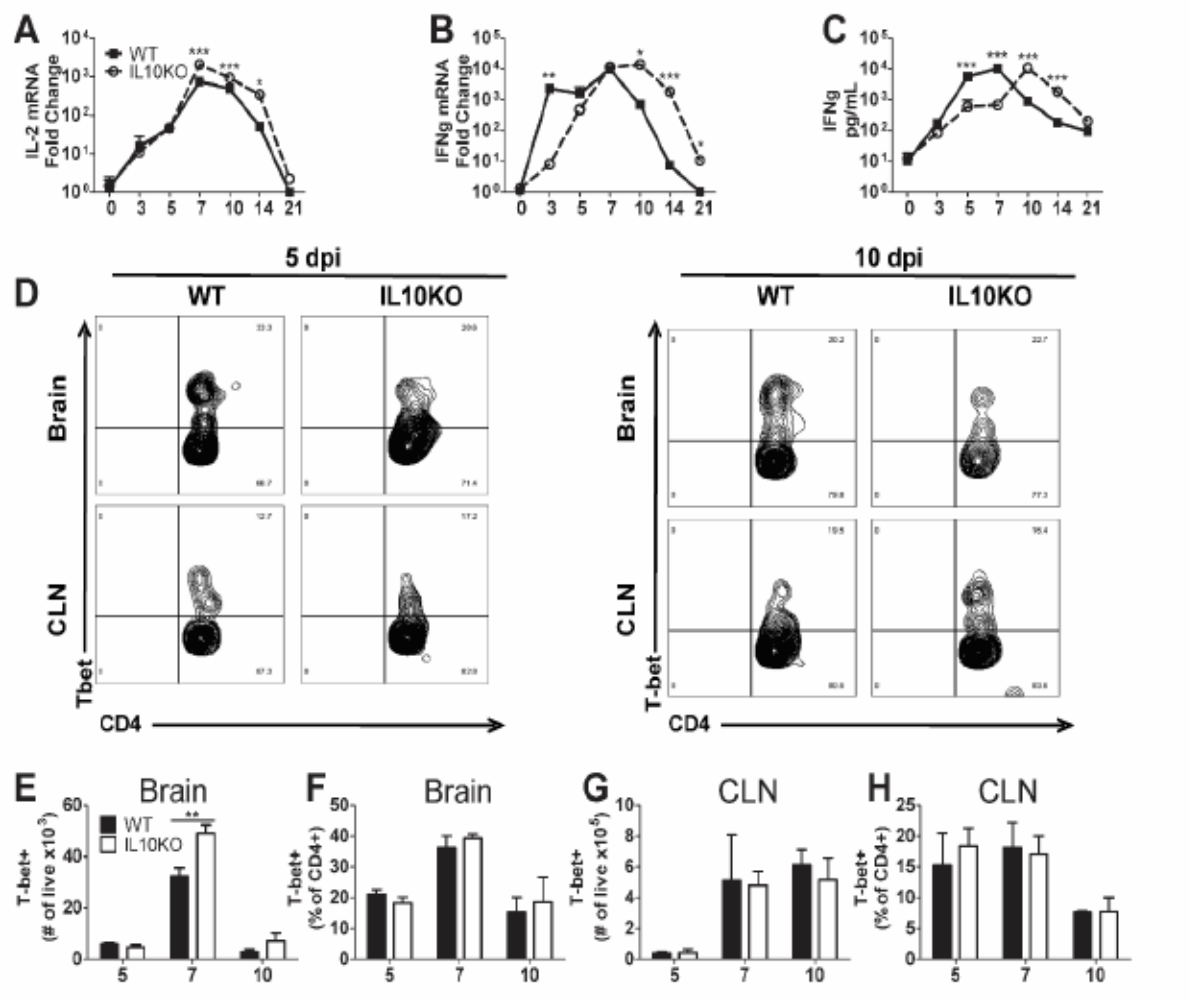

Analysis of IL-2 (A) and IFNγ (B) mRNA expression in the brains of WT (filled square, solid line) and IL-10KO (open circle, dashed line) mice during TE12 infection. Gene Ct values were normalized to GAPDH, and fold change was calculated relative to uninfected controls (ΔΔCt). Data are pooled from three independent experiments and presented as the mean ± SEM from 6 mice at each time point. *p <.05, **p < 0.01, ***p < 0.001. Analysis of IFN protein via EIA in the brains of WT (filled square, solid line) and IL-10KO (open circle, dashed line) mice during TE12 infection. Data are pooled from three independent experiments and presented as the mean ± SEM from 6 mice at each time point. ***p < 0.001. (D-H) Flow cytometric analysis of isolated cells pooled from the brains (n = 6) of WT (black bars) or IL10KO (white bars) mice at 5, 7 and 10 days post infection. TH1 cells were defined as CD3+CD4+ T cells expressing T-bet. Representative flow cytometry plots are shown in (D). The frequency and percent of CD4+ T cells in brain (D) and CLN (E) were determined. The data represent the mean ± SEM from two independent experiments. **p < .01.

Figure 3.5.10 IL-10 deficiency in TE12 infected mice does not alter type 17 immune response in brain and CLN tissues

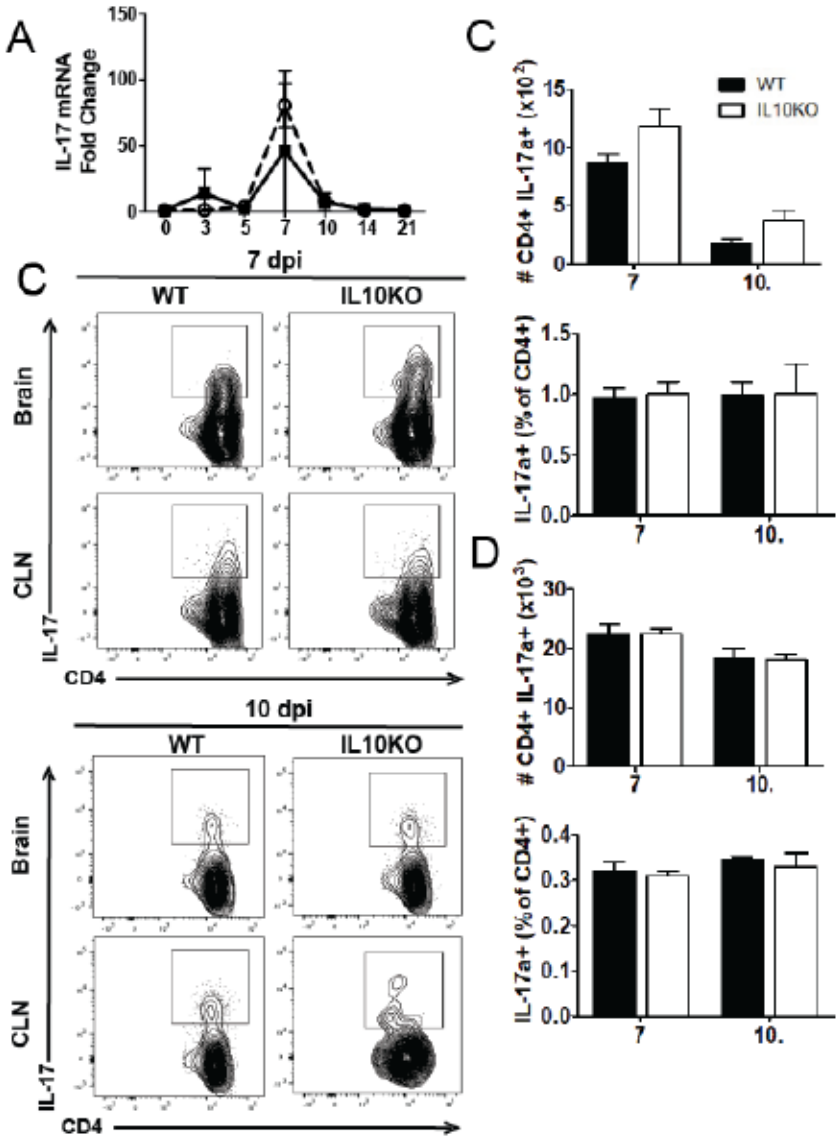

IL-10 deficiency does not alter TH17 response post TE12 infection. (A) Analysis of IL-17a mRNA expression in the brains of WT (filled square, solid line) and IL-10KO (open circle, dashed line) mice during TE12 infection. Gene Ct values were normalized to GAPDH, and fold change was calculated relative to uninfected controls (ΔΔCt). Data are pooled from two independent experiments and presented as the mean ± SEM from 6 mice at each time point. (B-D) Flow cytometric analysis of isolated cells pooled from the brains (n = 10) of WT (black bars) or IL10KO (white bars) mice at 7 and 10 days post infection. TH17 cells were defined as CD3+CD4+ T cells producing IL-17a. A representative flow cytometry plot is shown in (B). The percent of CD4+ T cells in brain (C) and CLN (D) were determined. The data represent the mean ± SEM from three independent experiments

Figure 3.5.11 IL-10 deficiency decreases the TH2 related response

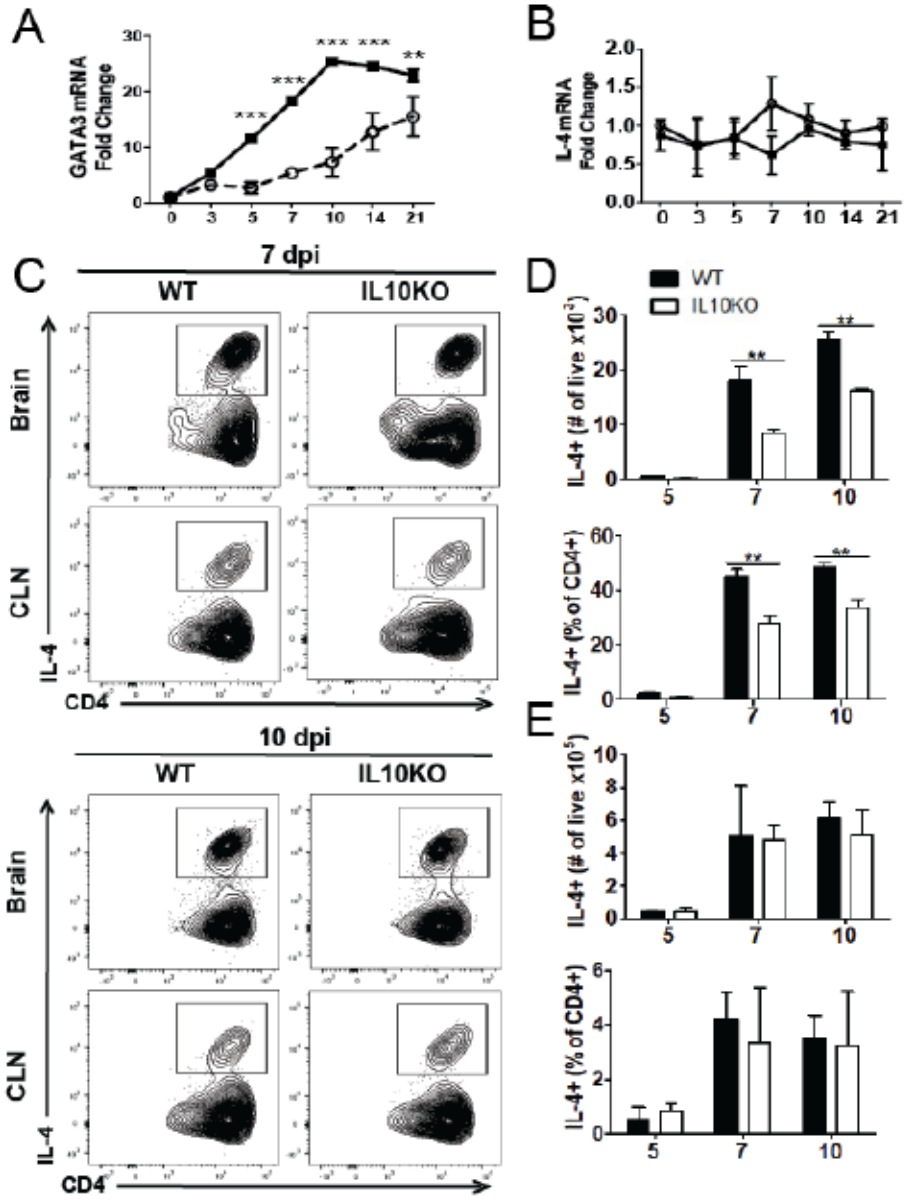

Analysis of GATA3 (A) and IL-4 (B) mRNA expression in the brains of WT (filled square, solid line) and IL-10KO (open circle, dashed line) mice during TE12 infection. Gene Ct values were normalized to GAPDH, and fold change was calculated relative to uninfected controls (ΔΔCt). Data are pooled from three independent experiments and presented as the mean ± SEM from 6 mice at each time point. **$p < 0.01$, ***$p < 0.001$. (C-E) Flow cytometric analysis of isolated cells pooled from the brains WT (black bars) or IL10KO (white bars) mice at 5 (n = 6), 7 (n = 10) and 10 (n = 10) days post infection. TH2 cells were defined as CD3+CD4+ T cells producing IL-4. A representative flow cytometry plot is shown in (C). The frequency and percent of CD4+ T cells in brain (D) and CLN (E) were determined. The data represent the mean ± SEM from three independent experiments. *$p < .05$.

Figure 3.5.12 IL-10 deficiency leads to lower numbers of ILC2s in the CNS

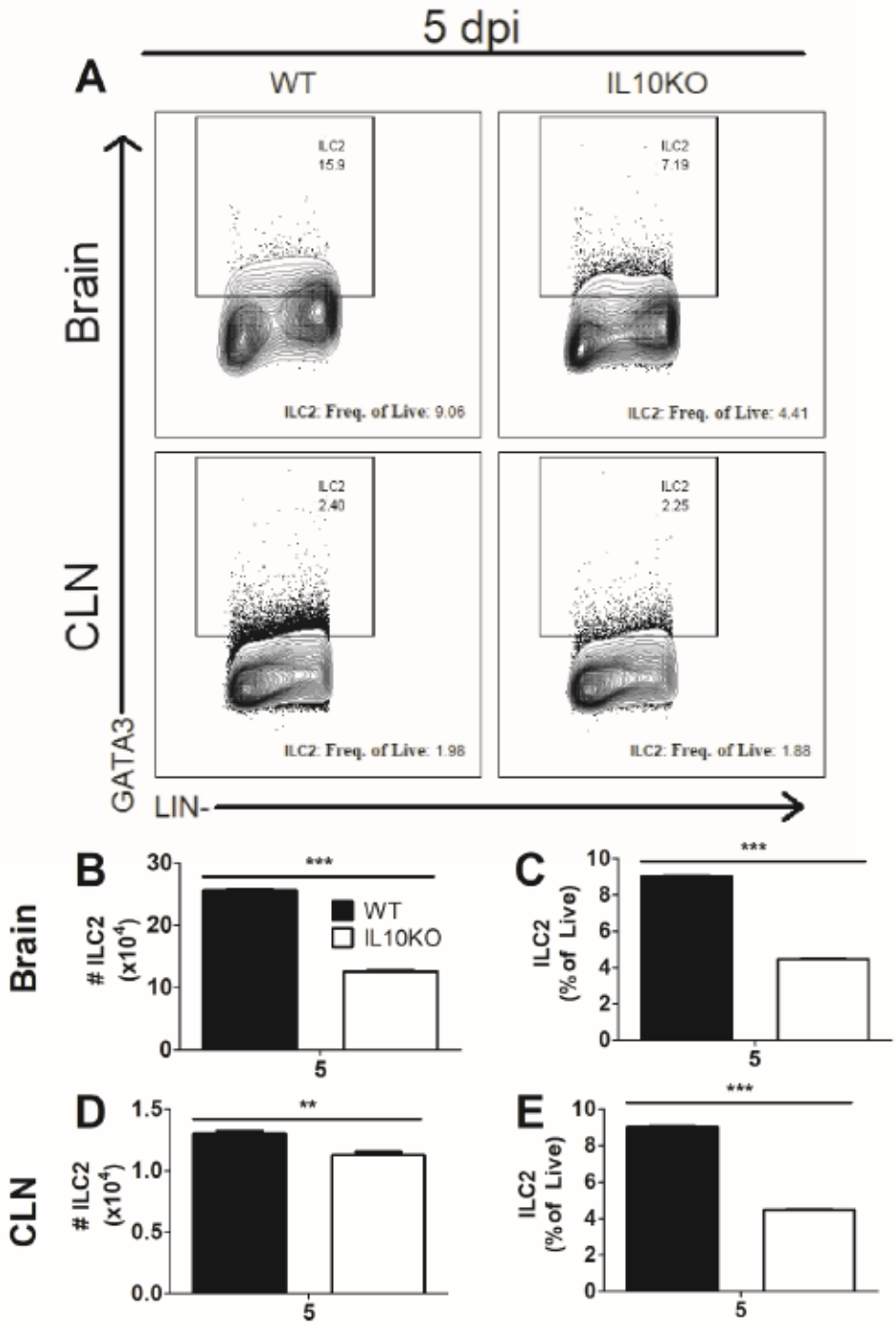

(A-E) Flow cytometric analysis of isolated cells pooled from the brains and CLN of 10 WT (black bars) and IL10KO (white bars) mice at 5 days post infection. ILC2 cells were defined as IL-7Ra+, Lineage-, Gata3+ cells. A representative flow cytometry plot is shown in (A). The frequency and percent of ILC2s in brain (B, C) and CLN (D, E) were determined. The data represent the mean ± SEM from three independent experiments. **p < .01, ***p <.001.

Figure 3.5.13 IL-10 deficiency leads to lower antibody production in the CNS

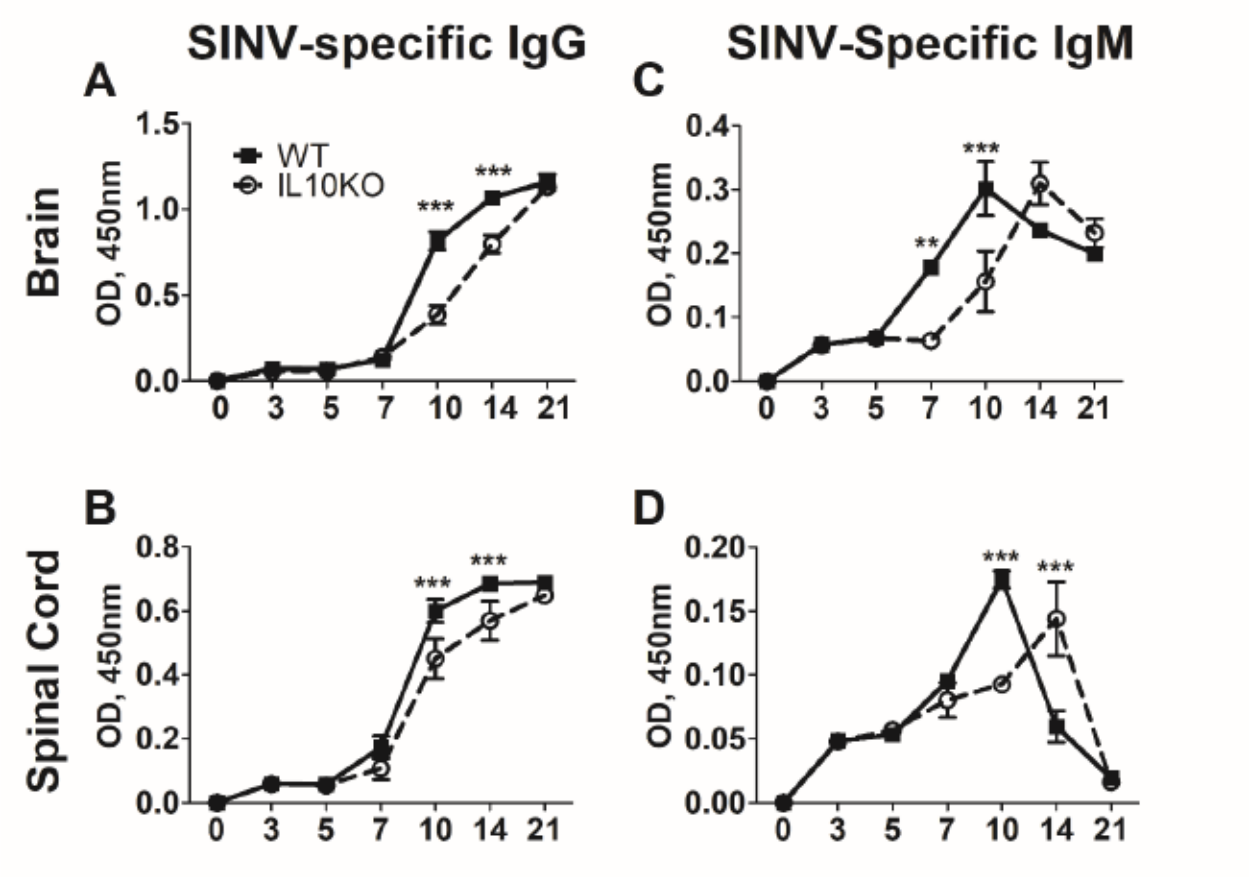

(A-D) Analysis of SINV-specific IgG (total) and IgM antibodies via EIA from WT (filled square, solid line) and IL10KO (open circle, dashed line) mice. Data were pooled from 2 independent experiments and represent the means ± SEM for 6 mice at each time point; ***$p < 0.001$. SINV-specific IgG1 from brain (A) and spinal cords (B). SINV-specific IgM from brain (C) and spinal cord (D).

Figure 3.5.14 IL-10 deficiency leads to lower numbers of CD19+ B cells in the CNS

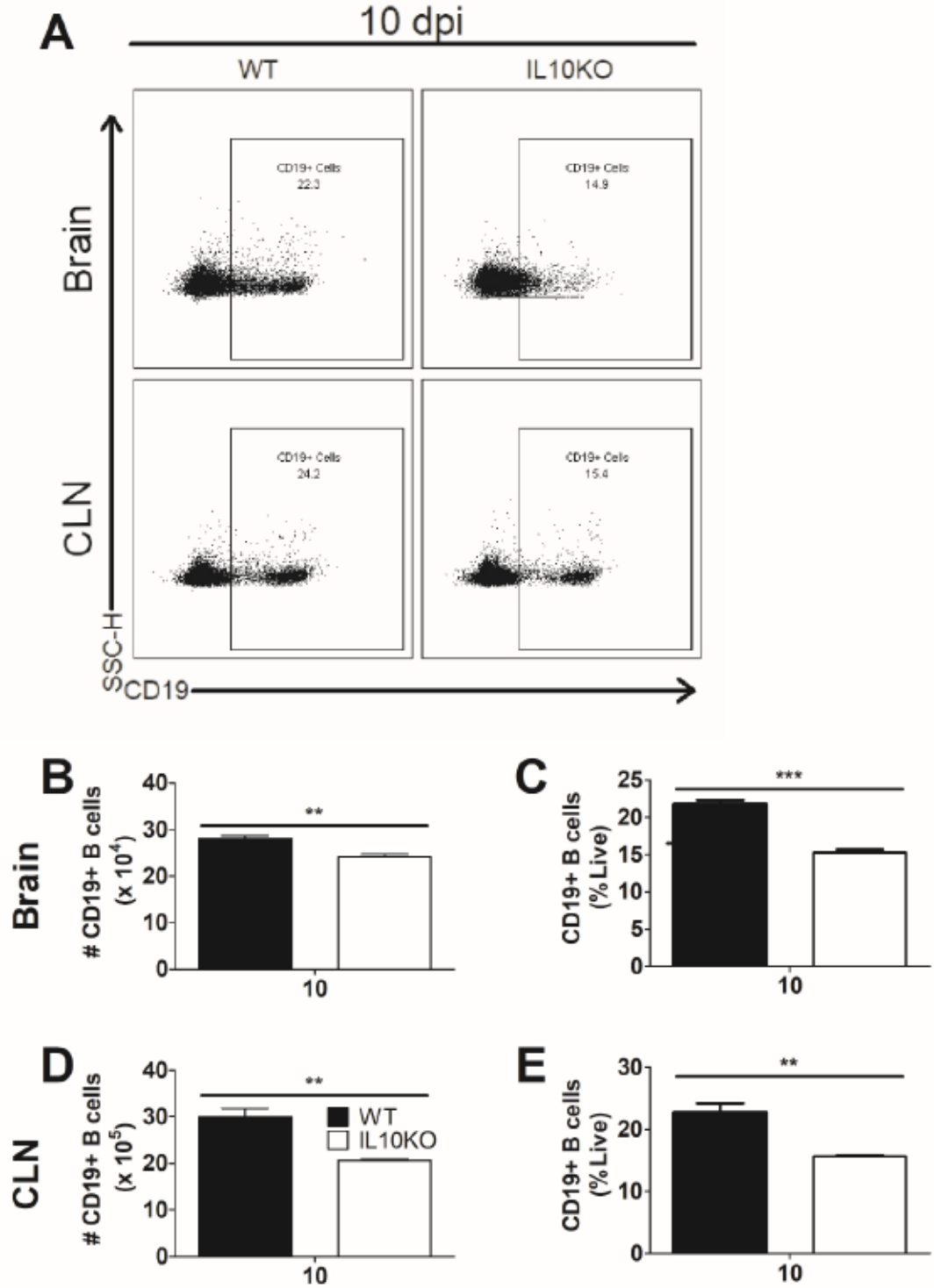

(A-E) Flow cytometric analysis of isolated cells pooled from the brains and CLN of 10 WT (black bars) and IL10KO (white bars) mice at 10 days post infection. A representative flow cytometry plot is shown in (A). The frequency and percent of CD19+ B cells in brain (B, C) and CLN (D, E) were determined. The data represent the mean ± SEM from three independent experiments. **p < .01, ***p <.001.

Figure 3.5.15 IL-10 deficiency leads to lower numbers of B Regs in the CNS

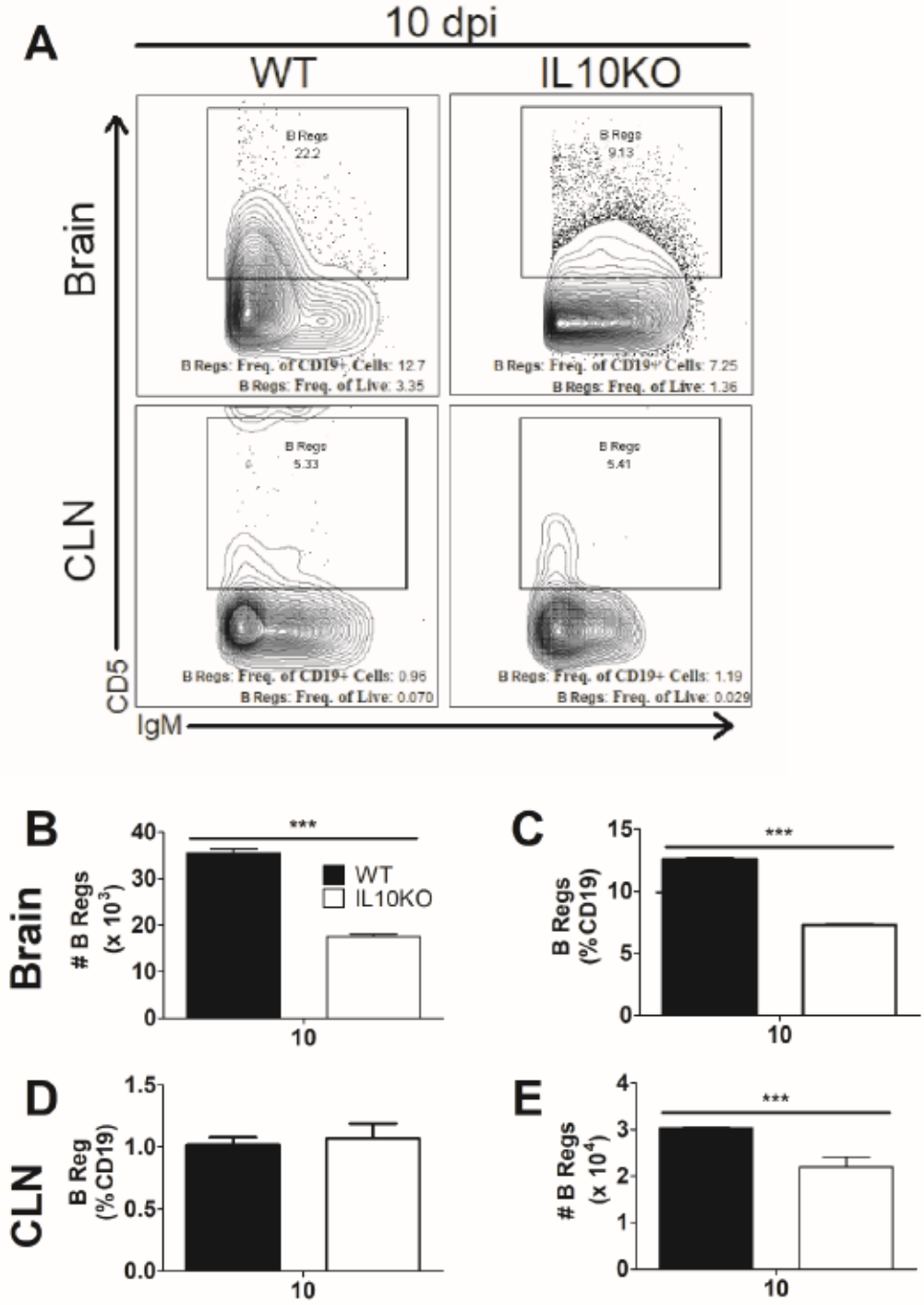

(A-E) Flow cytometric analysis of isolated cells pooled from the brains and CLN of 10 WT (black bars) and IL10KO (white bars) mice at 10 days post infection. A representative flow cytometry plot is shown in (A). Regulatory B cells are defined as CD19+ CD1dhi CD5+ IgM+ cells. The frequency and percent of B Regs in brain (B, C) and CLN (D, E) were determined. The data represent the mean ± SEM from three independent experiments. **p < .01, ***p <.001.

CHAPTER 4

TGFβ MODULATION OF IMMUNOPATHOGENESIS DURING AVIRULENT ALPHAVIRAL ENCEPHALOMYELITIS IN IL-10 DEFICIENT MICE

Nina M Martin, Diane E Griffin

ABSTRACT

Sindbis virus (SINV) strains of varying virulence have been produced to study factors leading to survival versus death during alphaviral encephalomyelitis. The avirulent strain of SINV, TE, has been used to study mechanisms that govern viral clearance and persistence. To date, the role of IL-10 during avirulent SINV infection represents a significant gap in our understanding of viral pathogenesis. In the absence of IL-10, mice infected with TE displayed clinical signs more quickly and for a prolonged period compared to WT controls. In addition, viral clearance was delayed in IL10KO mice. In response to infection, TE infection resulted in an up-regulation of TGFβ1 but not TGFβ3 in IL-10KO. There were no differences in IL-17 and TH17 responses, but IL-10 deficient mice had decreased B cell and regulatory T cell responses in the brain. These data support the hypothesis that TGFβ3 is more important than TGFβ1 for differentiation of pathogenic TH17 cells and immunopathology.

4.1 INTRODUCTION

Mosquito-borne diseases are a major global health threat that can lead to arthritis, fevers, neurological deficits, and death. Arthropod-borne viruses include New World alphaviruses, which are an important cause of viral encephalitis, an inflammatory disease of the CNS. Western, Eastern, and Venezuelan Equine Encephalitis are examples and are the cause of seasonal disease as well as periodic outbreaks of epidemic proportions [5, 106, 108, 148, 149, 172-174]. These diseases have high fatality rates and often leave survivors with permanent neurological deficits. Patients with viral encephalitis can only be placed on supportive care, there are no treatments available.

Sindbis virus (SINV) is a prototypical alphavirus with a positive sense RNA genome. SINV causes fever, rash, and arthritis in humans. In mice, SINV infects neurons and causes acute encephalomyelitis. The severity of disease is impacted by a range of host and virus factors, including age and genetic background, as well as virus strain [16, 19]. AR339 is the original isolate of SINV and causes fatal encephalomyelitis in newborn, but not adult mice. Neuroadapted SINV (NSV) was isolated after intracerebral serial passaging of AR339 in mice and causes severe and fatal encephalomyelitis in adult, C57Bl/6 mice. Fatal infection is associated with motor neuron cell death, a primary target of SINV infection. Recombinant avirulent strains of SINV have been created which allow the study of host and viral factors that mediate clearance of infectious virus and RNA. TE is an avirulent, recombinant strain that contains the E2 gene from NSV and the E1 gene from AR339 on an avirulent TOTO1101 background

[10]. TE causes mild encephalomyelitis in adult C57Bl/6 mice, with mice recovering from infection during the same time period that NSV-infected mice succumb due to CNS damage at about 7 to 10 days post-infection.

Studies with TE and NSV have shown that antibody and IFNγ made by T cells are essential for virus clearance while T cells are also implicated in immunopathology [30, 36, 113]. The deactivation and depletion of T cells and other inflammatory factors after CNS infection allow survival [113]. It is therefore important to understand how the immune response is regulated during SINV infection.

Interleukin-10 (IL-10) is a suppressor of inflammation and its dysregulation has been implicated in many diseases. Studies using influenza virus, experimental autoimmune encephalitis, trypanosome, plasmodium, listeria, mouse CMV, and hepatitis highlight a crucial role for IL-10 in limiting pathology caused by otherwise unchecked T cell responses [57, 58, 153, 175, 176]. These results are similar to observations of naturally occurring entercolitis in IL-10 knockout mice cause by uncontrolled T cell responses directed against gut flora [49]. IL-10 has pleiotropic effects in inflammation and regulation of immunity. IL-10 signaling results in the down-regulation in the expression of IL-12 by antigen-presenting cells thus effecting Th1 activation and the production of Th1 cytokines such as IFNγ and TNF. Additional effects on APCs include a reduction in MHC class II and costimulatory molecule production. IL-10 also enhances B cell survival, proliferation, and antibody production. [116].

Previous studies involving IL-10-deficient C57Bl/6 mice characterized the immune response following infection with the highly virulent strain NSV [15, 17]. IL-10 deficiency led to accelerated morbidity and mortality as well as an increase in TH17 cells

and pathogenic double positive IFNγ + IL17a+ producing TH17 cells and *Il17* mRNA in the CNS. Regulatory T cells were decreased in the absence of IL-10.

Chapter 2 hypothesized that the mechanism behind this immunopathology is an up-regulation of active TGFβ in the absence of IL-10. TGFβ suppresses pro-inflammatory cytokines such as IFNγ, can promote the differentiation of TH17 cells or Tregs depending on the concentration, and suppresses B cell responses. It is also hypothesized that different isoforms of TGFβ can promote differentiation of nonpathogenic or pathogenic TH17 cells, with TGFβ3 leading to pathogenic, double positive IL-17+ IFNγ+ TH17 cells, while TGFβ1 leads to nonpathogenic TH17 cells [80].

This current study determines the role of TGFβ in the absence of IL-10 during avirulent infection. TE infection induces increased TGFβ protein, but at a much lower level than during NSV infection. This level of TGFβ leads to suppression of B cell responses, but not promote differentiation of TH17 cells. These changes were associated with delayed viral clearance and accelerated and prolonged morbidity, but mice recovered from infection.

4.2 MATERIALS AND METHODS

4.2.1 Animals and virus

C57BL/6J WT and B6.129P2-Il10tm1Cgn/J (C57BL/6J IL10KO) mice were purchased from Jackson Laboratories and bred in house. All mice were sex and age (4-6-wk-old) matched. The TE strain of SINV was grown and assayed by plaque formation in BHK cells and administered intranasally at 10^5 pfu in PBS [10]. Morbidity and mortality was scored as previously reported in [15]. Briefly, the scoring system was: 0, no signs of disease; 1, abnormal hind-limb and tail posture, ruffled fur, and/or hunched back; 2, unilateral hind-limb paralysis; 3, bilateral hind-limb paralysis or full-body paralysis; 4, dead. For collection of cervical lymph nodes, brain, or spinal cords, mice were anesthetized with isoflurane, perfused with ice-cold PBS, and tissues collected used fresh or snap frozen and stored at −80°C. All experiments were performed according to guidelines approved by the Johns Hopkins University Institutional Animal Care and Use Committee.

4.2.2 Determination of viral titer

20% weight per volume brain and spinal cord tissue homogenates were made by thawing snap frozen tissues and homogenizing in PBS. Homogenates were serially diluted in DMEM+1% FBS and plated on BHK-21 cell monolayers. The infected monolayer was incubated for 1 hour, overlaid with 1.2% bactoagar, and incubated at 37°C with 5% CO_2 for 48 hours. After 48 hours, cells were stained with neutral red and plaques were counted. Each time point represents the mean of the $\log_{10}$ value of plaque

forming units per gram ± SEM. Samples in which no virus was detected at a 1:10 dilution were given a value midway between zero and the limit of detection for statistical analysis.

4.2.3 Mononuclear cell isolation

Mononuclear cells were isolated from brains and cervical lymph nodes collected from 6-10 WT or IL10KO mice at 5, 7, and 10 days post-infection unless otherwise noted. Cervical lymph nodes were pooled from 6-10 mice per group per time point in 10 mL of RPMI+1% FBS and homogenized in C tubes using the GentleMACS system (Miltenyi) spleen program 1 for 2 cycles. Brain tissue was collected from 6-10 mice per group per time point in ice cold Hanks Buffered Saline Solution. After tissue collection, 2 brains were pooled per C tube containing 4 mL of enzyme digest mix made up of RPMI + 1% FBS, 1 mg/mL collagenase (Roche), and 0.1 mg/mL DNase (Roche) and dissociated with scissors. Further dissociation was performed via GentleMACS (Miltenyi) brain program 3 (total of 5x with 2, 15 minute 37°C incubations with gentle rocking). All suspensions were filtered through 70 µm cell strainers and centrifuged. Red blood cells were lysed using 2 mL of red blood cell lysis buffer (Sigma #R-7757) for 3 minutes and then washed with PBS.

To remove debris, pellets were resuspended in 30% percoll, underlaid with 70% percoll for a 30/70% gradient and centrifuged for 30 minutes at 850xg at 4°C. The top debris layer was aspirated off and mononuclear cells at the interface were collected and washed with PBS + 2 mM EDTA. Pellets were suspended in PBS + 2 mM EDTA and live cells were counted using trypan blue exclusion.

4.2.4 Identification of cells by flow cytometry

To determine the number and type of infiltrating cells, ~1x10^6 cells were used for each panel. The cells were stained with a violet live/dead stain (Invitrogen #L345955), blocked with rat anti-mouse CD16/CD32 Block (BD #553142), surface stained for phenotyping, and then fixed using 1:1 dilution of 4% paraformaldehyde and FACS buffer, and data acquired.

The surface markers used were CD45-FITC (BD), CD3-APC (BD), CD4-PerCpCy5.5 (BD), CD8-PECy7 (BD), CD25-PE (BD), CD19-PerCPCy5.5 (eBiosciences). Cell types were defined as follows: T cells (CD3+), CD4 T cells (CD3+CD4+), CD8 T cells (CD3+CD8+), B cells (CD19+). Data was acquired using the BD FACS Canto II flow cytometer and FACS Diva software, and analyzed using FlowJo (v10.3.0).

4.2.5 Transcription factor staining by flow cytometry

For determination of T cell differentiation, transcription factors were assayed using Foxp3 Buffer Set (eBiosciences). After surface staining, cells were fixed, permeablized, and stained for GATA3, foxP3, RORγt, or Tbet. Cells were defined as follows: regulatory T cells (CD3+CD4+CD25+foxp3+), TH17 cells (CD3+CD4+RORgt+), TH1 cells (CD3+CD4+Tbet+).

4.2.6 Intracellular cytokine staining by flow cytometry

For determination of T cell cytokine production, 2-3x10^6 cells were stimulated with RPMI + 1% FBS containing 50 ng/mL of phorbol-12-myristate 13-acetate (PMA) and 1 µg/mL of ionomycin in the presence of GolgiPlug (BD #555029) for 4 hours. Cells were then washed and stained with the violet live/dead marker (Invitrogen #L345955), blocked with rat anti-mouse CD16/CD32 Block (BD #553142), and then stained for the surface markers for Helper T cells (CD3-APC and CD4-FITC). After surface staining, cells were fixed and permeabilzed using the BD CytoFix/CytoPerm kit (BD #554714). In CD4+ T cells, cytokine staining was performed either by itself or in conjunction with transcription factor staining. Cells were stained for IFNγ-PE, TGFb1-PE or IL-17a-PE. Cells were washed, suspended in FACS buffer and acquired using the BD FACS Canto II and FACS Diva, and analyzed using FlowJo software (v10.3.0).

4.2.7 Gene expression analysis using real-time PCR

RNA was extracted from snap frozen tissues using the RNeasy Lipid Mini RNA Isolation Kit (Qiagen #74804). After quantification via nanodrop, 500 ng of RNA was used to synthesize cDNA via High Capacity cDNA Reverse Transcription Kit (Life Technologies #4368814). Quantitative real-time PCR was performed using 2.5 µl of cDNA and TaqMan gene expression arrays in 2x Universal PCR Mastermix (Applied Biosystems, #4304437). The TaqMan gene expression arrays used were *Ifnγ, Il12b, Il18, Il10, Il17a, gata3*, and *foxp3*. *Gapdh* mRNA levels were determined using the rodent primer and probe set (Applied Biosystems, #4308313). All reactions were run on the Applied Biosystems 7500 Real-time PCR machine. Transcript levels were determined by

normalizing the target gene Ct value to the Ct value of the endogenous housekeeping gene Gapdh. This normalized value was used to calculate the fold-change relative to the average of the uninfected control (ΔΔCt method).

4.2.8 Statistical analysis

Unless otherwise noted, data from three independent experiments or at least 6 mice per group was used. All statistical analysis was done using GraphPad Prism 5 (v5.01). Survival was calculated using Kaplan-Meier survival curves [Log rank (Mantel Cox) Test]. Differences between groups during the course of infection were determined using a 2-way ANOVA and Bonferroni post-tests to compare the difference between groups at each time point (morbidity, cellular infiltrates, cytokine analysis, and viral titers).

4.3 RESULTS

4.3.1 IL-10 mRNA expression increases during TE infection

To determine if IL-10 is up-regulated post-TE infection, mRNA expression change compared to uninfected controls was measured during the course of infection in the brains and spinal cords of C57Bl/6 mice. *Il10* gene expression increases at day 3, peaks at day 10, and remains elevated out to 21 days post-infection in brain (Figure 4.5.1A). In the spinal cord, *Il10* gene expression begins to increase day 3 post-infection, peaks at day 5, and drops to low, but detectable levels at days 14 and 21 (Figure 4.5.1B).

4.3.2 IL-10 deficiency leads to accelerated and prolonged morbidity

To assess the effect of IL-10 deficiency on clinical outcomes, WT and IL10KO mice were infected with TE and assessed daily for weight, clinical score, and mortality. IL-10 deficiency did not alter survival as all mice survived infection, but did impact morbidity (Figure 4.5.2.A). IL10KO mice displayed clinical signs earlier than WT control mice for a longer period of time. Increased severity of disease was also indicated by percent weight change (Figure 4.5.2.B). IL10KO mice lost more weight than WT mice and took longer to regain weight during recovery.

4.3.3 IL-10 deficiency leads to delayed viral clearance and increased viral RNA

Next, we assessed the impact of IL-10 deficiency on viral replication, clearance, and viral RNA load. Increases in infectious virus occurred with the same kinetics at the

start of infection and the peak viral titers were similar between groups (Figure 4.5.3.A). IL-10 deficiency did, however, have an impact on viral clearance. IL10KO mice cleared virus more slowly than WT mice. IL-10 deficiency also impacted clearance of viral RNA load. IL10KO mice had more viral RNA present in both the brain and spinal cord on day 10 post-infection (Figure 4.5.3.C and D).

4.5.4 IL-10 deficiency leads to increased TGFβ1, but not TGFβ3 protein

To determine if TGFβ isoforms plays a compensatory role in the absence of IL-10 during TE infection, EIA was performed to measure TGFβ1 and TGFβ3 in brains and spinal cords post-TE infection. Both TGFβ1 and TGFβ3 were increased after infection in WT and IL10KO mice, but mice lacking IL-10 had elevated levels of TGFβ1 protein in the brain and spinal chord compared to the WT control mice (Figure 5.4A and B). Although TGFβ3 protein increased post-TE infection, there were no significant differences between groups in either brain or spinal cord (Figure 4.5.4C and D). These data identify a difference with responses to NSV infection (Chapter 2). TGFb3 is not significantly different in IL10KO or WT brains during TE infection, but is higher in IL10KO mice during NSV infection.

4.3.5 IL-10 deficiency does not impact *Il17a* mRNA expression, but does impact expression of IFNγ and IL-12b cytokine mRNA

To assess the impact of IL-10 deficiency on expression of pro-inflammatory cytokines, RT-qPCR was performed to assess changes in cytokine expression. *Il17a*, *Ccl20*, *Il23*, and *Il18* mRNA expression was not impacted by the absence of IL-10

(Figure 4.5.5 A-D). Conversely, IL-10-deficient TE-infected mice had lower levels of *Ifng* mRNA on day 3 post-infection and higher levels on day 10 post-infection (Figure 4.5.5, E). *Il12b* mRNA was also increased on day 7 post-infection (Figure 4.5.5, F).

4.3.6 IL-10 deficiency impacts recruitment of T cells in the SC and CLN, but not brain post TE infection

Because IL-10 regulates T cell responses, CD3+ T cells were measured via flow cytometry on day 7 and 10 post-infection (Figure 4.5.6). Percent and number of CD3+ T cells as well as total cell counts per mouse brain were not different (Figure 4.5.7, A, B, C). In spinal cord tissues, similar numbers of total cells and CD3+ T cells per mouse were isolated from WT and IL-10 deficient mice (Figure 4.5.7, D, E). Perhaps because of large variations in numbers of CD3+ T cells, percentages of CD3+ T cells were different on both 7 and 10 days post infection (Figure 4.5.7, F). Percent of CD3+ cells were decreased on day 7 while increased on day 10 post infection in IL-10 deficient mice compared to WT controls. In CLN, a similar trend was observed (Figure 4.5.7, G, H, I). Total cell counts per mouse and numbers of CD3+ T cells were similar between WT and IL-10 deficient mice on days 7 and 10 post infection. In terms of percentages of CD3+ T cells, IL-10KO mice had increased percentages on day 7 and decreased percentages on day 10. These changes may be because of variations in number of cells isolated per mouse.

4.3.7 IL-10 deficiency alters CD4+ T cell responses in the CNS

The impact of IL-10 deficiency on CD4+ T cell responses was determined via flow cytometry for brain, spinal cords, and CLN of WT and IL10KO mice (Figure 4.5.8, A). IL-10 deficient mice had higher percentages and numbers of CD4+ T cells at 7 days in the brain than WT control mice (Figure 4.5.8, B, C). On day 10 post infection, percentages of helper T cells were elevated in IL-10 deficient mice compared to WT control mice, while cell numbers where decreased. This discrepancy between frequency and percent could be because of variations in total cells isolated per mouse brain. In spinal cord tissues, IL-10 deficient mice had higher percentages of helper T cells on days 7 and 10 post infection compared to WT control mice (Figure 4.5.8, E). Numbers of isolated helper T cells from spinal cord tissues were not different (Figure 4.5.8, D). In the CLN, there were no differences in number of helper T cells (Figure 4.5.8, F). On day 7, but not 10, days post infection, there were greater percentages of helper T cells in CLN from IL-10 deficient mice compared to WT controls (Figure 4.5.8, G). Discrepancies between number and percentage of helper T cells could be because of variations in total cells isolated from CLN tissue as reported in Figure 4.5.7.

4.3.8 IL-10 deficiency does not alter CD8+ T cell responses in the brain

CD8+ T cell responses were minimally impacted by the absence of IL-10 as determined via flow cytometry (Figure 4.5.9, A). There were no significant differences in percent or number of CD8+ T cells in brain or CLN at days 7 or 10 post-TE infection (Figure 4.5.9, B, C, F, J). In spinal cords, there were higher percentages of CD8+ T cells on day 7 followed by a lower percentage on day 10 in IL-10-deficient mice (Figure 4.5.9,

E). There were no significant differences in the number of CD8+ T cells (Figure 4.5.9, D).

4.3.9 IL-10 deficiency alters regulatory T cell differentiation in the CNS

Because both IL-10 and TGFβ are important for the differentiation of regulatory T cells, we determined the impact of IL-10 deficiency on the number and percent of Tregs post-TE infection via flow cytometry analysis of CD25+ foxp3+ T cells (Figure 4.5.10, A). Differentiation of Tregs was significantly impacted by the absence of IL-10 in brain, spinal cord, and CLN. In the brain and the CLN, both number and percent were lower in IL10KO mice compared to WT animals (Figure 4.5.10, B, C, F, G). In spinal cords, Tregs were higher in IL10KO mice on day 7, but lower on day 10 (figure 4.5.10, D, E).

4.3.10 IL-10 deficiency alters production of SINV-specific IgM and IgG1 antibodies

The impact of IL-10 deficiency on the SINV-specific antibody response was measured via EIA. There was no impact on the production of SINV specific total IgG, IgG2a or IgG3 antibodies (data not shown). There were, however, lower levels of SINV-specific IgM (Figure 4.5.11, A, B) and IgG1 (Figure 4.5.11, C, D) antibody production in both the brain and spinal cord of mice lacking IL-10.

4.3.11 IL-10 deficiency decreases B cell responses

Because antibody production was altered in the absence of IL-10, we next determined via flow cytometry if recruitment of CD19+ B cells to the CNS was also impacted (Figure 4.5.12, A). On day 10 post-infection, CD19+ B cells were lower in both

number and the percent of live cells in the brains of IL10KO mice compared to WT mice (Figure 4.5.12, B, C). Number and percent of CD19+ B cells were not significantly different between groups in CLN (Figure 4.5.12, D, E).

4.4 DISCUSSION

Sindbis virus strains of varying virulence have been produced to study factors leading to survival versus death during alphaviral encephalomyelitis. The avirulent strain, TE, has been used to study the mechanism behind viral clearance and persistence. The role of IL-10 during avirulent infection was previously unknown. We report that in the absence of IL-10, mice infected with TE display clinical symptoms more quickly and for a prolonged period compared to WT control mice and viral clearance is delayed in IL10KO mice. Concomitant with these clinical consequences, levels of active TGFβ1 but not TGFβ3 are higher after TE infection in IL-10KO mice compared to WT control mice. These observations are associated with no changes in IL-17 and TH17 responses, decreased B cell responses, and decreased Treg responses in the brain. These data support the hypothesis that TGFβ3 and not TGFβ1 leads to differentiation of pathogenic TH17 cells. TGFβ1 does, however, lead to suppression of B cells. This will be discussed in more detail in Chapter 5.

4.5 FIGURES AND TABLES

Figure 4.5.1 IL-10 mRNA expression post TE infection in WT mice

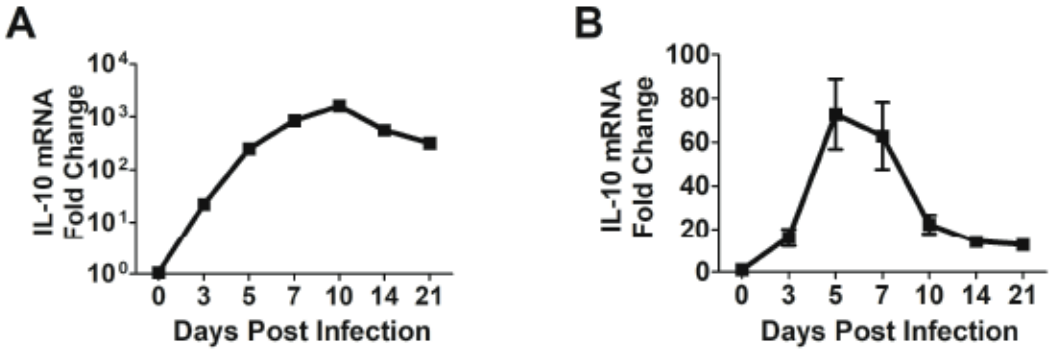

IL-10 is upregulated during TE infection. WT mice were intranasally infected with 10^5 pfu TE. (A) *Il10* mRNA expression measured by quantitative real-time PCR in the brains (A) and spinal cords (B) of TE-infected WT mice. Ct values were normalized to GAPDH. Ct values and fold change were calculated relative to uninfected controls (ΔΔCt). Data are pooled from two independent experiments and represent the mean ± SEM of 6 mice at each time point.

Figure 4.5.2 Morbidity and percent weight change post TE infection in WT versus IL10KO mice

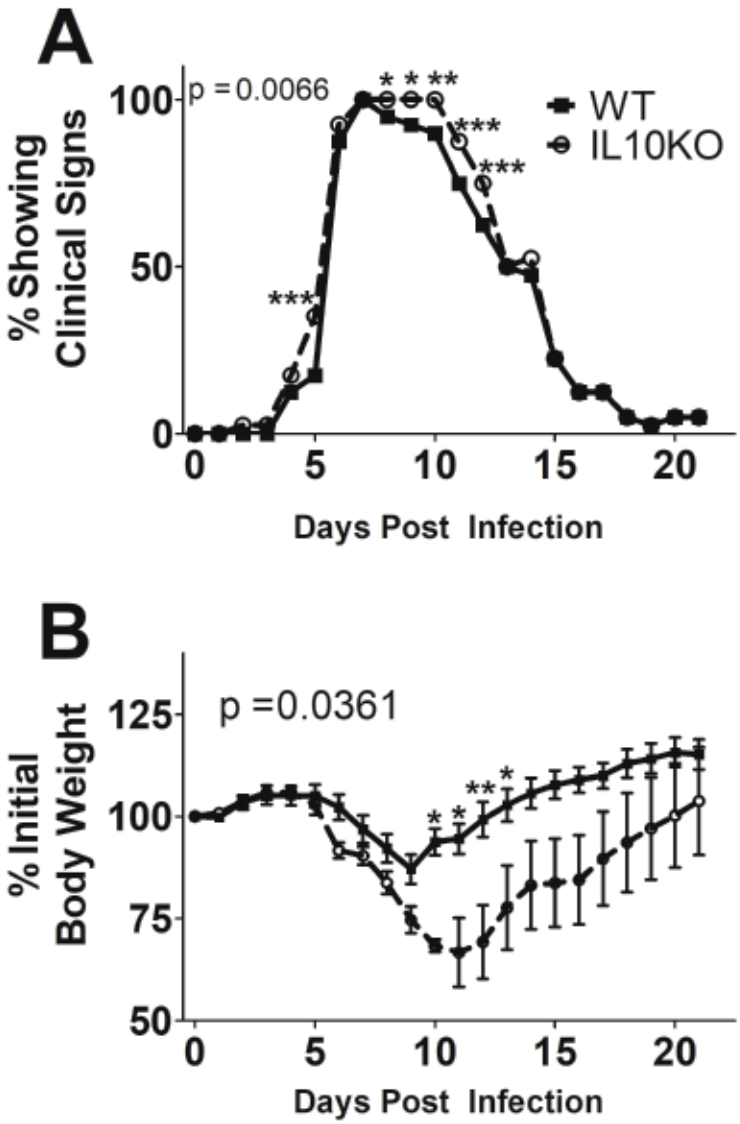

Signs of disease and weight change in WT (closed square, solid line) and IL10KO (open circle, dashed line) mice infected with TE were monitored daily. The clinical score scale was as follows: 0, no symptoms; 1, abnormal hind-limb and tail posture, ruffled fur, and/or hunched back; 2, unilateral hind-limb paralysis; 3, bilateral hind-limb paralysis and/or moribund; 4, dead. Data are pooled from three independent experiments for total of n = 40 and presented as the mean ± SEM; *p < .05, **p < .01, ***p < 0.001. (A) Percent of WT or IL10KO showing clinical symptoms. (B) Percent weight change was assessed by comparing daily measured weights to original weight of individual mice. Data are pooled from three independent experiments for a total of n = 40 for both groups and presented as the mean ± SEM; *p < .05, **p < .01, ***p < 0.001.

Figure 4.5.3 Infectious virus and viral load post TE infection in brains and spinal cords of WT versus IL10KO mice

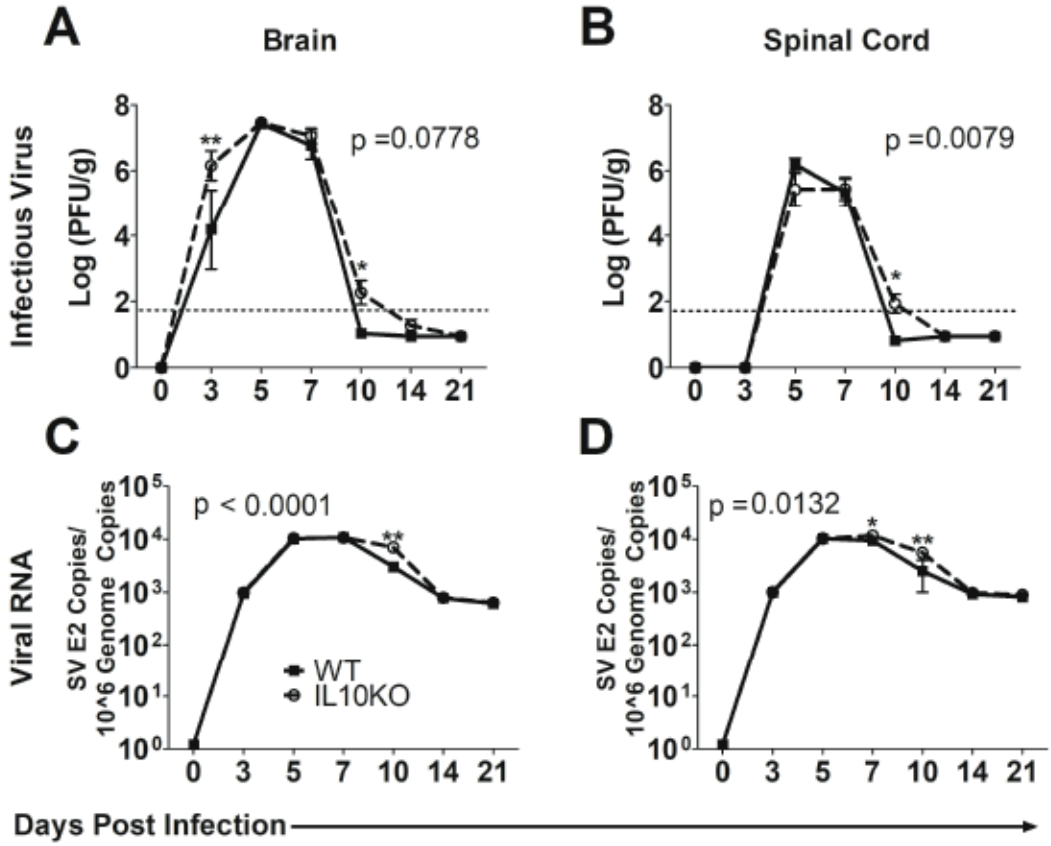

IL-10 is important in viral replication and clearance. (A and B) Virus titers were determined using brain (A) or spinal cord (B) homogenates prepared from WT (filled square, solid line) and IL10KO (open circle, dashed line) mice. Data are pooled from three independent experiments and presented as the mean ± SEM of 6 mice at each time point; * $p < .05$, ** $p < 0.01$. The limit of detection was calculated and displayed as the horizontal dotted line. Some data points are below the limit detection because for that time point, some mice had no plaque growth while others had plaque growth. (C and D) Viral RNA copy numbers were determined via PCR of RNA isolated from brain (C) or spinal cord (D) tissues. Data are pooled from three independent experiments and presented as the mean ± SEM of 6 mice at each time point; * $p < .05$, ** $p < 0.01$.

Figure 4.5.4 TGFβ1 but not TGFβ3 protein is increased in TE-infected IL10KO mice

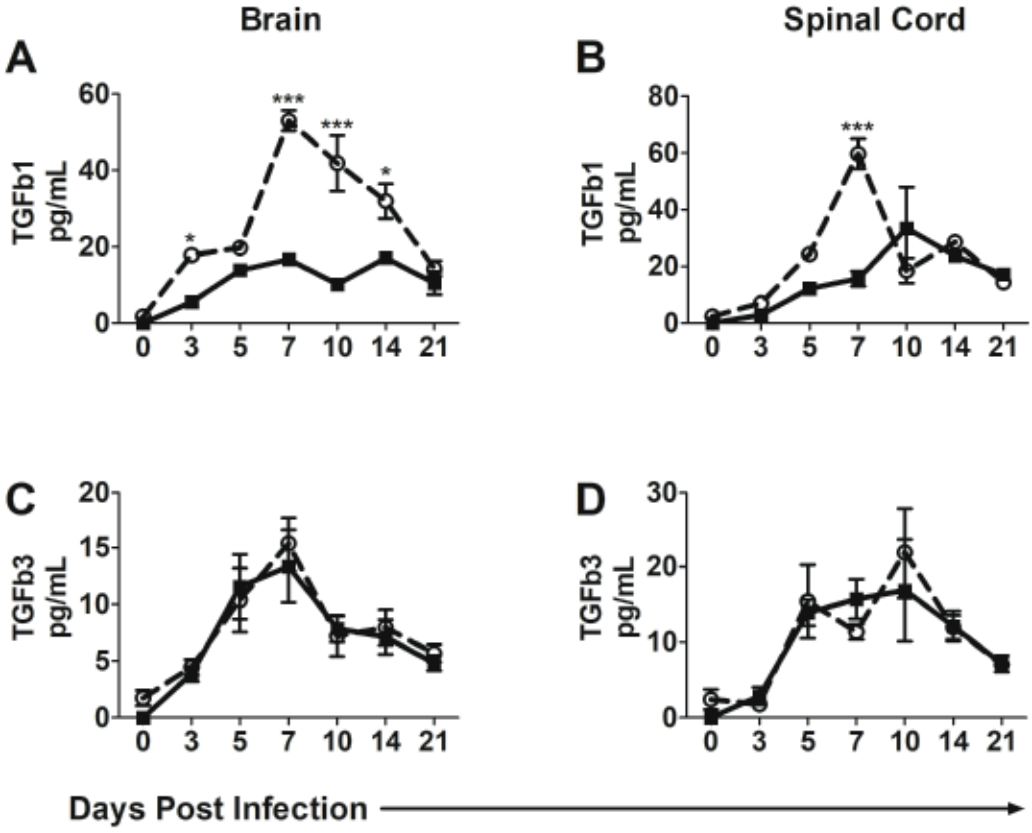

In the absence of IL-10, more TGFβ1 and TGFβ3 proteins are produced. (A-B) Protein levels of TGFβ1 and TGFβ3 were measured in brain (A & C) and spinal cord (B & D) tissues via EIA. Data were pooled from 2 independent experiments and represent the means ± SEM for 6 mice at each time point; *$p < 0.05$, ***$p < 0.001$.

Figure 4.5.5 IL-10 deficiency does not alter IL-17 mRNA expression, but does alter IFNγ.

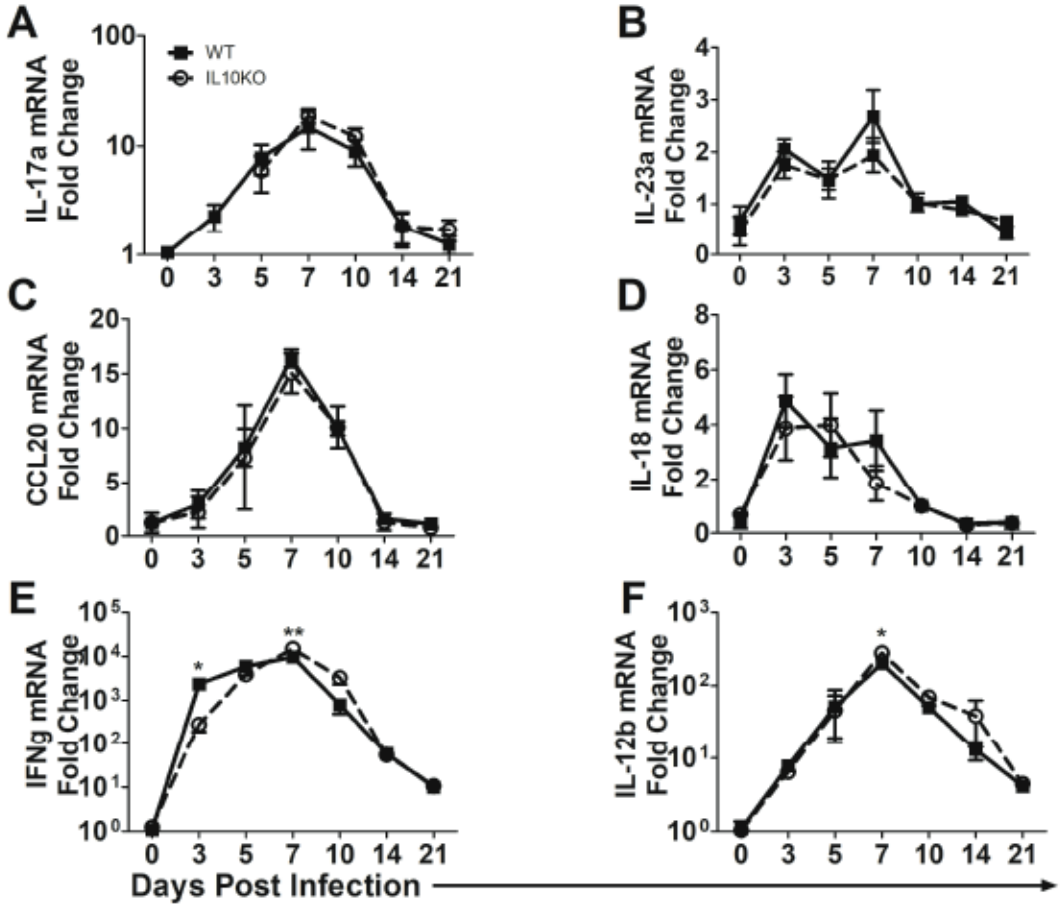

WT mice were intranasally infected with 10^5 pfu TE. Cytokine mRNA expression measured by quantitative real-time PCR in the brains of TE-infected WT (closed square, solid line) and IL10KO (open circle, dashed line) mice. Ct values were normalized to GAPDH. Ct values and fold change were calculated relative to uninfected controls ($\Delta\Delta$Ct). Data are pooled from two independent experiments and represent the mean ± SEM of 6 mice at each time point; *$p < .05$, **$p < .01$.

Figure 4.5.6 IL-10 deficiency and T cells, Example of Flow Cytometry Gating Strategy

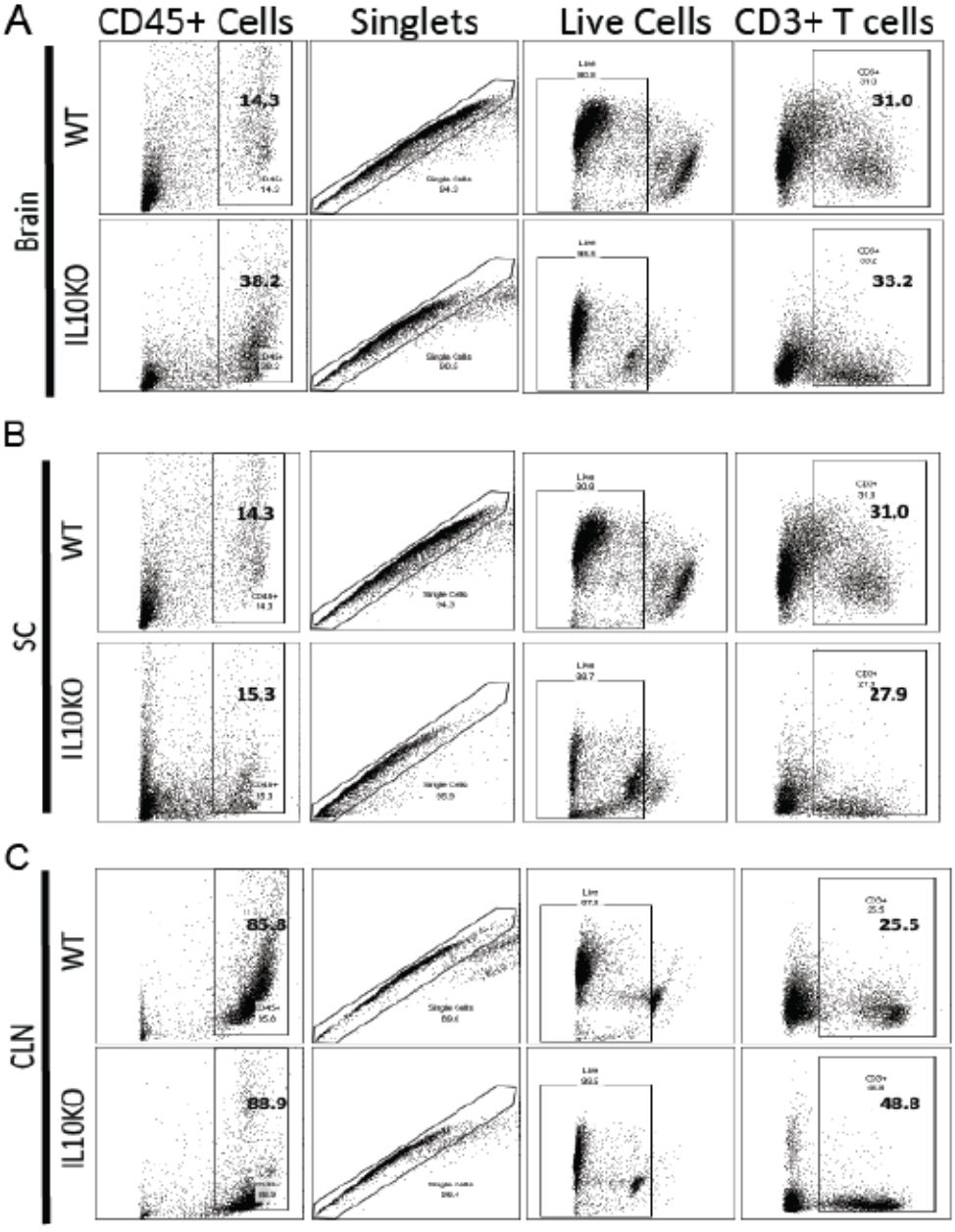

Representative flow cytometry gating and plots to determine percent and number of CD3+ T cells, CD4+ T cells, and CD8+ T cells.

Figure 4.5.7 IL-10 deficiency impacts T cell percentages in the spinal cord and CLN, but not brain

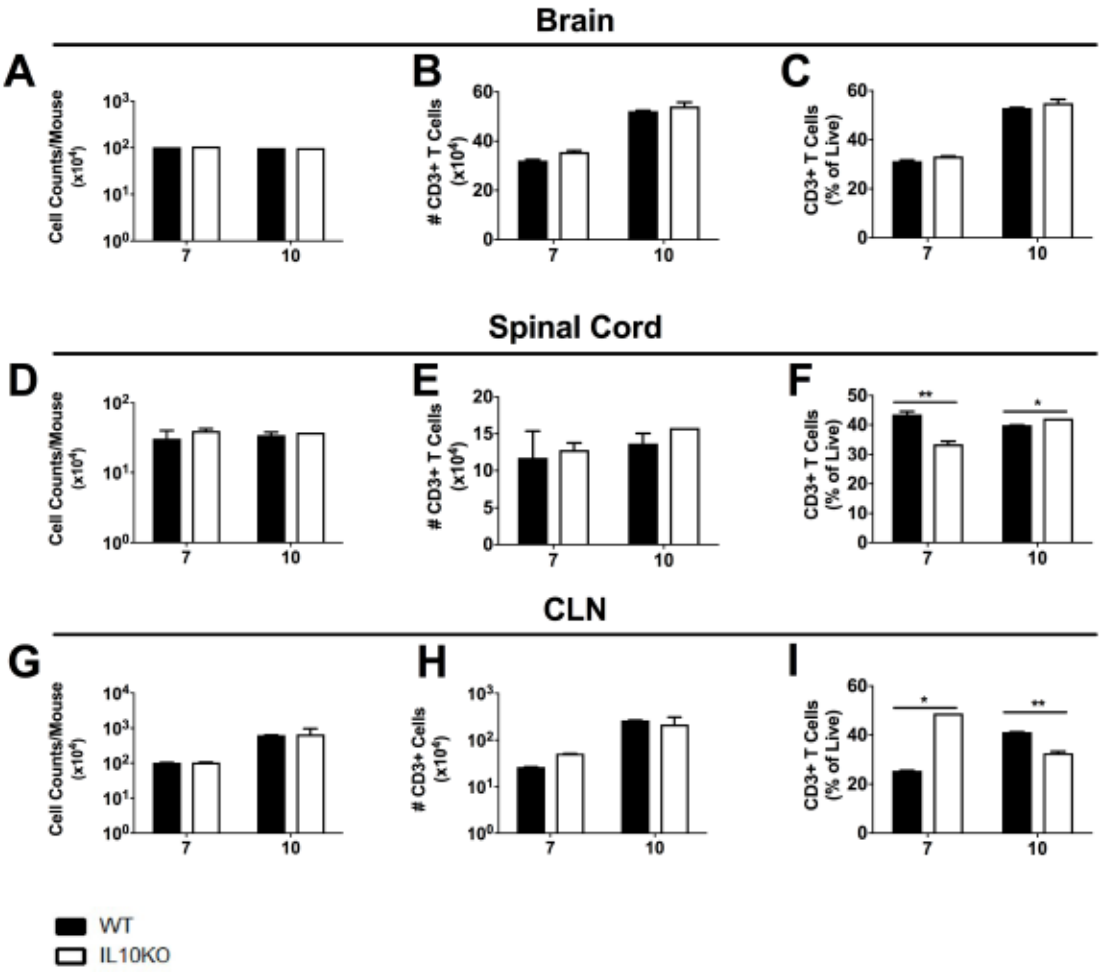

Lymphocytes were isolated from brain (A-C), spinal cord (D-F0, and CLN (G-I) from WT (black bars) or IL10KO (white bars) mice. Cells per mouse tissue were calculated (A, D, G). Flow cytometry was performed and CD3+ T cells as a number (B, E, H) and percent (C, F, I) of live cells was measured. Data were pooled from 2 independent experiments and represent the means ± SEM for 8 mice at each time point $p^* < .05$, $^{**}p < .01$.

Figure 4.5.8 IL-10 deficiency impacts recruitment of CD4+ T cells to the CNS

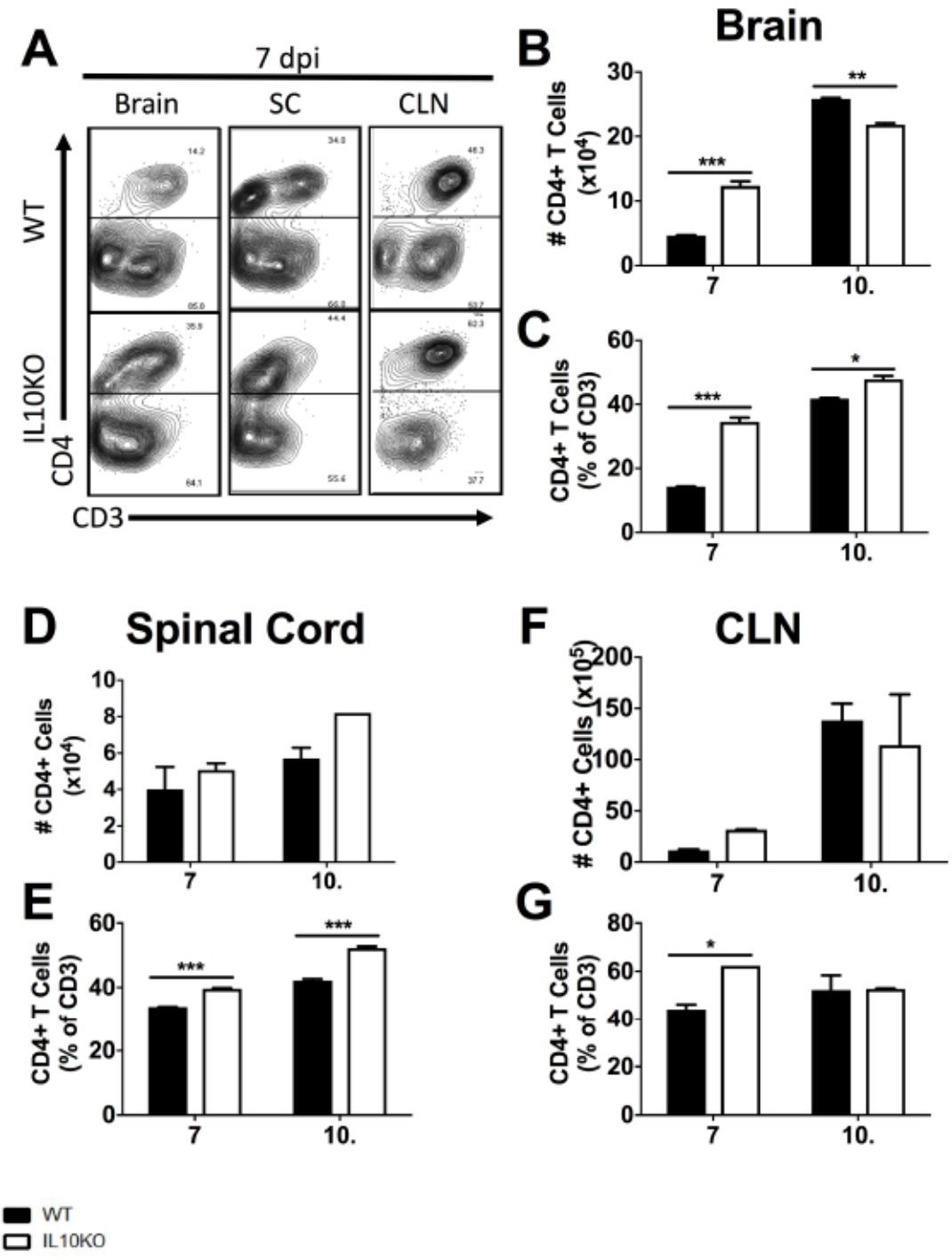

Flow cytometric analysis of isolated cells pooled from the brains of WT (black bars) or IL10KO (white bars) mice at 7 and 10 days post infection. Representative flow cytometry plots of cells isolated from WT or IL10KO are shown in (A). Number and percent of CD3+CD4+ cells were measured in brain (B, C), spinal cord (D, E), and CLN (F, G). The data represent the mean ± SEM from three independent experiments with n = 6; *p <.05, **p < .01, ***p < 0.001.

Figure 4.5.9 IL-10 deficiency impacts the percent of CD8+ T cells in the SC, but not in brain or CLN

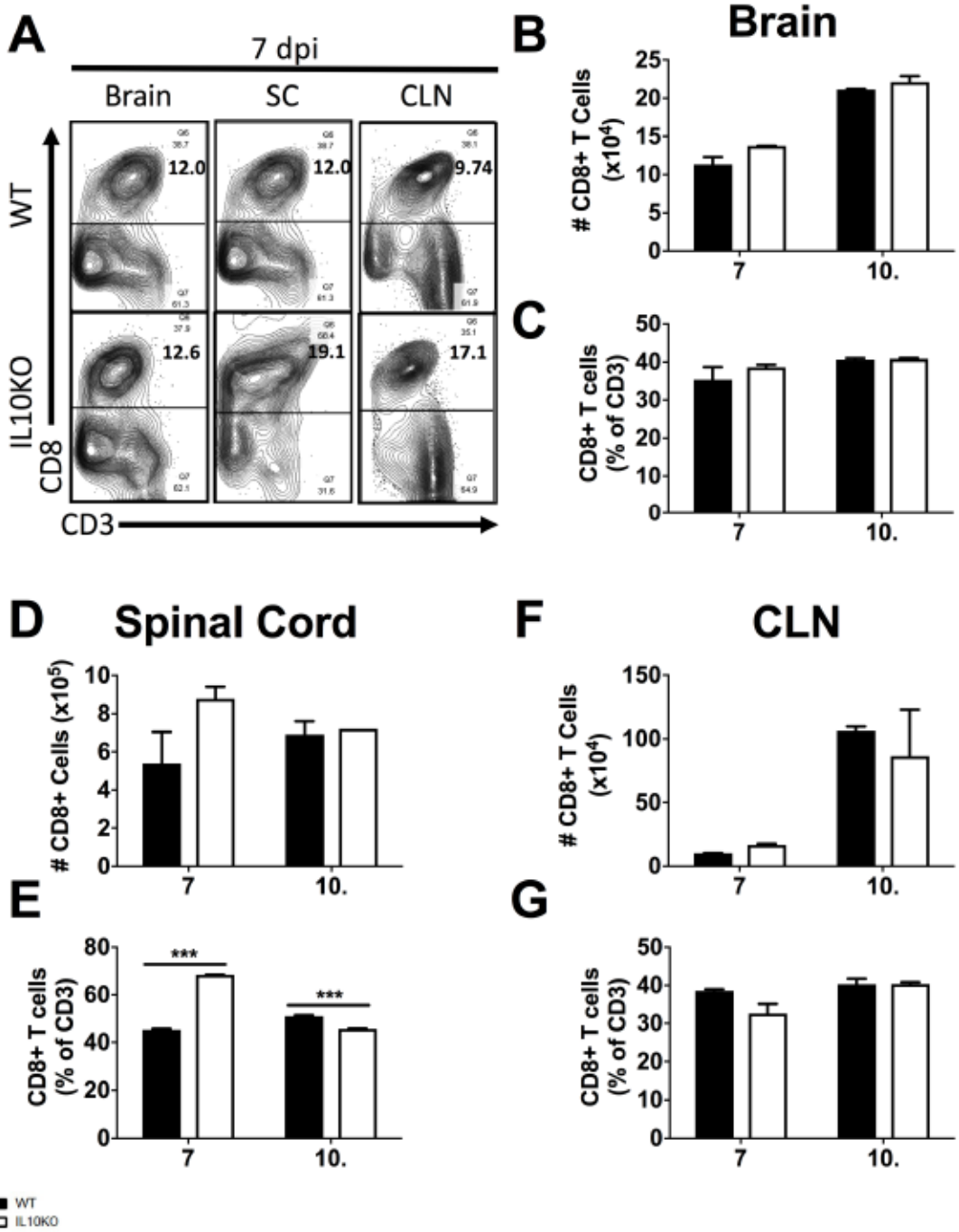

Flow cytometric analysis of isolated cells pooled from the brains of WT (black bars) or IL10KO (white bars) mice at 7 and 10 days post infection. Representative flow cytometry plots of cells isolated from WT or IL10KO are shown in (A). Number and percent of CD3+CD8+ cells were measured in brain (B, C), spinal cord (D, E), and CLN (F, G). The data represent the mean ± SEM from three independent experiments with n = 6; ***p < 0.001.

Figure 4.5.10 IL-10 deficiency impacts TRegs in the CNS

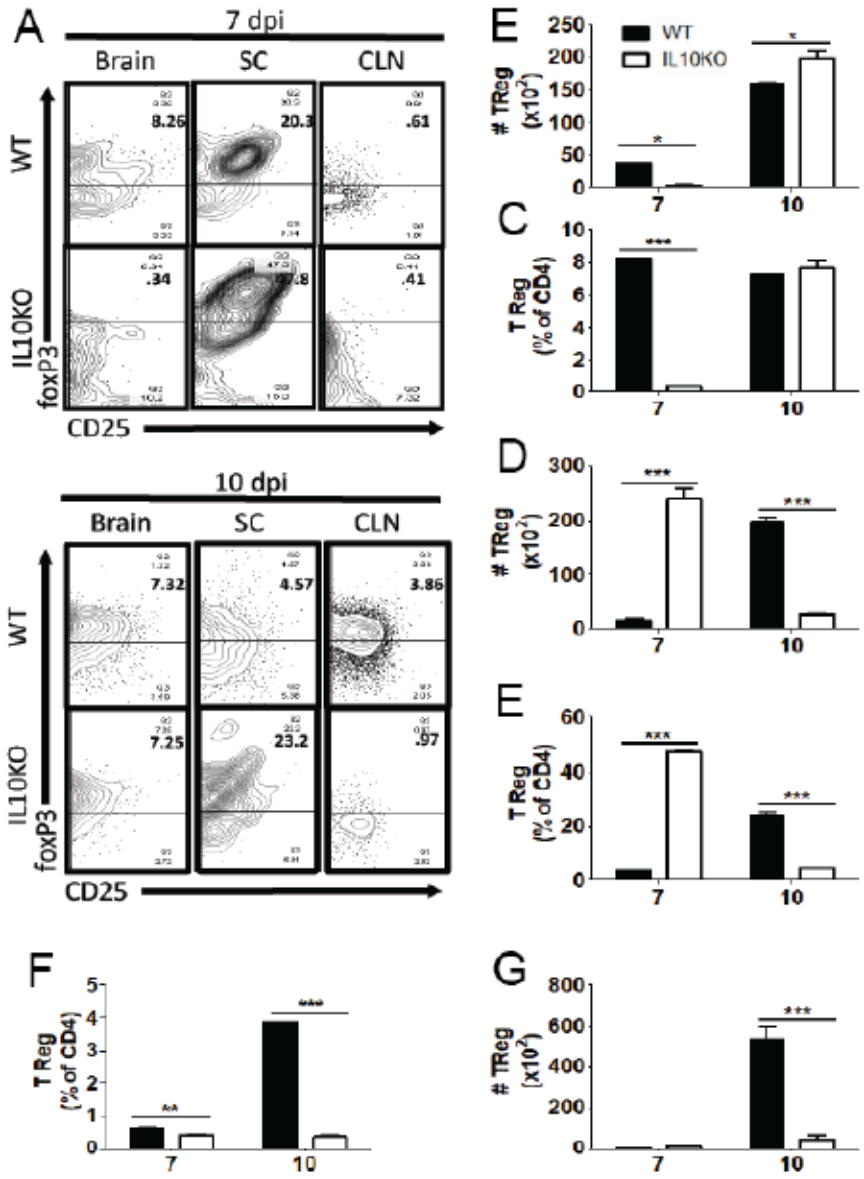

Flow cytometric analysis of isolated cells pooled from the brains of WT (black bars) or IL10KO (white bars) mice at 7 and 10 days post infection. Representative flow cytometry plots of cells isolated from WT or IL10KO are shown in (A). Number and percent of Tregs (CD3+CD4+CD25+foxP3+) cells were measured in brain (B, C), spinal cord (D, E), and CLN (F, G). The data represent the mean ± SEM from three independent experiments with n = 6; *p < .05, **p < .01, ***p < 0.001.

Figure 4.5.11 IL-10 deficiency impacts production of IgM and IgG1 SINV-specific antibodies

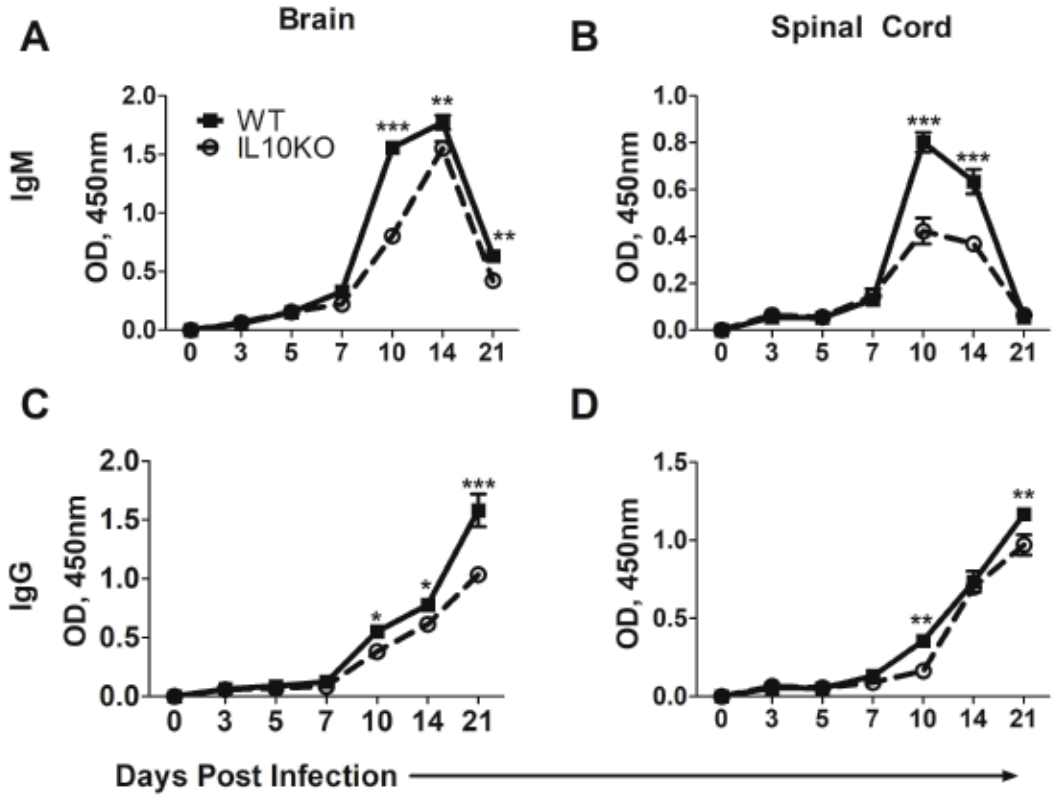

(A-D) Analyses of SINV-specific IgG1 and IgM antibodies via EIA from WT (filled square, solid line) and IL10KO (open circle, dashed line) mice. Data were pooled from 2 independent experiments and represent the means ± SEM for 6 mice at each time point; ***$p < 0.001$. SINV-specific IgM from brain (A) and spinal cords (B). SINV-specific IgG1 from brain (C) and spinal cord (D).

Figure 4.5.12 IL-10 deficiency alters B cell recruitment to the CNS post TE infection

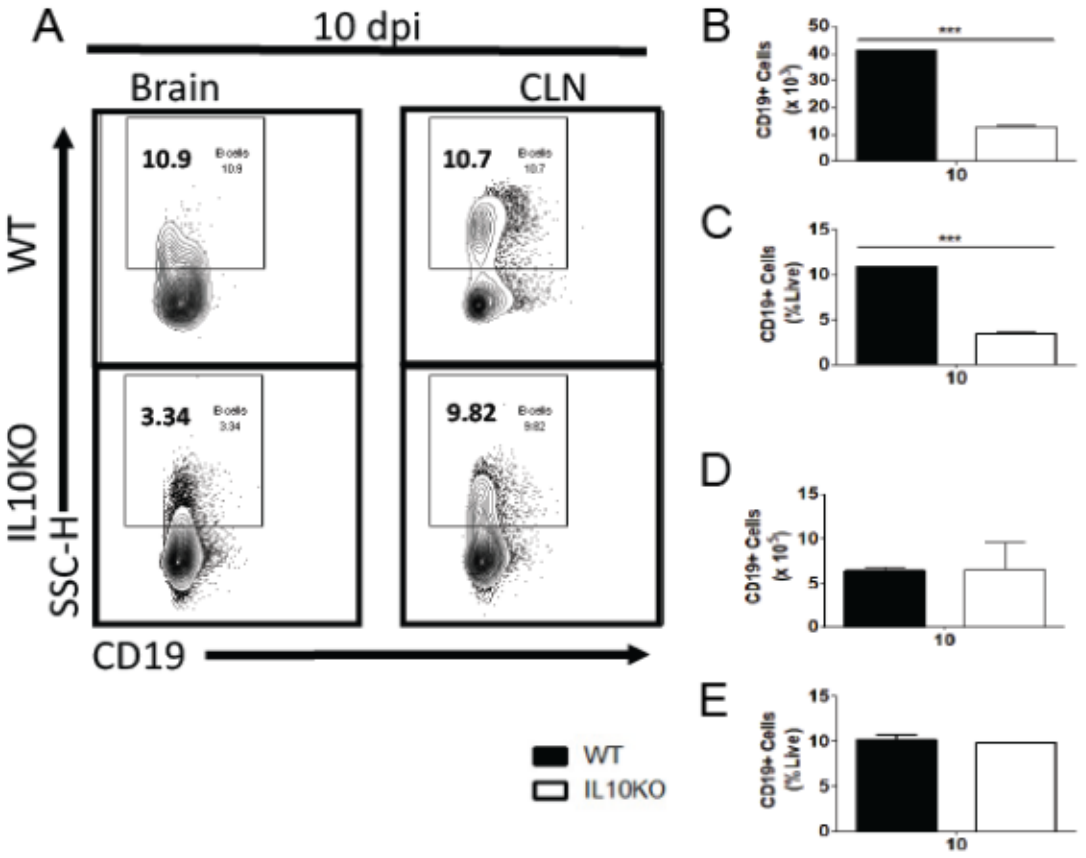

Flow cytometric analysis of isolated cells pooled from the brains of WT (black bars) or IL10KO (white bars) mice at 10 days post infection. Representative flow cytometry plots of cells isolated from WT or IL10KO are shown in (A). Number and percent of CD19+ B cells were measured in brain (B, C) and CLN (D, E). The data represent the mean ± SEM from three independent experiments with n = 8; ***$p < 0.001$.

CHAPTER 5 DISUSSION

5.1 DISCUSSION

5.1.1 Summary of main findings

Studies with SINV strains of varying virulence allow for analysis of mechanisms governing neuroprotection and survival versus immunopathogenicity and death. Because virulent NSV causes fatality in all mice by 10 days post-infection, studies with intermediate virulent strain TE12 and avirulent strain TE allow for longer term analysis of immunopathogenesis and clearance. Antibody and IFNγ are essential to infectious virus clearance and survival (**Figure 5.2.1**) [30, 36, 40, 45, 114]. Increasing numbers of TH17 cells and IL-17-producing ILC3s, as well as lower numbers of regulatory T and B cells are associated with immunopathogenesis [15-17, 177]. Integral to the control of immunopathogenesis is the cytokine IL-10, which suppresses T cell-mediated inflammation by down-regulating MHC Class II on APC and inhibiting pro-inflammatory cytokine production.

We found that SINV strains of varying virulence induce different amounts of TGFβ1 and TGFβ3 protein in the brains of WT mice after intranasal infection (**Figure 5.2.2, left**). The virulent SINV strain NSV induces the most TGFβ1 and TGFβ3 protein in brains; the intermediate virulent SINV strain, TE12, induces an intermediate amount of TGFβ1 and TGFβ3; and the avirulent SINV strain, TE, induces the lowest concentration of TGFβ1 and TGFβ3 in brains. Production of TGFβ1 and TGFβ3 in brains of IL10KO mice followed a similar pattern (**Figure 5.2.2, right**).

Comparisons of IL10KO and WT mice after infection with TE, TE12, and NSV show that NSV-infected IL10KO mice have greater amounts of both TGFβ1 and TGFβ3 proteins, while TE and TE12-infected IL10KO mice have greater induction of TGFβ1, but not TGFβ3 when compared to WT control mice (**Figure 5.2.3**). These findings support the hypothesis that TGFβ3, but not TGFβ1 is responsible for promotion of the differentiation of pathogenic TH17 cells [80]. TGFβ1 may play a role in the suppression of the TH2/B cell/antibody responses because this isoform was elevated and TH2 and antibody responses were suppressed after infection with all three strains in IL-10 deficient mice.

These different concentrations of TGFβ1 and TGFβ3 were associated with distinct immune responses in IL10KO compared to WT mice. NSV infection in IL-10 deficient mice was associated with the highest amount of TGFβ1 and TGFβ3 induction, increased TH17 cells, IL-17 producing ILC3s and IL-17 mRNA, as well as decreased B cell and antibody responses (**Figure 5.2.4**). These immune changes led to accelerated mortality and delayed viral clearance. Infection with intermediate virulent and avirulent SINV strains of mice lacking IL-10 induced a different immune response, as well as relatively intermediate and low concentrations of TGFβ1 and TGFβ3 (**Figure 5.2.5**). Contrary to NSV-induced immunopathogenesis, TE12- and TE-induced immunopathogenesis in IL-10 deficient mice was characterized by lower antibody production, decreased numbers of B cells, decreased numbers of regulatory T and B cells, and no changes in levels of mRNA or TH17 cells in the CNS compared to WT control mice.

These results show that NSV-, TE12-, and TE-induced immunopathologies were inherently different and the viruses induced different concentrations of TGFβ1 and TGFβ3 both in WT and IL10KO mice. During NSV-, but not TE12- or TE-induced immunopathogenesis, TGFβ3 and TH17 cells were increased in IL-10 deficient mice compared to WT control mice. This supports the hypothesis that TGFβ3, and not TGFβ1, is associated with the differentiation of pathogenic TH17 cells [80].

5.1.2 NSV-, TE12-, and TE-induced immunopathologies are inherently different – are different antigenic sites/epitopes recognized by the host's immune response leading to different immunopathologies?

Our results indicate that NSV-, TE12-, and TE-induced immunopathogenesis is inherently different and that IL-10 deficiency had strain-dependent effects on the immune response in the CNS. One potential explanation is that induced host immune responses are mounted against different epitopes and antigenic sites. The concept that over time, one antigenic site on an antigen will evolve to be immunodominant is reviewed in [178-180]; and different strains of the same pathogen can induce an array of fluctuating responses against multiple epitopes. Immunodominant epitopes to influenza A viruses and HIV have been the most studied, especially because understanding influenza immunodominant epitopes is important for increasing vaccine efficacy [181-183]. These studies have shown that immunodominance can change over time and that, for example, antigenic escape can occur when one epitope shifts immunodominance to other, potentially weaker, epitopes, thereby altering immunopathogenesis and virulence [184]. Amount of influenza virus can also impact immunodominance through changes in

antigen presentation and T cell avidity [185]. NSV replicates to a higher titer in the brain and spinal cords and spreads to more areas than TE and TE12; this difference could be leading to changes in immunodominance and immunopathogenesis [186]. Further study will be required to address this possibility.

5.1.3 NSV-, TE12-, and TE-induced immunopathologies are inherently different – what is the role of viral 3' and 5' UTRs in modulating the immune response?

The genomes of positive sense RNA viruses like alphaviruses are translated immediately following entry into a host cell and have evolved mechanisms to evade the antiviral immune responses to establish infection. Two such mechanisms include (1) limiting myeloid cell tropism and replication and/or (2) antagonizing myeloid cell responses to virus infection. Important to this latter aspect is the poorly understood role of the 3' and 5' untranslated regions (UTRs) of the SINV RNA genome in immunopathogenesis. **Figure 5.2.6** shows the general structure of the alphavirus genome. **Figure 5.2.7.A** maps the structural and non-structural differences of NSV, TE12, and TE, while **Figure 5.2.7.B** indicates the differences in their 5' UTRs. As reviewed in [187], the UTRs of alphaviral genomes play critical roles in the regulation of RNA replication and translation, as well as interaction with the host cellular machinery. The 5' UTR of NSV is different from that of TE12 and TE, which were both made on the TOTO1101 background (**Figure 5.2.7.B**). NSV has a G at nucleotide 5 while TE12 has an A. TE was created similarly to TE12 and therefore the nucleotide at position 5 is an A like TE12. A potential area of future study would be to explore the role of UTRs in induction of distinct immune responses.

Figure 5.2.8 summarizes how host immune factors can interact with the 5' UTR of alphaviruses to restrict viral replication [188]. There has been a resurgence of interest in these host viral replication blockers to identify new classes of drugs that activate these genes. Antiviral drugs that target host proteins instead of viral proteins could in theory minimize the emergence of resistance [189]. The IFITs are a family of IFN-stimulated proteins that block viral replication by interacting with the 5' UTR of viruses [187, 189-191]. IFIT1 regulates alphavirus translation dependent on the sequence of the 5'UTR [191]. Higher eukaryotic mRNAs and many viral RNAs have 5' caps that are methylated at the N-7 and 2'-O positions of the cap by specific nuclear and cytoplasmic methyltransferases (MTases), respectively [190]. IFITs, which are up-regulated upon viral infection and activation of type I interferon responses, can recognize RNA that is unmethylated at the 2'-O position of the 5' cap, can block translation, and target the RNA for decay or destruction [190]. Alphaviruses lack this modification, but can evade IFIT1 inhibition by altering the structure of the 5'UTR [192]. Figure 3 of Hyde et al [192] shows effects of switching nucleotide 5 from A to G in SINV on pathogenicity via IFIT1. There was significant binding of IFIT1 to A3 RNA, but less binging to G3 RNA[192]. Similar to SINV, a single point mutation in nucleotide 8 in the 5'UTR of VEEV was sufficient to decrease virulence and allow IFIT-dependent replication restriction [193]. Further study could explore how the differences in the 5'UTRs of NSV, TE12, and TE are contributing to immunopathogenesis. A hypothesis for how NSV escapes IFIT1 detection, leading to higher virulence and more severe immunopathogenesis when compared to TE-induced immunopathogenesis is summarized in **Figure 1.9.9.**

The 3' UTR is essential for synthesis of negative sense RNA required for synthesis of positive RNA virus genomes [187]. All alphaviruses have a conserved sequence element (CSE) immediately prior to the poly(A) tail (**Figure 5.2.5**) [187]. Because differences were found in the 5' UTR of NSV, TE12, and TE, an analysis was made of the 3' UTR. The 3' UTR sequences were identical. Conservation of this sequence across strains is most likely because deviations from this sequence (and corresponding secondary structure) will lead to SINV replication restriction [152].

In eukaryotic cells, micro RNAs (miRNAs) play an important role in regulating mRNA translation and different miRNAs can lead to protein synthesis or mRNA decay. miRNA can also interact with virus 3' UTRs [187]. These interactions can be beneficial or detrimental to the host as some miRNAs can interact with 3'UTRs to shut down viral replication while other miRNAs work to increase replication and activation of cellular machinery necessary for attachment to ribosomes. For example, in hematopoietic/myeloid cells, miR-142-3p binds to miR-142-3p binding sites in the 3' UTR of EEEV, blocking translation of the viral genome and induction of type I IFN and other innate immune effectors and limits prodromal disease. This allows EEEV to replicate essentially undetected by host defense responses, which exacerbates disease in animal models.

miRNAs are also involved in immune responses to viruses, which can lead to clearance and/or immunopathology. For example, Epstein Barr Virus, JEV, and HBV can induce miR-146a to escape detection by the immune response by modulating lymphocyte function [194-198]. Dengue virus specifically up=regulates miR-146a that interferes with interferon signaling via TRAF6 [199]. Other miRNAs that are induced by viruses will

activate host immune responses and lead to virus clearance, and may also control immunopathology. miRNA 155 is up-regulated in response to JEV infection and decreases JEV-induced immunopathology by inhibiting SHIP-1 and increase anti-viral activity via Type I interferons [200].

5.1.4 Immunomodulatory therapies for treatment of viral encephalitis

Currently there are no FDA-approved vaccines or anti-viral therapies for the treatment of alphaviral encephalomyelitis. There are, however, many ongoing clinical trials using immunomodulatory approaches to treating viral encephalitis. For example, IVIG therapy is being tested in clinical trials for the treatment of JEV [201]. Although there were no differences in mortality between groups, JEV-positive children treated with IVIG had 16x higher JEV-specific neutralizing antibody titres and had higher levels of IL-4 and IL-6 than children that were not treated [201]. The shortcoming of this treatment is that human antibodies are in short supply and take a long time to produce in the quantities necessary for treatment. Passive transfer of non-human antibodies has not been successful because of the host's anti-antibody response is rapidly produced. To counteract this problem, a recent study reported the creation of a transchromosomic (Tc) bovine that can produce human anti-VEEV antibodies [202]. This is possible by engineering these bovines to possess a human artificial chromosome containing the human antibody heavy chain and kappa chain and 'hyper' immunizing them with VEEV [202]. These VEEV immunized Tc bovines produce as much as 300 g of human IgG/animal/month, allowing the production of highly concentrated antibody preparations

in a very short time frame, with no further processing being required for therapeutic use. VEEV specific antibodies from these bovines protected mice from fatal infection [202].

Because of the varied success of these immunomodulatory approaches to treat viral encephalomyelitis, it remains important to continue to investigate new therapies. IL-10 immune therapy remains the focus of many clinical trials for the treatment of inflammatory diseases [168-171]. Because there are currently zero therapeutic interventions for viral encephalomyelitis, understanding the potential of using IL-10 as a therapeutic agent remains of high importance.

5.2 Figures and Tables

Figure 5.2.1 Framework 1

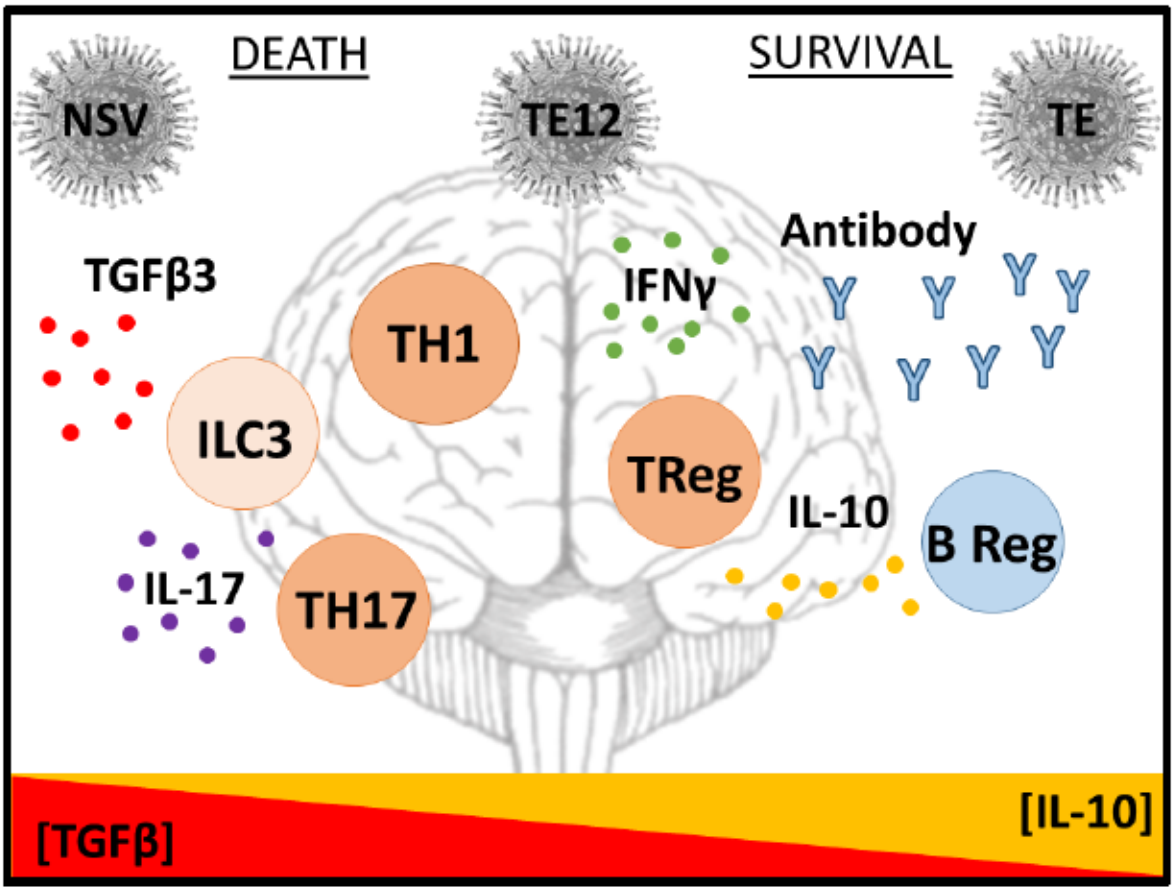

Source: Created by Martin, NM, August 2017

Overview of immune factors leading to survival versus death in adult C57Bl/6 mice after infection with the virulent NSV strain, the TE12 strain of intermediate virulence, and the avirulent TE strain of SINV. T cells have been implicated in immunopathogenesis of fatal disease while antibody and IFN are essential for virus clearance and recovery. Pathogenic TH17 cells and increased levels of IL-17 have been associated with accelerated mortality.

Figure 5.2.2 TGF induction: NSV > TE12 > TE

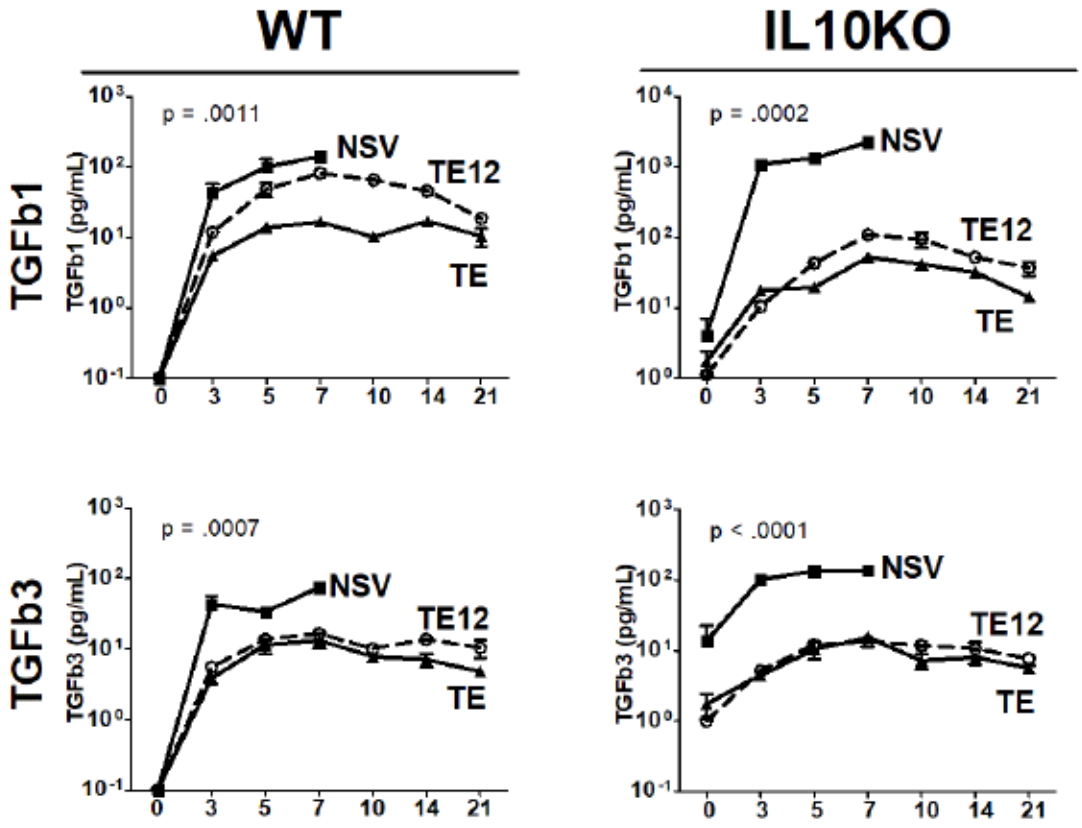

Measurement of levels of TGFβ1 and TGFβ3 protein in brains of WT and IL10KO mice via EIA after intranasal infection with NSV, TE12, or TE SINV strains.

Figure 5.2.3 TGF induction: NSV > TE12 > TE

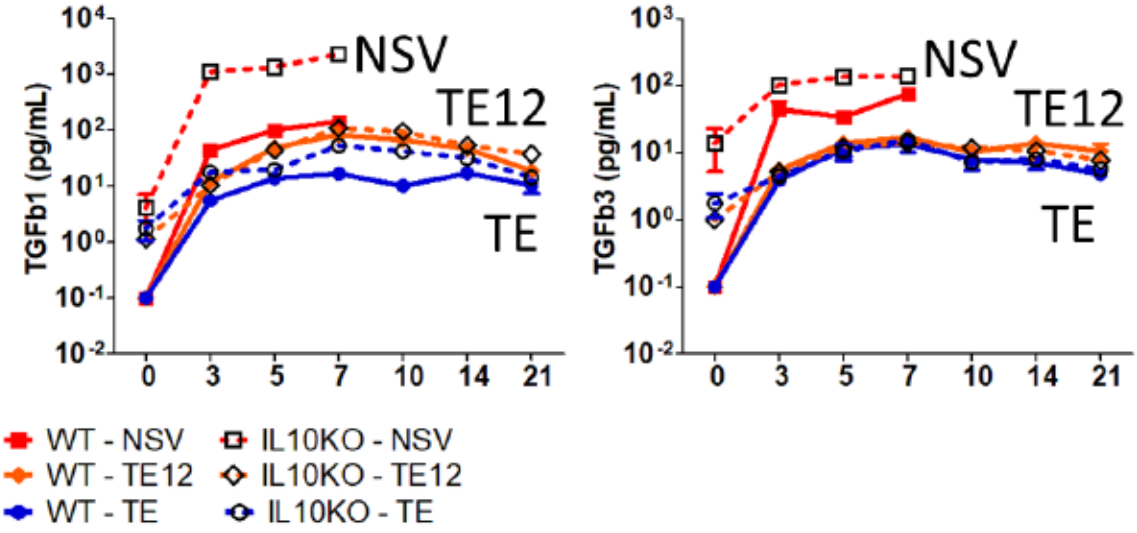

Measurement of levels of TGFβ1 and TGFβ3 protein in brains of WT and IL10KO mice via EIA after intranasal infection with NSV, TE12, or TE SINV strains.

Figure 5.2.4 Framework 2: Effects of TGFβ1 and TGFβ3 during fatal alphaviral encephalomyelitis in IL-10 deficient mice

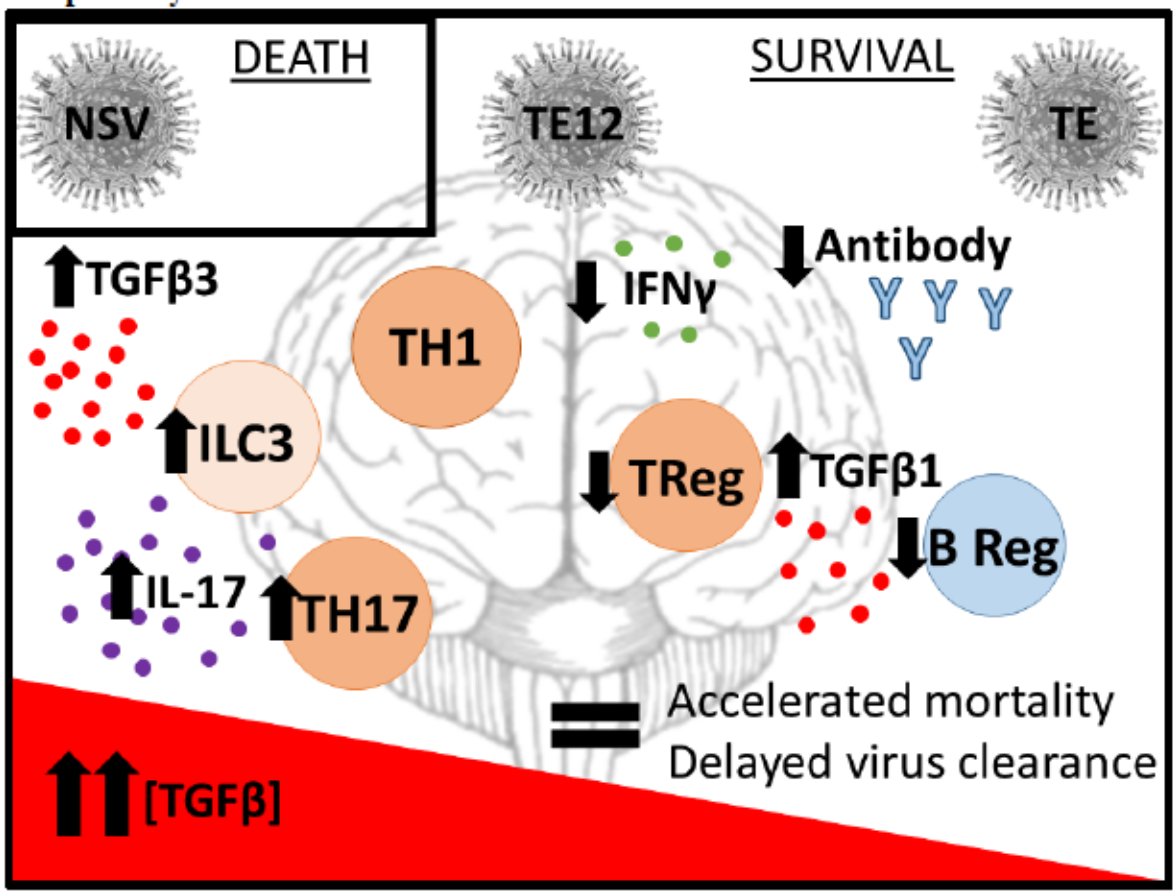

Source: created by Martin, NM, August 2017

Summary of findings from Chapter 2 regarding the upregulation of TGFβ1 and TGFβ3 in the absence of IL-10 and associated impacts on helper T cells, cytokine production, B cells, and antibody production.

Figure 5.2.5 Framework 3: Effects of TGFβ1 and TGFβ3 during avirulent and intermediate virulent alphaviral encephalomyelitis in IL-10 deficient mice

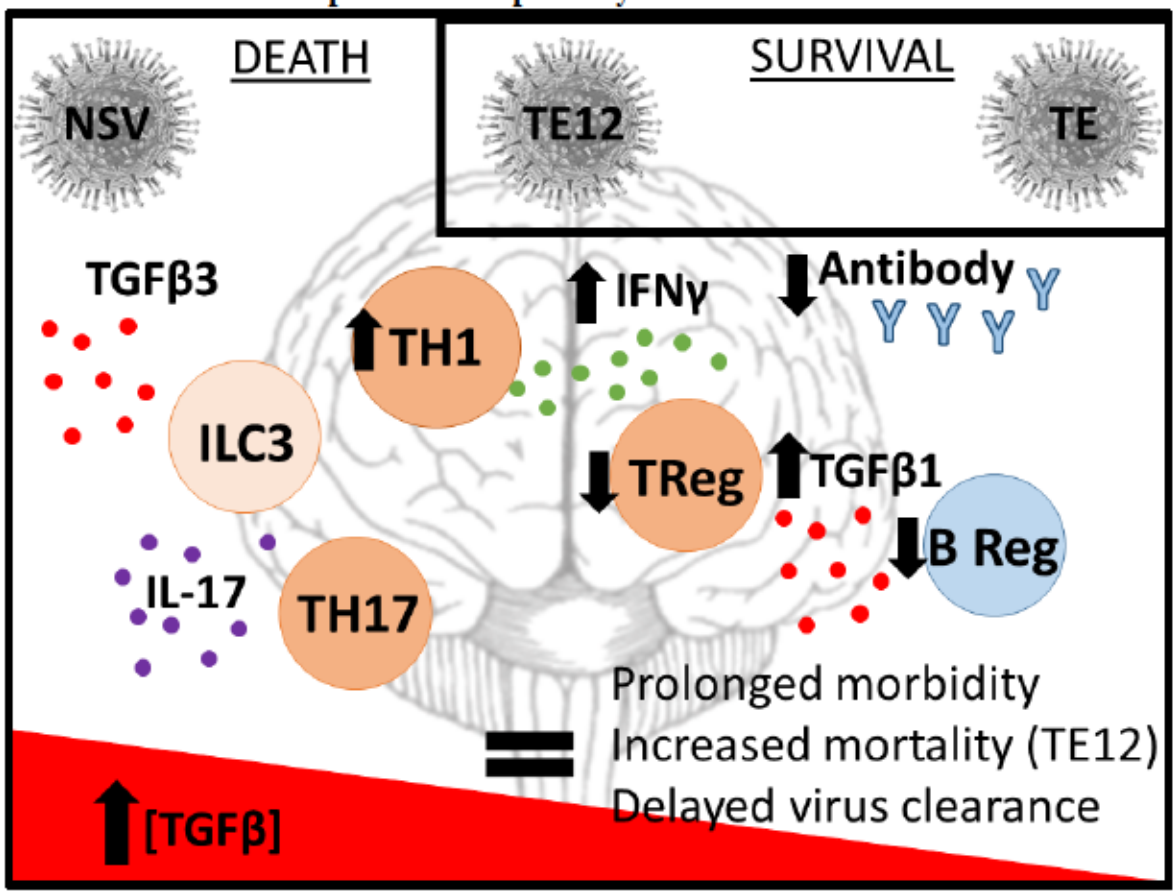

Summary of findings from Chapter 3 & 4 regarding the upregulation of TGFβ1 and TGFβ3 in the absence of IL-10 and associated impacts on helper T cells, cytokine production, B cells, and antibody production.

Figure 5.2.6 The 5' and 3' untranslated region of alphaviruses

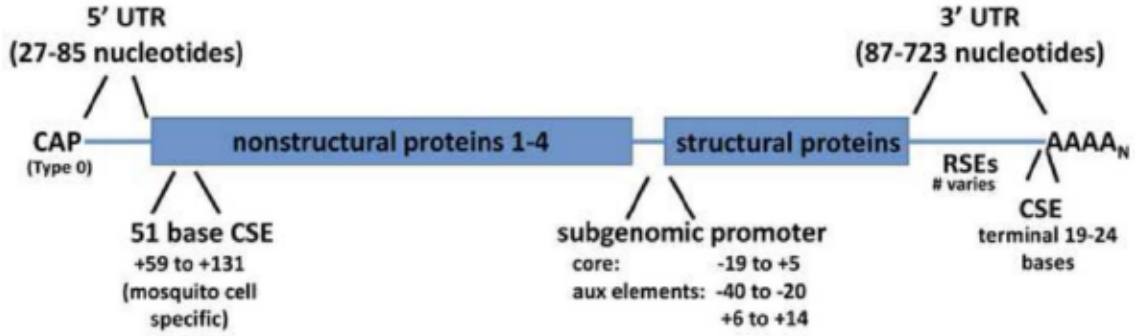

SOURCE: [187]

Overview of organization and regulatory landmarks of the alphavirus genome. Major RNA regulatory elements and open reading frames are indicated. The positions of the 51 base CSE and subgenomic promoter are given relative to the start site of their associated open reading frame. This diagram is based on studies of Sindbis virus.

Figure 5.2.7 NSV, TE12, and TE genome structures

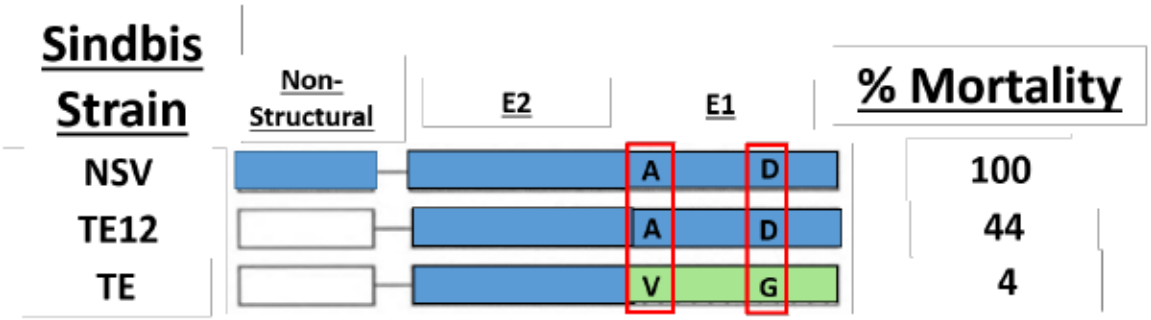

Figure 5.2.7.A Structural and non-structural proteins of NSV, TE12, and TE

Adapted by Martin, NM from [19]

Figure 5.2.7.B Nucleotide changes in position 5 of the 5'UTR in NSV, TE12, and TE

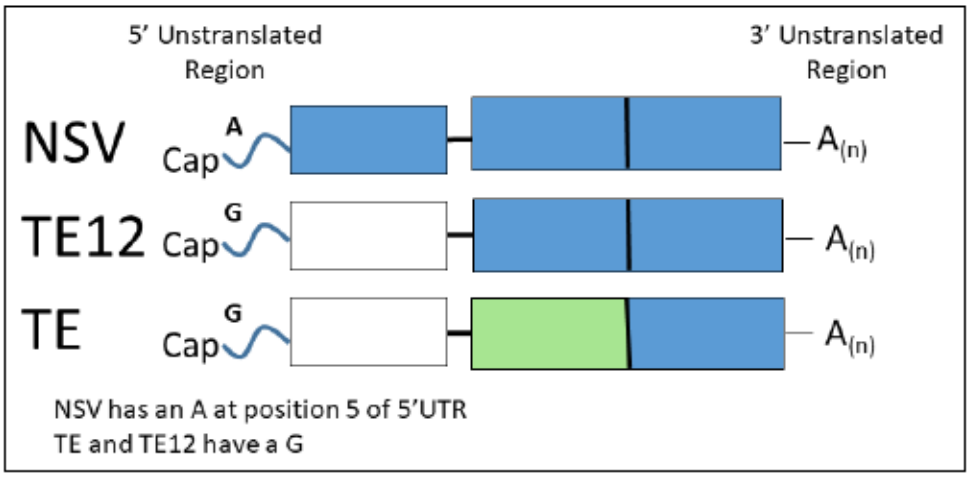

Source: Martin, NM, August 2017. Based on data from Griffin, DE and Hauer, D.

Virulent NSV strain was made by serially passaging the original isolate AR339 in brains. TE and TE12 are recombinant SINV strains made on the TOTO1101 background. TE and TE12 have the same nonstructural proteins and contain the same E2 structural protein from NSV. TE's E1 structural protein comes from AR339, while TE12's E2 structural protein is from NSV. For TE and TE12, the 5' UTR has an A at nucleotide 5 while NSV has a G. There are no sequence differences in the 3'UTR.

Figure 5.2.8 Summary of known immune regulatory elements in the 3' and 5' UTRs of alphaviruses

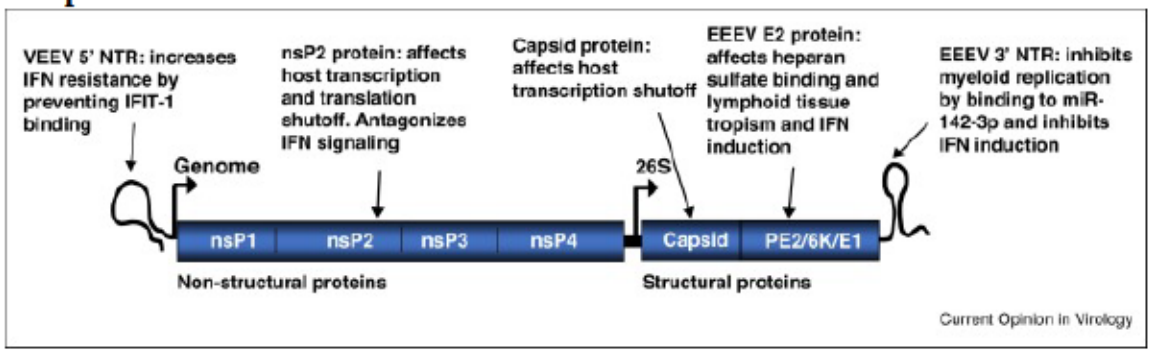

Source: [188]

Figure 5.2.9 IFIT1-dependent inhibition of SINV RNA replication

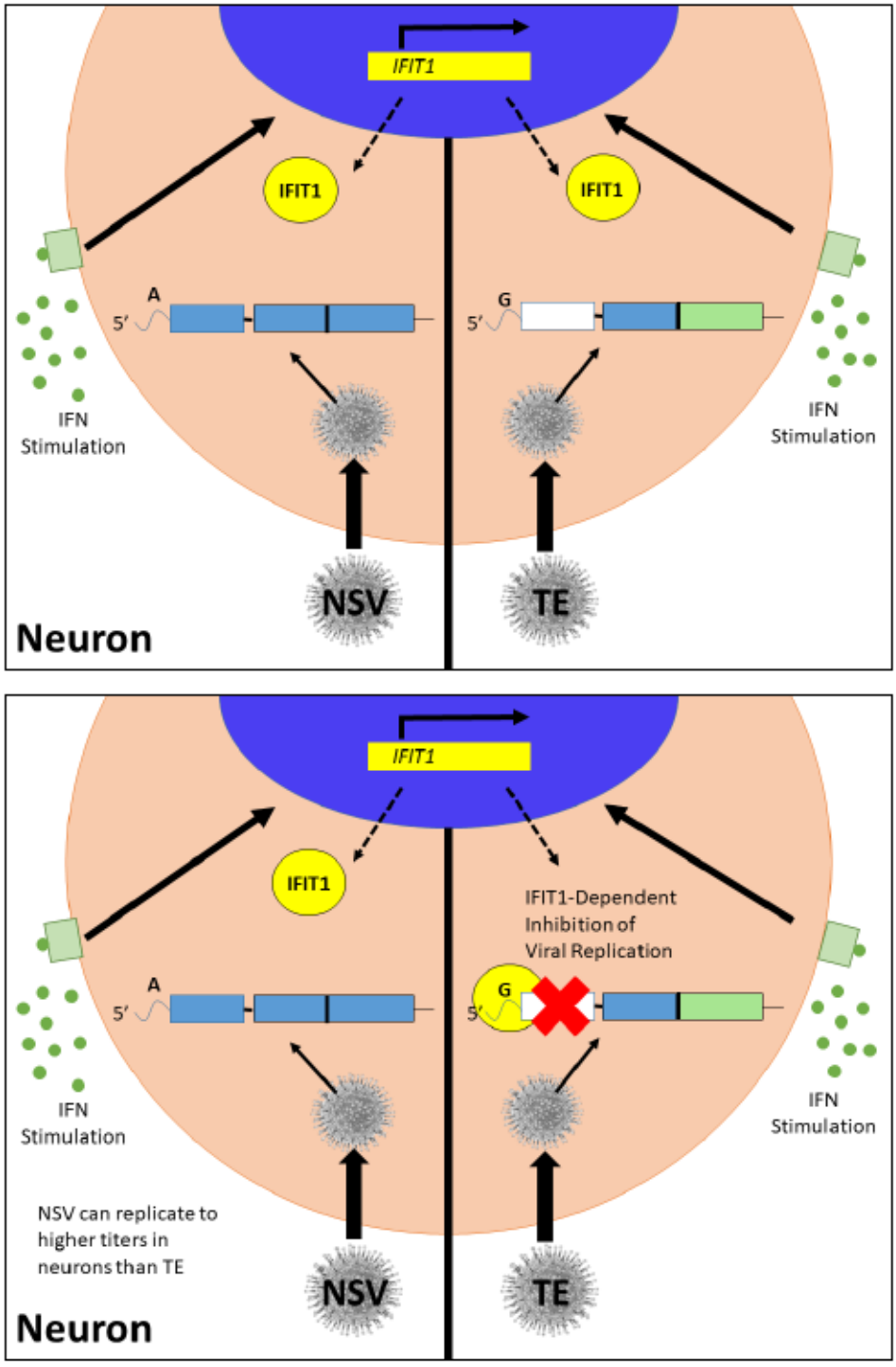

Mice infected with NSV and TE produce interferon. Interferon stimulates infected cells to synthesize IFIT1, a protein that can recognize and restrict RNA without 2'O methylation. SINV RNA does not have 2'O methylation, but can evade IFIT1 detection by changing the nucleotide in position 5 of the cap. NSV has an A at position 5 while TE and TE12 have a G. NSV is able to replicate to higher titers in neurons than TE because of this nucleotide change.

CHAPTER 6 BIBLIOGRAPHY

1. Tucker, P.C. and D.E. Griffin, *Mechanism of altered Sindbis virus neurovirulence associated with a single-amino-acid change in the E2 Glycoprotein.* J Virol, 1991. **65**(3): p. 1551-7.
2. Ryman, K.D. and W.B. Klimstra, *Host responses to alphavirus infection.* Immunol Rev, 2008. **225**: p. 27-45.
3. Control, C.f.D. *Arboviral Encephalitis*. 2014; Available from: http://www.cdc.gov/ncidod/dvbid/arbor/.
4. Kurkela, S., et al., *Sindbis virus infection in resident birds, migratory birds, and humans, Finland.* Emerg Infect Dis, 2008. **14**(1): p. 41-7.
5. Derlet, R., *Venezuelan Equine Encephalitis.* Medscape, 2016.
6. Rice, C.M. and J.H. Strauss, *Nucleotide sequence of the 26S mRNA of Sindbis virus and deduced sequence of the encoded virus structural proteins.* Proc Natl Acad Sci U S A, 1981. **78**(4): p. 2062-6.
7. Fuller, S.D., *The T=4 envelope of Sindbis virus is organized by interactions with a complementary T=3 capsid.* Cell, 1987. **48**(6): p. 923-34.
8. Byrnes, A.P. and D.E. Griffin, *Binding of Sindbis virus to cell surface heparan sulfate.* J Virol, 1998. **72**(9): p. 7349-56.
9. Griffin, D.E. and T. Metcalf, *Clearance of virus infection from the CNS.* Curr Opin Virol, 2011. **1**(3): p. 216-21.
10. Lustig, S., et al., *Molecular basis of Sindbis virus neurovirulence in mice.* J Virol, 1988. **62**(7): p. 2329-36.
11. Thach, D.C., T. Kimura, and D.E. Griffin, *Differences between C57BL/6 and BALB/cBy mice in mortality and virus replication after intranasal infection with neuroadapted Sindbis virus.* J Virol, 2000. **74**(13): p. 6156-61.
12. Griffin, D.E., et al., *Age-dependent susceptibility to fatal encephalitis: alphavirus infection of neurons.* Arch Virol Suppl, 1994. **9**: p. 31-9.
13. Tucker, P.C., et al., *Amino acid changes in the Sindbis virus E2 glycoprotein that increase neurovirulence improve entry into neuroblastoma cells.* J Virol, 1997. **71**(8): p. 6106-12.

14. Vernon, P.S. and D.E. Griffin, *Characterization of an in vitro model of alphavirus infection of immature and mature neurons.* J Virol, 2005. **79**(6): p. 3438-47.
15. Kulcsar, K.A., et al., *Interleukin 10 modulation of pathogenic Th17 cells during fatal alphavirus encephalomyelitis.* Proc Natl Acad Sci U S A, 2014. **111**(45): p. 16053-8.
16. Kulcsar, K.A., et al., *Distinct Immune Responses in Resistant and Susceptible Strains of Mice during Neurovirulent Alphavirus Encephalomyelitis.* J Virol, 2015. **89**(16): p. 8280-91.
17. Kulcsar, K.A. and D.E. Griffin, *T cell-derived interleukin-10 is an important regulator of the Th17 response during lethal alphavirus encephalomyelitis.* J Neuroimmunol, 2016. **295-296**: p. 60-7.
18. Dropulic, L.K., J.M. Hardwick, and D.E. Griffin, *A single amino acid change in the E2 glycoprotein of Sindbis virus confers neurovirulence by altering an early step of virus replication.* J Virol, 1997. **71**(8): p. 6100-5.
19. Tucker, P.C., et al., *Viral determinants of age-dependent virulence of Sindbis virus for mice.* J Virol, 1993. **67**(8): p. 4605-10.
20. Kimura, T. and D.E. Griffin, *Extensive immune-mediated hippocampal damage in mice surviving infection with neuroadapted Sindbis virus.* Virology, 2003. **311**(1): p. 28-39.
21. Griffin, D.E. and R.T. Johnson, *Role of the immune response in recovery from Sindbis virus encephalitis in mice.* J Immunol, 1977. **118**(3): p. 1070-5.
22. Labrada, L., et al., *Age-dependent resistance to lethal alphavirus encephalitis in mice: analysis of gene expression in the central nervous system and identification of a novel interferon-inducible protective gene, mouse ISG12.* J Virol, 2002. **76**(22): p. 11688-703.
23. Griffin, D.E., *Arboviruses and the central nervous system.* Springer Semin Immunopathol, 1995. **17**(2-3): p. 121-32.
24. Dahm, T., et al., *Neuroinvasion and Inflammation in Viral Central Nervous System Infections.* Mediators Inflamm, 2016. **2016**: p. 8562805.
25. Nayak, D., T.L. Roth, and D.B. McGavern, *Microglia development and function.* Annu Rev Immunol, 2014. **32**: p. 367-402.

26. Chen, C.J., et al., *Glial activation involvement in neuronal death by Japanese encephalitis virus infection.* J Gen Virol, 2010. **91**(Pt 4): p. 1028-37.
27. Tsai, T.T., et al., *Microglia retard dengue virus-induced acute viral encephalitis.* Sci Rep, 2016. **6**: p. 27670.
28. Lannes, N., et al., *Interactions of human microglia cells with Japanese encephalitis virus.* Virol J, 2017. **14**(1): p. 8.
29. Griffin, D.E., *Immune responses to RNA-virus infections of the CNS.* Nat Rev Immunol, 2003. **3**(6): p. 493-502.
30. Byrnes, A.P., J.E. Durbin, and D.E. Griffin, *Control of Sindbis virus infection by antibody in interferon-deficient mice.* J Virol, 2000. **74**(8): p. 3905-8.
31. Frolova, E.I., et al., *Roles of nonstructural protein nsP2 and Alpha/Beta interferons in determining the outcome of Sindbis virus infection.* J Virol, 2002. **76**(22): p. 11254-64.
32. Schultz, K.L., P.S. Vernon, and D.E. Griffin, *Differentiation of neurons restricts Arbovirus replication and increases expression of the alpha isoform of IRF-7.* J Virol, 2015. **89**(1): p. 48-60.
33. Burdeinick-Kerr, R., D. Govindarajan, and D.E. Griffin, *Noncytolytic clearance of sindbis virus infection from neurons by gamma interferon is dependent on Jak/STAT signaling.* J Virol, 2009. **83**(8): p. 3429-35.
34. !!! INVALID CITATION !!! {}.
35. Eberl, G., J.P. Di Santo, and E. Vivier, *The brave new world of innate lymphoid cells.* Nat Immunol, 2015. **16**(1): p. 1-5.
36. Binder, G.K. and D.E. Griffin, *Interferon-gamma-mediated site-specific clearance of alphavirus from CNS neurons.* Science, 2001. **293**(5528): p. 303-6.
37. Baxter, V.K. and D.E. Griffin, *Interferon gamma modulation of disease manifestation and the local antibody response to alphavirus encephalomyelitis.* J Gen Virol, 2016. **97**(11): p. 2908-2925.
38. Griffin, D.E., et al., *The immune response in viral encephalitis.* Semin Immunol, 1992. **4**(2): p. 111-9.
39. Griffin, D., et al., *The role of antibody in recovery from alphavirus encephalitis.* Immunol Rev, 1997. **159**: p. 155-61.

40. Levine, B., et al., *Antibody-mediated clearance of alphavirus infection from neurons.* Science, 1991. **254**(5033): p. 856-60.
41. Ubol, S., et al., *Roles of immunoglobulin valency and the heavy-chain constant domain in antibody-mediated downregulation of Sindbis virus replication in persistently infected neurons.* J Virol, 1995. **69**(3): p. 1990-3.
42. Despres, P., J.W. Griffin, and D.E. Griffin, *Antiviral activity of alpha interferon in Sindbis virus-infected cells is restored by anti-E2 monoclonal antibody treatment.* J Virol, 1995. **69**(11): p. 7345-8.
43. Despres, P., J.W. Griffin, and D.E. Griffin, *Effects of anti-E2 monoclonal antibody on sindbis virus replication in AT3 cells expressing bcl-2.* J Virol, 1995. **69**(11): p. 7006-14.
44. Ulug, E.T., R.F. Garry, and H.R. Bose, Jr., *Inhibition of Na+K+ATPase activity in membranes of Sindbis virus-infected chick cells.* Virology, 1996. **216**(2): p. 299-308.
45. Burdeinick-Kerr, R., J. Wind, and D.E. Griffin, *Synergistic roles of antibody and interferon in noncytolytic clearance of Sindbis virus from different regions of the central nervous system.* J Virol, 2007. **81**(11): p. 5628-36.
46. Metcalf, T.U., et al., *Recruitment and retention of B cells in the central nervous system in response to alphavirus encephalomyelitis.* J Virol, 2013. **87**(5): p. 2420-9.
47. Moore, K.W., et al., *Interleukin-10 and the interleukin-10 receptor.* Annu Rev Immunol, 2001. **19**: p. 683-765.
48. Fiorentino, D.F., M.W. Bond, and T.R. Mosmann, *Two types of mouse T helper cell. IV. Th2 clones secrete a factor that inhibits cytokine production by Th1 clones.* J Exp Med, 1989. **170**(6): p. 2081-95.
49. Kuhn, R., et al., *Interleukin-10-deficient mice develop chronic enterocolitis.* Cell, 1993. **75**(2): p. 263-74.
50. Zdanov, A., et al., *Crystal structure of interleukin-10 reveals the functional dimer with an unexpected topological similarity to interferon gamma.* Structure, 1995. **3**(6): p. 591-601.

51. Liu, Y., et al., *Expression cloning and characterization of a human IL-10 receptor.* J Immunol, 1994. **152**(4): p. 1821-9.
52. Ho, A.S., et al., *Functional regions of the mouse interleukin-10 receptor cytoplasmic domain.* Mol Cell Biol, 1995. **15**(9): p. 5043-53.
53. Meraz, M.A., et al., *Targeted disruption of the Stat1 gene in mice reveals unexpected physiologic specificity in the JAK-STAT signaling pathway.* Cell, 1996. **84**(3): p. 431-42.
54. Riley, J.K., et al., *Interleukin-10 receptor signaling through the JAK-STAT pathway. Requirement for two distinct receptor-derived signals for anti-inflammatory action.* J Biol Chem, 1999. **274**(23): p. 16513-21.
55. Verhoeven, D. and S. Perry, *Differential mucosal IL-10-induced immunoregulation of innate immune responses occurs in influenza infected infants/toddlers and adults.* Immunol Cell Biol, 2017. **95**(3): p. 252-260.
56. Tun, M.M., et al., *Protective role of TNF-alpha, IL-10 and IL-2 in mice infected with the Oshima strain of Tick-borne encephalitis virus.* Sci Rep, 2014. **4**: p. 5344.
57. McKinstry, K.K., et al., *IL-10 deficiency unleashes an influenza-specific Th17 response and enhances survival against high-dose challenge.* J Immunol, 2009. **182**(12): p. 7353-63.
58. Cheeran, M.C., et al., *Reduced lymphocyte infiltration during cytomegalovirus brain infection of interleukin-10-deficient mice.* J Neurovirol, 2009. **15**(4): p. 334-42.
59. Marques, C.P., et al., *Interleukin-10 attenuates production of HSV-induced inflammatory mediators by human microglia.* Glia, 2004. **47**(4): p. 358-66.
60. Eberhardt, M.K., et al., *Exploitation of Interleukin-10 (IL-10) Signaling Pathways: Alternate Roles of Viral and Cellular IL-10 in Rhesus Cytomegalovirus Infection.* J Virol, 2016. **90**(21): p. 9920-9930.
61. Young, V.P., et al., *Modulation of the Host Environment by Human Cytomegalovirus with Viral Interleukin 10 in Peripheral Blood.* J Infect Dis, 2017. **215**(6): p. 874-882.

62. Gorshkova, E.A. and E.S. Shilov, *Possible Mechanisms of Acquisition of Herpesvirus Virokines.* Biochemistry (Mosc), 2016. **81**(11): p. 1350-1357.
63. O'Neill, E.J., M.J. Day, and D.C. Wraith, *IL-10 is essential for disease protection following intranasal peptide administration in the C57BL/6 model of EAE.* J Neuroimmunol, 2006. **178**(1-2): p. 1-8.
64. Zhang, J., et al., *Treatment with IL-10 producing B cells in combination with E2 ameliorates EAE severity and decreases CNS inflammation in B cell-deficient mice.* Metab Brain Dis, 2015. **30**(5): p. 1117-27.
65. Kim, K., et al., *Role of excitatory amino acid transporter-2 (EAAT2) and glutamate in neurodegeneration: opportunities for developing novel therapeutics.* J Cell Physiol, 2011. **226**(10): p. 2484-93.
66. Kulkarni, A.B., et al., *Transforming growth factor beta 1 null mutation in mice causes excessive inflammatory response and early death.* Proc Natl Acad Sci U S A, 1993. **90**(2): p. 770-4.
67. Rifkin, D.B., *Latent transforming growth factor-beta (TGF-beta) binding proteins: orchestrators of TGF-beta availability.* J Biol Chem, 2005. **280**(9): p. 7409-12.
68. Saharinen, J. and J. Keski-Oja, *Specific sequence motif of 8-Cys repeats of TGF-beta binding proteins, LTBPs, creates a hydrophobic interaction surface for binding of small latent TGF-beta.* Mol Biol Cell, 2000. **11**(8): p. 2691-704.
69. Annes, J.P., J.S. Munger, and D.B. Rifkin, *Making sense of latent TGFbeta activation.* J Cell Sci, 2003. **116**(Pt 2): p. 217-24.
70. Taipale, J., et al., *Latent transforming growth factor-beta 1 associates to fibroblast extracellular matrix via latent TGF-beta binding protein.* J Cell Biol, 1994. **124**(1-2): p. 171-81.
71. Yu, Y., et al., *TGF-beta, BMPS, and their signal transducing mediators, Smads, in rat fracture healing.* J Biomed Mater Res, 2002. **60**(3): p. 392-7.
72. Kim, S.J., et al., *Post-transcriptional regulation of the human transforming growth factor-beta 1 gene.* J Biol Chem, 1992. **267**(19): p. 13702-7.
73. Itoh, S., et al., *The transcriptional co-activator P/CAF potentiates TGF-beta/Smad signaling.* Nucleic Acids Res, 2000. **28**(21): p. 4291-8.

74. Valdimarsdottir, G., et al., *Smad7 and protein phosphatase 1alpha are critical determinants in the duration of TGF-beta/ALK1 signaling in endothelial cells.* BMC Cell Biol, 2006. 7: p. 16.

75. Malhotra, N. and J. Kang, *SMAD regulatory networks construct a balanced immune system.* Immunology, 2013. **139**(1): p. 1-10.

76. Malhotra, N., E. Robertson, and J. Kang, *SMAD2 is essential for TGF beta-mediated Th17 cell generation.* J Biol Chem, 2010. **285**(38): p. 29044-8.

77. Martinez, G.J., et al., *Smad2 positively regulates the generation of Th17 cells.* J Biol Chem, 2010. **285**(38): p. 29039-43.

78. Martinez, G.J., et al., *Smad3 differentially regulates the induction of regulatory and inflammatory T cell differentiation.* J Biol Chem, 2009. **284**(51): p. 35283-6.

79. Zhou, L., et al., *TGF-beta-induced Foxp3 inhibits T(H)17 cell differentiation by antagonizing RORgammat function.* Nature, 2008. **453**(7192): p. 236-40.

80. Sharma, M., S.V. Kaveri, and J. Bayry, *Th17 cells, pathogenic or not? TGF-beta3 imposes the embargo.* Cell Mol Immunol, 2013. **10**(2): p. 101-2.

81. Gershon, R.K. and K. Kondo, *Cell interactions in the induction of tolerance: the role of thymic lymphocytes.* Immunology, 1970. **18**(5): p. 723-37.

82. Duffy, S.S., et al., *The role of regulatory T cells in nervous system pathologies.* J Neurosci Res, 2017.

83. Danikowski, K.M., S. Jayaraman, and B.S. Prabhakar, *Regulatory T cells in multiple sclerosis and myasthenia gravis.* J Neuroinflammation, 2017. **14**(1): p. 117.

84. Komatsu, N., et al., *Pathogenic conversion of Foxp3(+) T cells into TH17 cells in autoimmune arthritis.* Nat Med, 2014. **20**(1): p. 62-8.

85. Oukka, M., *Interplay between pathogenic Th17 and regulatory T cells.* Ann Rheum Dis, 2007. **66 Suppl 3**: p. iii87-90.

86. Han, J., et al., *Role of regulatory b cells in neuroimmunologic disorders.* J Neurosci Res, 2016. **94**(8): p. 693-701.

87. Roosendaal, S.D. and F. Barkhof, *Imaging phenotypes in multiple sclerosis.* Neuroimaging Clin N Am, 2015. **25**(1): p. 83-96.

88. Wolf, S.D., et al., *Experimental autoimmune encephalomyelitis induction in genetically B cell-deficient mice.* J Exp Med, 1996. **184**(6): p. 2271-8.
89. Fillatreau, S., et al., *B cells regulate autoimmunity by provision of IL-10.* Nat Immunol, 2002. **3**(10): p. 944-50.
90. Matsushita, T., et al., *Regulatory B cells (B10 cells) and regulatory T cells have independent roles in controlling experimental autoimmune encephalomyelitis initiation and late-phase immunopathogenesis.* J Immunol, 2010. **185**(4): p. 2240-52.
91. Matsushita, T., et al., *Regulatory B cells inhibit EAE initiation in mice while other B cells promote disease progression.* J Clin Invest, 2008. **118**(10): p. 3420-30.
92. Pennati, A., et al., *Regulatory B Cells Induce Formation of IL-10-Expressing T Cells in Mice with Autoimmune Neuroinflammation.* J Neurosci, 2016. **36**(50): p. 12598-12610.
93. Carter, N.A., et al., *Mice lacking endogenous IL-10-producing regulatory B cells develop exacerbated disease and present with an increased frequency of Th1/Th17 but a decrease in regulatory T cells.* J Immunol, 2011. **186**(10): p. 5569-79.
94. Flores-Borja, F., et al., *CD19+CD24hiCD38hi B cells maintain regulatory T cells while limiting TH1 and TH17 differentiation.* Sci Transl Med, 2013. **5**(173): p. 173ra23.
95. Cen, Z., et al., *IL-10-producing B cells involved in the pathogenesis of Coxsackie virus B3-induced acute viral myocarditis.* Int J Clin Exp Pathol, 2015. **8**(1): p. 830-5.
96. Guo, Y., et al., *Increased circulating interleukin 10-secreting B cells in patients with dilated cardiomyopathy.* Int J Clin Exp Pathol, 2015. **8**(7): p. 8107-14.
97. Liu, F., et al., *Role of IL-10-producing regulatory B cells in modulating T-helper cell immune responses during silica-induced lung inflammation and fibrosis.* Sci Rep, 2016. **6**: p. 28911.
98. Hu, X., et al., *A Lower Proportion of Regulatory B Cells in Patients with Henoch-Schoenlein Purpura Nephritis.* PLoS One, 2016. **11**(3): p. e0152368.

99. Wang, X.F. and F. Korangy, *Intrahepatic landscape of regulatory T-cell subsets in chronically HCV-infected patients with cirrhosis and HCC.* Hepatology, 2014. **60**(5): p. 1461-2.

100. Wang, L., et al., *Increased numbers of CD5+CD19+CD1dhighIL-10+ Bregs, CD4+Foxp3+ Tregs, CD4+CXCR5+Foxp3+ follicular regulatory T (TFR) cells in CHB or CHC patients.* J Transl Med, 2014. **12**: p. 251.

101. Yanaba, K., et al., *A regulatory B cell subset with a unique CD1dhiCD5+ phenotype controls T cell-dependent inflammatory responses.* Immunity, 2008. **28**(5): p. 639-50.

102. Olkhanud, P.B., et al., *Tumor-evoked regulatory B cells promote breast cancer metastasis by converting resting CD4(+) T cells to T-regulatory cells.* Cancer Res, 2011. **71**(10): p. 3505-15.

103. Mutnal, M.B., et al., *Infiltrating regulatory B cells control neuroinflammation following viral brain infection.* J Immunol, 2014. **193**(12): p. 6070-80.

104. Kulcsar, K., *PhD Thesis Work*, in *Molecular Microbiology & Immunology*. 2014, Johns Hopkins School of Public Health: Unpublished.

105. Griffin, D.E., *Emergence and re-emergence of viral diseases of the central nervous system.* Prog Neurobiol, 2010. **91**(2): p. 95-101.

106. Adams, A.P., et al., *Venezuelan equine encephalitis virus activity in the Gulf Coast region of Mexico, 2003-2010.* PLoS Negl Trop Dis, 2012. **6**(11): p. e1875.

107. Aguilar, P.V., et al., *Genetic characterization of Venezuelan equine encephalitis virus from Bolivia, Ecuador and Peru: identification of a new subtype ID lineage.* PLoS Negl Trop Dis, 2009. **3**(9): p. e514.

108. Aguilar, P.V., et al., *Endemic Venezuelan equine encephalitis in the Americas: hidden under the dengue umbrella.* Future Virol, 2011. **6**(6): p. 721-740.

109. Griffin, D.E., *Role of the immune response in age-dependent resistance of mice to encephalitis due to Sindbis virus.* J Infect Dis, 1976. **133**(4): p. 456-64.

110. Hirsch, R.L. and D.E. Griffin, *Development of age-dependent resistance to sindbis virus encephalitis: correlation with inactivation of virus within the blood stream.* Antiviral Res, 1981. **1**(4): p. 263-7.

111. Sherman, L.A. and D.E. Griffin, *Pathogenesis of encephalitis induced in newborn mice by virulent and avirulent strains of Sindbis virus.* J Virol, 1990. **64**(5): p. 2041-6.

112. Kimura, T. and D.E. Griffin, *The role of CD8(+) T cells and major histocompatibility complex class I expression in the central nervous system of mice infected with neurovirulent Sindbis virus.* J Virol, 2000. **74**(13): p. 6117-25.

113. Rowell, J.F. and D.E. Griffin, *Contribution of T cells to mortality in neurovirulent Sindbis virus encephalomyelitis.* J Neuroimmunol, 2002. **127**(1-2): p. 106-14.

114. Burdeinick-Kerr, R. and D.E. Griffin, *Gamma interferon-dependent, noncytolytic clearance of sindbis virus infection from neurons in vitro.* J Virol, 2005. **79**(9): p. 5374-85.

115. Donnelly, R.P., et al., *The expanded family of class II cytokines that share the IL-10 receptor-2 (IL-10R2) chain.* J Leukoc Biol, 2004. **76**(2): p. 314-21.

116. Couper, K.N., D.G. Blount, and E.M. Riley, *IL-10: the master regulator of immunity to infection.* J Immunol, 2008. **180**(9): p. 5771-7.

117. Zhou, Z., et al., *IL-10 promotes neuronal survival following spinal cord injury.* Exp Neurol, 2009. **220**(1): p. 183-90.

118. Berg, D.J., et al., *Enterocolitis and colon cancer in interleukin-10-deficient mice are associated with aberrant cytokine production and CD4(+) TH1-like responses.* J Clin Invest, 1996. **98**(4): p. 1010-20.

119. Ito, S., et al., *Interleukin-10 inhibits expression of both interferon alpha- and interferon gamma- induced genes by suppressing tyrosine phosphorylation of STAT1.* Blood, 1999. **93**(5): p. 1456-63.

120. Malisan, F., et al., *Interleukin-10 induces immunoglobulin G isotype switch recombination in human CD40-activated naive B lymphocytes.* J Exp Med, 1996. **183**(3): p. 937-47.

121. Go, N.F., et al., *Interleukin 10, a novel B cell stimulatory factor: unresponsiveness of X chromosome-linked immunodeficiency B cells.* J Exp Med, 1990. **172**(6): p. 1625-31.

122. Gorelik, L. and R.A. Flavell, *Abrogation of TGFbeta signaling in T cells leads to spontaneous T cell differentiation and autoimmune disease.* Immunity, 2000. **12**(2): p. 171-81.

123. Gorelik, L. and R.A. Flavell, *Transforming growth factor-beta in T-cell biology.* Nat Rev Immunol, 2002. **2**(1): p. 46-53.

124. Korn, T., et al., *IL-17 and Th17 Cells.* Annu Rev Immunol, 2009. **27**: p. 485-517.

125. Yoshimura, A., Y. Wakabayashi, and T. Mori, *Cellular and molecular basis for the regulation of inflammation by TGF-beta.* J Biochem, 2010. **147**(6): p. 781-92.

126. Xu, A., et al., *TGF-beta-Induced Regulatory T Cells Directly Suppress B Cell Responses through a Noncytotoxic Mechanism.* J Immunol, 2016. **196**(9): p. 3631-41.

127. Lee, Y., et al., *Induction and molecular signature of pathogenic TH17 cells.* Nat Immunol, 2012. **13**(10): p. 991-9.

128. Sun, L., H. Jin, and H. Li, *GARP: a surface molecule of regulatory T cells that is involved in the regulatory function and TGF-beta releasing.* Oncotarget, 2016. **7**(27): p. 42826-42836.

129. Meisel, M., et al., *The kinase PKCalpha selectively upregulates interleukin-17A during Th17 cell immune responses.* Immunity, 2013. **38**(1): p. 41-52.

130. Yamashita, T., et al., *IL-6-mediated Th17 differentiation through RORgammat is essential for the initiation of experimental autoimmune myocarditis.* Cardiovasc Res, 2011. **91**(4): p. 640-8.

131. Hatfield, J.K. and M.A. Brown, *Group 3 innate lymphoid cells accumulate and exhibit disease-induced activation in the meninges in EAE.* Cell Immunol, 2015. **297**(2): p. 69-79.

132. Takatori, H., et al., *Lymphoid tissue inducer-like cells are an innate source of IL-17 and IL-22.* J Exp Med, 2009. **206**(1): p. 35-41.

133. Gladiator, A. and S. LeibundGut-Landmann, *Innate lymphoid cells: new players in IL-17-mediated antifungal immunity.* PLoS Pathog, 2013. **9**(12): p. e1003763.

134. Moro, K., et al., *Innate production of T(H)2 cytokines by adipose tissue-associated c-Kit(+)Sca-1(+) lymphoid cells.* Nature, 2010. **463**(7280): p. 540-4.

135. Halim, T.Y., *Group 2 innate lymphoid cells in disease.* Int Immunol, 2016. **28**(1): p. 13-22.

136. Russi, A.E., et al., *Cutting edge: c-Kit signaling differentially regulates type 2 innate lymphoid cell accumulation and susceptibility to central nervous system demyelination in male and female SJL mice.* J Immunol, 2015. **194**(12): p. 5609-13.

137. Kim, B.S. and D. Artis, *Group 2 innate lymphoid cells in health and disease.* Cold Spring Harb Perspect Biol, 2015. 7(5).

138. Besnard, A.G., et al., *IL-33-mediated protection against experimental cerebral malaria is linked to induction of type 2 innate lymphoid cells, M2 macrophages and regulatory T cells.* PLoS Pathog, 2015. **11**(2): p. e1004607.

139. Lohning, M., et al., *T1/ST2 is preferentially expressed on murine Th2 cells, independent of interleukin 4, interleukin 5, and interleukin 10, and important for Th2 effector function.* Proc Natl Acad Sci U S A, 1998. **95**(12): p. 6930-5.

140. Walzl, G., et al., *Inhibition of T1/ST2 during respiratory syncytial virus infection prevents T helper cell type 2 (Th2)- but not Th1-driven immunopathology.* J Exp Med, 2001. **193**(7): p. 785-92.

141. Nawijn, M.C., et al., *Enforced expression of GATA-3 in transgenic mice inhibits Th1 differentiation and induces the formation of a T1/ST2-expressing Th2-committed T cell compartment in vivo.* J Immunol, 2001. **167**(2): p. 724-32.

142. Mangan, N.E., et al., *T1/ST2 expression on Th2 cells negatively regulates allergic pulmonary inflammation.* Eur J Immunol, 2007. **37**(5): p. 1302-12.

143. Korn, T., et al., *The dynamics of effector T cells and Foxp3+ regulatory T cells in the promotion and regulation of autoimmune encephalomyelitis.* J Neuroimmunol, 2007. **191**(1-2): p. 51-60.

144. Huber, S., et al., *Th17 cells express interleukin-10 receptor and are controlled by Foxp3(-) and Foxp3+ regulatory CD4+ T cells in an interleukin-10-dependent manner.* Immunity, 2011. **34**(4): p. 554-65.

145. Forkel, M. and J. Mjosberg, *Dysregulation of Group 3 Innate Lymphoid Cells in the Pathogenesis of Inflammatory Bowel Disease.* Curr Allergy Asthma Rep, 2016. **16**(10): p. 73.

146. Ramos, M.M., et al., *Epidemic dengue and dengue hemorrhagic fever at the Texas-Mexico border: results of a household-based seroepidemiologic survey, December 2005.* Am J Trop Med Hyg, 2008. **78**(3): p. 364-9.

147. Thomas, D.L., et al., *Reemergence of Dengue in Southern Texas, 2013.* Emerg Infect Dis, 2016. **22**(6): p. 1002-7.

148. Saxton-Shaw, K.D., et al., *The first outbreak of eastern equine encephalitis in Vermont: outbreak description and phylogenetic relationships of the virus isolate.* PLoS One, 2015. **10**(6): p. e0128712.

149. Pisano, M.B., et al., *Venezuelan equine encephalitis viruses (VEEV) in Argentina: serological evidence of human infection.* PLoS Negl Trop Dis, 2013. 7(12): p. e2551.

150. Lindholm, D.A., et al., *Mosquito Exposure and Chikungunya and Dengue Infection Among Travelers During the Chikungunya Outbreak in the Americas.* Am J Trop Med Hyg, 2017. **96**(4): p. 903-912.

151. Oviedo-Pastrana, M., et al., *Epidemic outbreak of Chikungunya in two neighboring towns in the Colombian Caribbean: a survival analysis.* Arch Public Health, 2017. **75**: p. 1.

152. Kuhn, R.J., et al., *Attenuation of Sindbis virus neurovirulence by using defined mutations in nontranslated regions of the genome RNA.* J Virol, 1992. **66**(12): p. 7121-7.

153. Mutnal, M.B., et al., *Excess neutrophil infiltration during cytomegalovirus brain infection of interleukin-10-deficient mice.* J Neuroimmunol, 2010. **227**(1-2): p. 101-10.

154. Ho, A.S. and K.W. Moore, *Interleukin-10 and its receptor.* Ther Immunol, 1994. **1**(3): p. 173-85.

155. Zhu, J., et al., *Cellular mRNA expression of interferon-gamma, IL-4 and transforming growth factor-beta (TGF-beta) by rat mononuclear cells stimulated with peripheral nerve myelin antigens in experimental allergic neuritis.* Clin Exp Immunol, 1994. **98**(2): p. 306-12.

156. Reuter, D., et al., *Foxp3+ regulatory T cells control persistence of viral CNS infection.* PLoS One, 2012. 7(3): p. e33989.

157. Jung, M.K. and E.C. Shin, *Regulatory T Cells in Hepatitis B and C Virus Infections.* Immune Netw, 2016. **16**(6): p. 330-336.
158. Zhang, Z., et al., *Distribution of Foxp3(+) T-regulatory cells in experimental autoimmune neuritis rats.* Exp Neurol, 2009. **216**(1): p. 75-82.
159. Sojka, D.K. and D.J. Fowell, *Regulatory T cells inhibit acute IFN-gamma synthesis without blocking T-helper cell type 1 (Th1) differentiation via a compartmentalized requirement for IL-10.* Proc Natl Acad Sci U S A, 2011. **108**(45): p. 18336-41.
160. Trandem, K., et al., *Virally expressed interleukin-10 ameliorates acute encephalomyelitis and chronic demyelination in coronavirus-infected mice.* J Virol, 2011. **85**(14): p. 6822-31.
161. Singh, S.K., et al., *Acute Encephalitic Syndrome in Adults and its Correlation with Cytokine Levels in Serum and Cerebrospinal Fluid.* Jpn J Infect Dis, 2016.
162. Freyschmidt, E.J., et al., *Skin inflammation arising from cutaneous regulatory T cell deficiency leads to impaired viral immune responses.* J Immunol, 2010. **185**(2): p. 1295-302.
163. Howell, J. and K. Visvanathan, *The role of natural killer cells in hepatitis C infection.* Antivir Ther, 2013. **18**(7): p. 853-65.
164. Amadei, B., et al., *Activation of natural killer cells during acute infection with hepatitis C virus.* Gastroenterology, 2010. **138**(4): p. 1536-45.
165. Golden-Mason, L. and H.R. Rosen, *Natural killer cells: multifaceted players with key roles in hepatitis C immunity.* Immunol Rev, 2013. **255**(1): p. 68-81.
166. Sun, C., et al., *TGF-beta1 down-regulation of NKG2D/DAP10 and 2B4/SAP expression on human NK cells contributes to HBV persistence.* PLoS Pathog, 2012. **8**(3): p. e1002594.
167. Rubtsov, Y.P. and A.Y. Rudensky, *TGFbeta signalling in control of T-cell-mediated self-reactivity.* Nat Rev Immunol, 2007. **7**(6): p. 443-53.
168. Ni, G., et al., *Manipulating IL-10 signalling blockade for better immunotherapy.* Cell Immunol, 2015. **293**(2): p. 126-9.
169. Li, W., et al., *Blocking the function of inflammatory cytokines and mediators by using IL-10 and TGF-beta: a potential biological immunotherapy for*

intervertebral disc degeneration in a beagle model. Int J Mol Sci, 2014. **15**(10): p. 17270-83.

170. Dobrzanski, M.J., et al., *Immunotherapy with IL-10- and IFN-gamma-producing CD4 effector cells modulate "Natural" and "Inducible" CD4 TReg cell subpopulation levels: observations in four cases of patients with ovarian cancer.* Cancer Immunol Immunother, 2012. **61**(6): p. 839-54.
171. Lou, W., et al., *Enhancement of the frequency and function of IL-10-secreting type I T regulatory cells after 1 year of cluster allergen-specific immunotherapy.* Int Arch Allergy Immunol, 2012. **159**(4): p. 391-8.
172. Paniz-Mondolfi, A.E., et al., *Venezuelan equine encephalitis: How likely are we to see the next epidemic?* Travel Med Infect Dis, 2017.
173. Oliver, J., et al., *Geography and Timing of Cases of Eastern Equine Encephalitis in New York State from 1992 to 2012.* Vector Borne Zoonotic Dis, 2016. **16**(4): p. 283-9.
174. Garlick, J., et al., *Locally Acquired Eastern Equine Encephalitis Virus Disease, Arkansas, USA.* Emerg Infect Dis, 2016. **22**(12): p. 2216-2217.
175. Perona-Wright, G., et al., *Systemic but not local infections elicit immunosuppressive IL-10 production by natural killer cells.* Cell Host Microbe, 2009. **6**(6): p. 503-12.
176. Loevenich, K., et al., *DC-Derived IL-10 Modulates Pro-inflammatory Cytokine Production and Promotes Induction of CD4+IL-10+ Regulatory T Cells during Plasmodium yoelii Infection.* Front Immunol, 2017. **8**: p. 152.
177. Martin, N., *Role of TGFβ During Fatal Alphavirus Encephalomyelitis in IL-10 Deficient Mice on TH17 Responses.* 2017.
178. Kim, A. and S. Sadegh-Nasseri, *Determinants of immunodominance for CD4 T cells.* Curr Opin Immunol, 2015. **34**: p. 9-15.
179. Angeletti, D., et al., *Defining B cell immunodominance to viruses.* Nat Immunol, 2017. **18**(4): p. 456-463.
180. Dale, G.A., J.R. Shartouny, and J. Jacob, *Quantifying the shifting landscape of B cell immunodominance.* Nat Immunol, 2017. **18**(4): p. 367-368.

181. Akram, A. and R.D. Inman, *Immunodominance: a pivotal principle in host response to viral infections.* Clin Immunol, 2012. **143**(2): p. 99-115.
182. Grant, E.J., et al., *T-cell immunity to influenza A viruses.* Crit Rev Immunol, 2014. **34**(1): p. 15-39.
183. Angeletti, D. and J.W. Yewdell, *Is It Possible to Develop a "Universal" Influenza Virus Vaccine? Outflanking Antibody Immunodominance on the Road to Universal Influenza Vaccination.* Cold Spring Harb Perspect Biol, 2017.
184. Popova, L., et al., *Immunodominance of antigenic site B over site A of hemagglutinin of recent H3N2 influenza viruses.* PLoS One, 2012. 7(7): p. e41895.
185. Luciani, F., et al., *Increasing viral dose causes a reversal in CD8+ T cell immunodominance during primary influenza infection due to differences in antigen presentation, T cell avidity, and precursor numbers.* J Immunol, 2013. **190**(1): p. 36-47.
186. Griffin, D.E., *A review of alphavirus replication in neurons.* Neurosci Biobehav Rev, 1998. **22**(6): p. 721-3.
187. Hyde, J.L., et al., *The 5' and 3' ends of alphavirus RNAs--Non-coding is not non-functional.* Virus Res, 2015. **206**: p. 99-107.
188. Trobaugh, D.W. and W.B. Klimstra, *Alphaviruses suppress host immunity by preventing myeloid cell replication and antagonizing innate immune responses.* Curr Opin Virol, 2017. **23**: p. 30-34.
189. Diamond, M.S. and M. Farzan, *The broad-spectrum antiviral functions of IFIT and IFITM proteins.* Nat Rev Immunol, 2013. **13**(1): p. 46-57.
190. Daffis, S., et al., *2'-O methylation of the viral mRNA cap evades host restriction by IFIT family members.* Nature, 2010. **468**(7322): p. 452-6.
191. Reynaud, J.M., et al., *IFIT1 Differentially Interferes with Translation and Replication of Alphavirus Genomes and Promotes Induction of Type I Interferon.* PLoS Pathog, 2015. **11**(4): p. e1004863.
192. Hyde, J.L., et al., *A viral RNA structural element alters host recognition of nonself RNA.* Science, 2014. **343**(6172): p. 783-7.

193. White, L.J., et al., *Role of alpha/beta interferon in Venezuelan equine encephalitis virus pathogenesis: effect of an attenuating mutation in the 5' untranslated region.* J Virol, 2001. **75**(8): p. 3706-18.

194. Cameron, J.E., et al., *Epstein-Barr virus latent membrane protein 1 induces cellular MicroRNA miR-146a, a modulator of lymphocyte signaling pathways.* J Virol, 2008. **82**(4): p. 1946-58.

195. Sharma, N., et al., *miR-146a suppresses cellular immune response during Japanese encephalitis virus JaOArS982 strain infection in human microglial cells.* J Neuroinflammation, 2015. **12**: p. 30.

196. Bandiera, S., et al., *Hepatitis C Virus-Induced Upregulation of MicroRNA miR-146a-5p in Hepatocytes Promotes Viral Infection and Deregulates Metabolic Pathways Associated with Liver Disease Pathogenesis.* J Virol, 2016. **90**(14): p. 6387-400.

197. Deng, M., et al., *miR-146a negatively regulates the induction of proinflammatory cytokines in response to Japanese encephalitis virus infection in microglial cells.* Arch Virol, 2017. **162**(6): p. 1495-1505.

198. Tian, T., et al., *MiR-146a and miR-196a-2 polymorphisms are associated with hepatitis virus-related hepatocellular cancer risk: a meta-analysis.* Aging (Albany NY), 2017. **9**(2): p. 381-392.

199. Wu, S., et al., *miR-146a facilitates replication of dengue virus by dampening interferon induction by targeting TRAF6.* J Infect, 2013. **67**(4): p. 329-41.

200. Thounaojam, M.C., et al., *MicroRNA 155 regulates Japanese encephalitis virus-induced inflammatory response by targeting Src homology 2-containing inositol phosphatase 1.* J Virol, 2014. **88**(9): p. 4798-810.

201. Rayamajhi, A., et al., *A preliminary randomized double blind placebo-controlled trial of intravenous immunoglobulin for Japanese encephalitis in Nepal.* PLoS One, 2015. **10**(4): p. e0122608.

202. Gardner, C.L., et al., *Antibody Preparations from Human Transchromosomic Cows Exhibit Prophylactic and Therapeutic Efficacy against Venezuelan Equine Encephalitis Virus.* J Virol, 2017. **91**(14).

CHAPTER 7 CURRICULM VITAE

SUMMARY: A proven leader in health science advocacy and communication as founder of Public Health United, Inc. Innovator in health & science education via Gordis Teaching Fellowship, Teaching As Research Fellowship, & teaching "Communicating Science" course at Hopkins. Over twenty years of experience in scientific research, including current doctoral work in Molecular Microbiology & Immunology and international research in Africa and France. Avid social media user.

EMPLOYMENT AFTER GRADUATION:

- *Policy, Advocacy, and Communications Associate*, International Vaccine Access Center, Johns Hopkins School of Public Health
- *Adjunct Faculty*, University of Maryland School of Medicine
    - Will be teaching "Science Communication"
- *CEO*, Public Health United, Inc. "Saving Lives with Better Science Communication", Baltimore, MD

EDUCATION:

Johns Hopkins Bloomberg School of Public Health, Baltimore, Maryland, 2012-2017

Program:

- 2012-2017 PhD in Department of Molecular Microbiology & Immunology

Fellowships:

- 2016-2017 Johns Hopkins Teaching As Research Fellowship
- 2016-2017 Johns Hopkins School of Public Health Gordis Teaching Fellowship, 3 semesters

Awards:

- 2015 SOURCE Champion of the Month (community service award)
- 2014 Voted "Top 100 Sites for Real Science of Immunizations"
- 2013 & 2012 Frances Coventry Fund Scholarship

Elected Leadership Positions:

- 2017 & 2016 Vice President, Public Health Promotion Executive Member of JHSPH Student Assembly
- 2017 & 2016 American Public Health Association Campus Liaison
- 2015-2013 Student Coordinator for Departmental Weekly Seminars

University of Pennsylvania, Philadelphia, PA, 2004-2009

Program: Post-baccalaureate Pre-Health Program

- Advanced Science GPA: 3.5/4.0 (10 courses)
- Concurrent volunteer work in laboratory (10-20 hours/week) & hospital

Colby College, Waterville, ME, 2000- 2004

Degree: Bachelor of Arts

Major: French Studies; Minor: Science, Technology and Society

Honors:

- Magna Cum Laude
- 2004-2003, Senior Scholar
- 2003 & 2002 Mellon Grant: award for summer environmental research projects on mosquito control
- 2003-2002 Certificat d'Etudes Politiques from the Institut d'Etudes Politques, France, diploma for completed course work

Programs:

- 2004-2003, Senior Scholar's Program, Colby College (thesis on permanent dispay, yearlong honors research project entitled: "Pesty Business: A History of Human-Mosquito Interactions in the North Shore Region of Massachusetts."
- 2003-2002, Wellesley-in-Aix, Aix-En-Provence, France Yearlong study abroad at the Institut d'Etudes Politiques Law School in
- 2000, Colby-in-Dijon: semester study abroad at the University de Dijon in Dijon, France

SCIENCE COMMUNICATION EXPERIENCE:

- Present-2013 CEO & Founder, Public Health United, Inc. www.publichealthunited.org
  - Improving science & public health communication through podcasts, articles, & outreach.
- September 2017, Invited Speaker, Introduction to Public Health, University of Mississippi
  - Talk title: Vaccine Communication for Pro-Vaxxers
- August 2017, Invited Speaker, Introduction to Biomedical Sciences, JHPSH.
  - Talk title: Science Communication for Public Health Students
- July 2017, Oral presentation, American Society for Microbiology Conference for Undergraduate Educators
  - Talk title: Effectiveness of A Flipped Classroom Active Learning Approach To Teaching Practical Science Communication
- June 2017, Fellow, Science Alliance Leadership Training, New York Academy of Sciences
- June 2017, Oral presentation, Johns Hopkins University, Center for Education Research
  - Talk title: Effectiveness of A Flipped Classroom Active Learning Approach To Teaching Practical Science Communication
- June 2017, Invited speaker, JHSPH Postdoctoral Association
  - Talk title: The Science of Science Communication
- May 2017, invited speaker, Johns Hopkins University, PHIIX Annual Symposium
  - Panelist & speaker on innovative ideas in public health
- April 2017, Invited speaker, Johns Hopkins University Undergraduate Public Health Conference
- June 2016, Trainee, Alan Alda Center for Communicating Science Bootcamp
  - Week long science communication training program for scientists
- June 2016, invited speaker, International Vaccine Access Center, JHSPH
  - Talk title: "Vaccine Communication Mistakes Everyone Makes"

- June 2016, oral presentation, American Society for Virology
    - Talk title: TGFb modulation of virus clearance during intermediate virulent alphaviral encephalomyelitis in IL-10 deficient mice
- September 2015, invited speaker, TEDxMidAtlantic, Washington, D.C
    - Talk title: "Fifty Shades of Science"
- July 2015, oral presentation, American Society for Virology Annual Meeting
    - Talk Title: Impact of IL-10 Deficiency on Antibody During Fatal Alphaviral Infection
- June 2015, Invited speaker, Ignite Baltimore, Baltimore, MD
    - Talk title: "Vaccinate!" (vaccine communication issues)
- June 2013, Invited speaker, Ignite Hopkins, Baltimore, MD
    - Talk title: "To Speak or Not To Speak: How Dysfunctional Communication Hurts Public Health Progress"

*Videos available at http://www.publichealthunited.org/videos/

TEACHING EXPERIENCE:

- 2017-2015, Science Communication Professor via Gordis Teaching Fellowship
    - Won fellowship to independently design and teach course to Hopkins undergraduate students in the Public Health Studies Department
    - Awarded for three semesters
    - Course Title: Communicating Science: Skills to Analyze & Communicate Science News
- 2017-2016, Teaching As Research Fellow
    - Fellowship awarded to formally research teaching methods in self-designed Gordis course
    - Title: "Effectiveness of A Flipped Classroom Active Learning Approach To Teaching Practical Science Communication"
    - Includes project design, IRB application, collection of data from my course, presentation, and publication of research results.
- 2017-2016: Preparing Future Faculty Fellow
    - Completed (September 2017) certificate program with the Johns Hopkins Teaching Academy
    - Requirements: 3 stages of courses, workshops, and teaching experience.
    - Learned formal teaching methods and gained experience teaching
- Present-2016, Immunology Tutor:
    - Provided intensive tutoring to public health masters students with little science background enrolled in required Immunology course.
- Present- 2013, Introduction to Biomedical Sciences, JHSPH, Primary Instructor: Dr. Gundula Bosch (past: Dr. Noel Rose)
    - Independently designed & taught two class sessions for incoming public health students: "Introduction to the Musculoskeletal System" & "Introduction to the Cardiovascular System"
    - Co-developer and instructor for third session "Introduction to Molecular Biology: An Active Learning Based Class on How to Study an Unknown Outbreak"

RESEARCH EXPERIENCE:

PhD Program, Johns Hopkins Bloomberg School of Public Health Department of Molecular Microbiology & Immunology

- Jan 2014-Fall 2017, **Thesis Work, Laboratory of Dr. Diane Griffin,**
  - Project: Pathogenesis & Regulation of T cell mediated viral encephalitis
- Sept-Nov 2013, **Special Field Research Project, Laboratory of Dr. Rhoel Dinglasan**
  - Project: Development of Saliva-Based Malaria Rapid Diagnostic Test
  - Location: Yaounde, Cameroon & surrounding villages
  - Description: Collected saliva and blood samples from children at 6 schools in rural Cameroon for the development of a rapid diagnostic test for malaria.
- **PhD Rotation #1, Laboratory of Dr. Marcelo Jacobs-Lorena**
  - Project: Role of p38 in LL3 nuclear localization in Plasmodium berghei infected mosquitoes
- **PhD Rotation #2, Laboratory of Dr. George Dimopoulos**
  - Project: Interactions of the midgut microbiota with field & laboratory strains of Aedes aegypti
- **PhD Rotation #3, Laboratory of Dr. Rhoel Dinglasan**
  - Project: Immunofocusing of the malaria transmission blocking vaccine target recombinant Anopheline-delta N-APN1

2012-2010, Lab Manager/Technician C, Dr. Dario Altieri (Principal Investigator) Cancer Center, Wistar Institute, Philadelphia, PA

- Projects:
  Role of Ran In Pancreatic Islet Beta Cells
  Role of CypD-KO Cell Xenografts in Nude Mice
  Metastasis of CypD-KO MEF Cells from Spleen To Liver in Nude Mice

2010-2008, Lab Technician C/Manager, Dr. Jorge Sepulveda (Principal Investigator), Department of Pathology, Veteran's Affairs Medical Center, Philadelphia, PA

- Projects:
  Elucidate the molecular markers of hypertrophy in mouse model.
  Includes ILK and cholesterol studies, Cre/Lox mouse husbandry, genotyping, PCR, transfection, cardiac myocyte cell culture, and Western Blotting.

2008-2006, Lab Technician II, Dr. Steve Douglas (Department of Immunology Chair), Flow Cytometry Core, Children's Hospital of Philadelphia, Philadelphia, PA

- Projects:
  Development of CFSE lymphocyte proliferation assay
  Effects of anti-PD1 & anti-PDL1 on lymphocyte proliferation
  Effects of mitogen and antigen stimulation on intracellular cytokine expression in lymphocytes

2006-2004, Lab Technician (Unpaid Volunteer), The Wistar Institute, Philadelphia, PA

- **HIV Immunopathogenesis Laboratory** (Dr. Luis Montaner, PI)
- Projects:
  NK cell cytolytic function against tumor and HIV infected targets.
  PBMC preparation from blood of HIV-infected individuals.
  Tissue culture and preparation of viral stocks.
- **Cancer Cell Biology Laboratory** (Dr. Dorothee Herlyn, PI)
  Purification and immuno-testing of hmEGR and mEGP

2004-2001, Research Assistant, James Webb, PhD (Principal Investigator, Professor) **History Department, Colby College, Waterville, ME**

Assisted Professor Webb in his research into the history of malaria in West Africa and India. This included searching for primary sources, taking notes, and making historical-epidemiological maps for his books

Summer 2003, Researcher, Station Biologique de la Tour du Valat, Le Sambuc, France

Researched and wrote a report in French analyzing how mosquito control operations are organized and conducted in France.

Summer 2002, Researcher, Toxics Action Center, Boston, MA

Conducted investigation into nuisance mosquito control operations in MA

Summer 1999, Lab Technician, W. R. Grace & Company, Cambridge, MA

Received Grace Research Award to study effects of freezing on intumescent paints

PUBLICATIONS:

- Caino MC, Chae YC, Vaira V, Ferrero S, Nosotti M, Martin NM, Weeraratna A, O'Connell M, Jernigan D, Fatatis A, Languino LR, Bosari S, Altieri DC. Metabolic stress regulates cytoskeletal dynamics and metastasis of cancer cells. J Clin Invest. 2013 Jul 1;123(7):2907-20.
- Vaira V, Faversani A, Martin NM, Garlick DS, Ferrero S, Nosotti M, Kissil JL, Bosari S, Altieri DC. Regulation of lung cancer metastasis by Klf4-Numb-like signaling. Cancer Res. 2013 Apr 15;73(8):2695-705.
- Tavecchio M, Lisanti S, Lam A, Ghosh JC, Martin NM, O'Connell M, Weeraratna AT, Kossenkov AV, Showe LC, Altieri DC. Cyclophilin D extramitochondrial signaling controls cell cycle progression and chemokine-directed cell motility. J Biol Chem. 2013 Feb 22;288(8):5553-61.
- Xia, Fang, Dohi, Takehiko, Martin, Nina M., Raskett, Christopher M., Liu, Qin, & Altieri, Dario C. Essential Role of the Small GTPase Ran In Postnatal Pancreatic Islet Development. *PLoS One*. 2011;6(11):e27879. Epub 2011 Nov 17.
- Martin, Nina. "Pesty Business: A History of Human-Mosquito Interactions on the North Shore of Boston, MA." *Senior Scholars*. Miller Library Collections. Colby College. May, 2004.

ADDITIONAL SKILLS AND ACTIVITIES:

Language:

- Fluent in English and French
- Proficient in oral and written Spanish

Computer:

- Excel, PowerPoint, Photoshop, EndNote, Illustrator, CellQuest, FloJo, Lucy, KC Junior, JavaScript, Access, SQL

Activities:

- Spin & Body Pump Instructor (2009-Present)
- Marathons: Great Wall of China Marathon, NYC Marathon, Philly Marathon
- Drummer (1989-Present)
- Baker (2006-Present)